Kyutech
Kyushu Institute of Technology

Controlling the Orientation of Semiconducting Polymers in Floating Film for Anisotropic Charge Transport in Organic Field Effect Transistor

DISSERTATION

FOR THE DEGREE OF

DOCTOR OF PHYLOSOPHY

MANISH PANDEY

Supervisor: SHYAM S. PANDEY

Division of Green Electronics

Graduate School of Life Sciences and Systems Engineering

Kyushu Institute of Technology

2017

Dedicated

To

Late Prof. Wataru Takashima

Abstract

Conjugated polymers (CPs) are among the most investigated semi-conducting material for their potential application in next generation electronic devices by roll-to-roll printing technique such as thin film transistors, photovoltaics, light emitting diodes etc. The performance of the any CP depends on the ease with which charge carriers can be transported in them. Although in the past two decades extensive research has been done by the scientific community to understand the charge transport mechanism in CPs, consensus have been well established that that morphology of CP in their thin films serves as the deceive parameter which influences the device parameter. In this perspective, orienting CPs in one direction has been focal point of many researchers to improve the overall device performance. This thesis presents a detailed investigation of orientation characteristics in a newly developed method for fabrication of oriented thin films named "floating film transfer method (FTM)". The orientation characteristics of some of well-known CPs such as Non-regiocontrolled poly(3-hexylthiophene) (NR-P3HT), Regioregular poly(3-hexylthiophene), Poly(3,3‴-didodecyl-quarterthiophene), Poly[2,5-bis(3-tetradecylthiophen-2-yl)thieno[3,2-b]thiophene] (PBTTT), Poly(9,9-dioctylfluorene), and Poly(9,9-dioctylfluorene-alt-bithiophene) have been carried out by polarized absorption spectroscopy, atomic force microscopy, X-ray diffraction, polarized Fourier transform spectroscopy, polarized Raman spectroscopy. The influence the microstructures on the electrical parameters were investigated by fabricating thin film transistors.

This investigation related to the orientation characteristics of CPs in FTM revealed that the casting conditions of the floating film on liquid substrate serves the most important role for optimizing the orientation intensity of individual CP. However, investigations revealed that the given polymer will only be able to orient if they are of liquid crystalline nature in particular lyotropic or thermotropic. Preliminary results observed by optimizing the orientation of one of the well-known amorphous NR-P3HT revealed very high orientation with nanofibrous domains. When the influence of these oriented domains on charge transport in transistors were studied they showed drastic enhancement of field effect mobility in comparison to isotropic films. A greater insight of orientation and charge transport was further investigated by blending amorphous NR-P3HT with crystalline material (PBTTT) in order to see changes in the orientation and their effect on charge transport. We have shown that that the orientation in oriented fibrous domain can be further enhanced by slight addition of the guest material, which results in to synergistic improvement of

orientation as well as the mobility, which also revealed that the resulting orientation and mobility depends on the individual constituent.

In order to extend the use of optimization techniques for orientation further, an air stable high performance thienothiophene PBTTT were highly oriented and detailed characterization revealed the formation of large scale domains with uni-directional orientation resulting in to high performance along the orientation direction with mobility reaching 1.24 cm^2/Vs, representing one of the best reported for this material system.

Looking at the limitations of the other orientation techniques utilized till now, layer by layer coating in order to prepare solution processed and multilayer oriented films while retaining the morphological features of underlying layers is one of the most cumbersome task. Since in FTM, casting and coating procedures are isolated and no solvent comes in this process, which can interfere with the underlying morphology in terms of orientation intensity as well as crystallite orientation. In order to demonstrate this, we have also carried out layer-by-layer coating of CPs by parallel and orthogonal coating. The detailed characterization these films suggested no morphological changes have taken place with layer by layer coating, which is an exciting results in sense of fabricating future organic electronic devices having multilayered oriented as well as isotropic thin films of CPs.

Table of Contents

Chapter 1: Introduction

1.1 Background Introduction

Now as days, where the whole modern world is driven by fast growing electronics, there is huge demand for making the fast growing technology more and more better to meet the ever increasing expectations. The miniaturization carried by the development of macroelectronics/microelectronics in modern circuitry have become an integral part of our life in the form high speed electronic device we use in our day to day life and the list of such devices is endless.

Since 19th century, immense efforts have been done for the development of inorganic semiconductors following the typical silicon based material owing to its unique characteristics. However, necessity to produce very high purity silicon (crystalline) wafer that rates over the existing purity level, is obtained by various sophisticated and energy consuming techniques and purification of raw material has become a tough challenge for further lowering down the cost. In addition to this, there is an absolute necessity for high class clean rooms or fabrication and processing of devices. Both of these issues make the initial production cost very high. It would have been a lot cheaper, if these necessities could be either avoided or minimized. There is a class of materials, known as organic semiconductors, which offer convenience not only in terms of processing but also the cost. It is important to note here that performance of organic materials cannot compete with single crystal silicon and in fact it not required too rather it is better to search for some other alternate and cost effective applications.

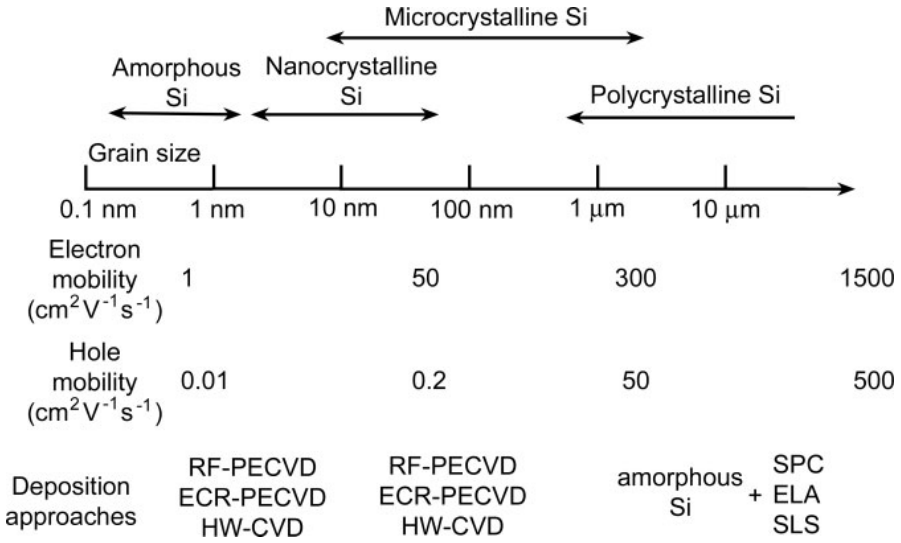

Figure 1.1 Grain sizes and carrier mobilities of Si films with various crystallinities grown via dry processes. Abbreviations: RF-PECVD, radiofrequency plasma-enhanced chemical vapor deposition; ECR-PECVD, electron cyclotron resonance plasma-enhanced chemical vapor deposition; HW-CVD, hot-wire chemical vapor deposition; SPC, solid-phase crystallization; ELA, excimer-laser annealing; SLS, sequential lateral solidification. Reproduced with Permission,[1] Copyright 2007 WILEY-VCH.

Although the performance of the amorphous silicon having the mobility of 1 cm^2/Vs (**Figure 1.1**), which is much below to that of single crystal silicon; however, they serve to be an excellent candidate for their wide use in display technology as backplane circuitry, Radio frequency identification (RFID) tags, smart cards etc. Till date, the techniques widely accepted for depositing thin films of amorphous silicon utilizes conventional chemical vapor deposition, moreover, at the same time much progress have also been made in the development of inorganic materials with even higher mobilities.[1] However, in spite of all the progress made in inorganic semiconductors, they cannot justify low-cost, large scale flexible circuits as deposition procedures should be simplified and the overall device processing cost needs to be reduced.

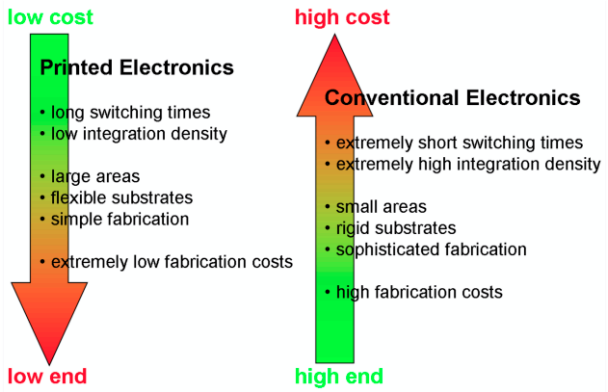

Figure 1.2 Comparison of printed electronics and conventional electronics.[2]

Considering the above issues, organic semiconductors, especially conjugated polymers offer various merits for the production of low cost flexible/printed electronics (**Figure 1.2**). This can be gauged by the researches conducted in the area of organic semiconductors to compete with the amorphous silicon technology.[3] Unique advantage of organic semiconductors over amorphous silicon lies in the fact that they can be synthesized with varying functionalities to be suitable for particular applications, where amorphous silicon technology lags.[4] It is important to note here that actual goal of the organic electronics is not to compete with crystalline silicon technology, but to replace amorphous silicon technology and other beneficial applications through unique properties of organic semiconductors in other fields.[5,6] **Figure 1.3** shows some typical devices made in the recent past utilizing organic semiconductors.

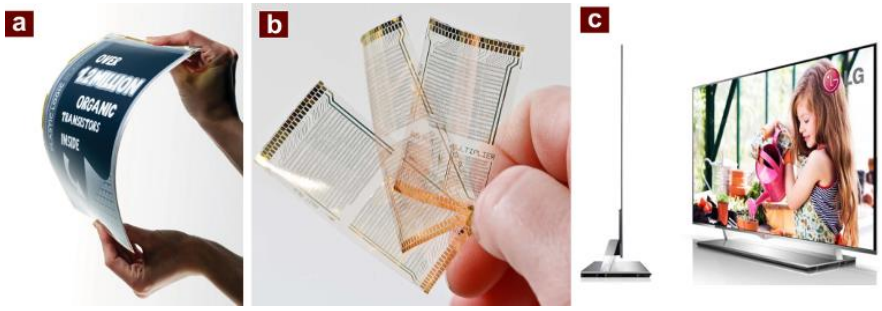

Figure 1.3 Photograph of (a) Flexible electrophoretic ink display containing 1.2 million OFETs [source: plastic logic]; (b) 8-bit microprocessors on plastic foil, Reproduced with permission,[7] Copyright 2012, IEEE; (c) OLED TV from LG electronics.[8]

Particularly amongst organic semiconductors, conjugated polymer offers various advantages over small organic molecules in terms of solution processability and mechanical flexibility, however, performance of conjugated polymer for electronic devices stringently depends on many parameters such as morphology, molecular weight, interface etc. due to their one-dimensional nature (conjugated backbone). A typical recent example of such class of materials is recently developed high performance organic semiconductor material poly[4-(4,4-dihexadecyl-4H-cyclopenta[1,2-b:5,4-b']dithiophen-2-yl)-*alt*-[1,2,5] thiadiazolo[3,4-c]pyridine] (PCDTPT) is shown in the **Figure 1.4**, where the performance of this conjugated polymer was enhanced remarkably when polymer chains were oriented in the desired channel direction. In this perspective, development of easy solution based procedures to deposit oriented conjugated polymers will offer various advantages over other widely used procedures such as spin coating, zone-casting, doctor blade coating etc. This thesis is going to primarily focus on development of new solution based orientation technique floating film transfer method (FTM) and their potential applications, precisely organic field effect transistors (OFETs) and will be discussed in the subsequent chapters.

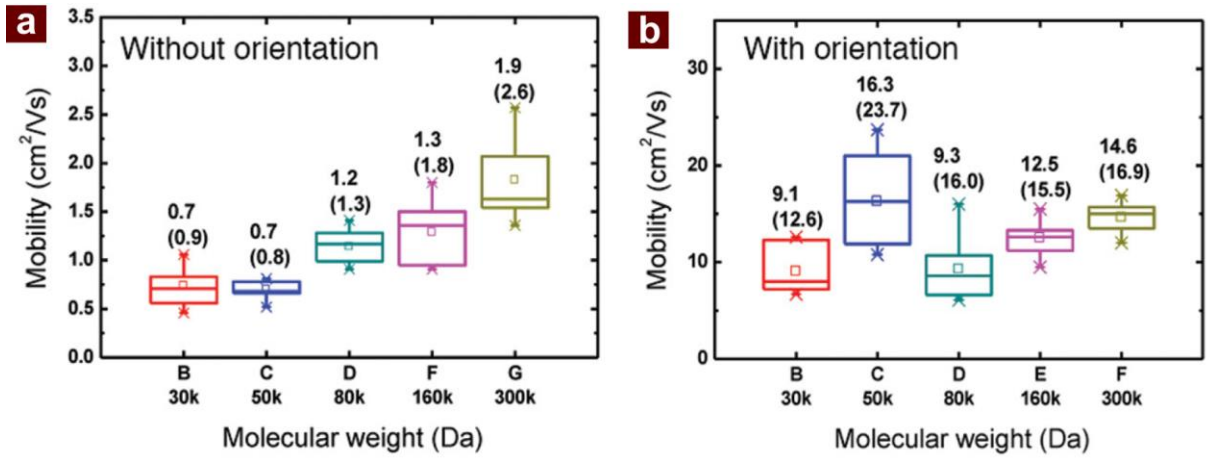

Figure 1.4 Mobility of PCDTPT OFETs after annealing at 200 °C. The mobility value and the value in parentheses represent mean and maximum values obtained from 10 independent OFETs. (A) Devices fabricated by drop casting. (B) Devices fabricated by slow drying in the tunnel-like configuration. The horizontal lines in the box denote the 25th, 50th, and 75th percentile values. The error bars denote the 5th and 95th percentile values. The open square inside the box denotes the mean value. Reproduced with Permission,[9] Copyright 2014 WILEY-VCH.

1.2 Theory of Conjugated Polymers

Polymers are referred to chains of connecting monomer repeat units. In general polymers, the carbon atoms connecting these monomer units are sp^3 hybridized and form 4 σ bonds with adjacent atoms. Such σ bonds in these types of polymer offers no electrical conductivity, and widely used as an insulating materials. However, conjugated polymers have the backbones adjoining carbon atoms that are sp^2 hybridized and valence electrons resides in the p_z orbitals along orthogonally to other 3 σ bonds and 1 π bond. These alternating p_z orbitals are delocalized along the polymeric

backbones and form 1-dimentional electronic band and the electrons belonging to this band under any under can possesses metallic or semi-conducting nature. Chemical structure of some very common conjugated polymers is shown in **Figure 1.5**.

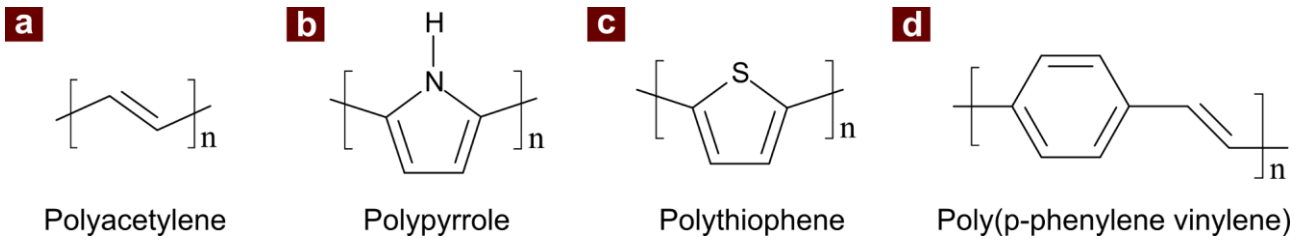

Figure 1.5 Chemical structure of some well-known conjugated polymers.

In general these conjugated polymers do not possess intrinsic charge carriers but the charge carriers can be supplied by partial oxidation (p-type doping) or by partial reduction (n-type doping), which introduce charged defects such as polaron, bipolaron and solitons.[10] According to band theory, the phenomenon about the doping induced changes can be understood as shown in **Figure 1.6**. By analogy to inorganic semiconductor, the highest occupied band is called valence band (VB) and lowest unoccupied band is called conduction band (CB). Basically the difference between these two bands (bandgap (EG)) decides the nature of the material to be conductor, semi-conductor or insulator. Electrons needs certain amount of energy to move from VB to CB.[10,11] For metals, the CB overlaps with the VB (EG =0) and the electrons in the CB become electrically conductive. Conjugated polymers do possess a narrow bandgap (Figure 1.2 (b)) and doping can change their band structure in both the way by either taking electrons from VB (p-type doping) or adding electrons to CB (n-type doping).

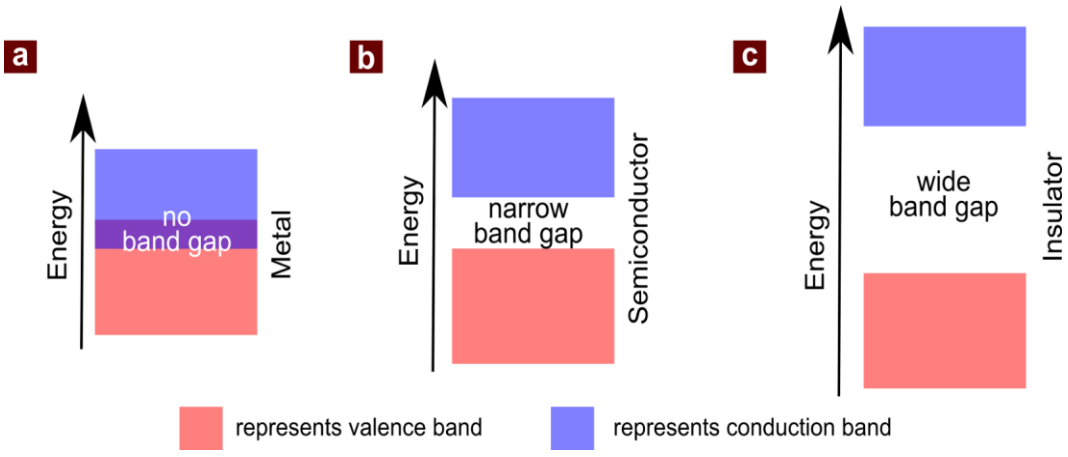

Figure 1.6 Schematic represents energy gaps in (a) metal, (b) semiconductor and (c) insulator.

When an electron is added (removed) to the bottom of CB (from top of VB) of conjugated polymer (**Figure 1.7**), the CB (VB) ends up being partially filled and radical anion (cation), termed as polaron is created.[12] The formation polaron causes the injection of states from the bottom of the CB and top of the VB in the EG. A polaron carries both charge (1/2) and charge (e^-). Addition (removal) of a secondary electron on a chain already having a negative (positive) polaron results in the formation of bipolaron (spin-less) trough dimerization of two polarons with a degenerate ground state (i.e. two equivalent resonance forms), like *trans*-polyacetylene, the bipolaron can further lower their energy by dissociating into two spin-less solitons at one half of the gap energy.[12]

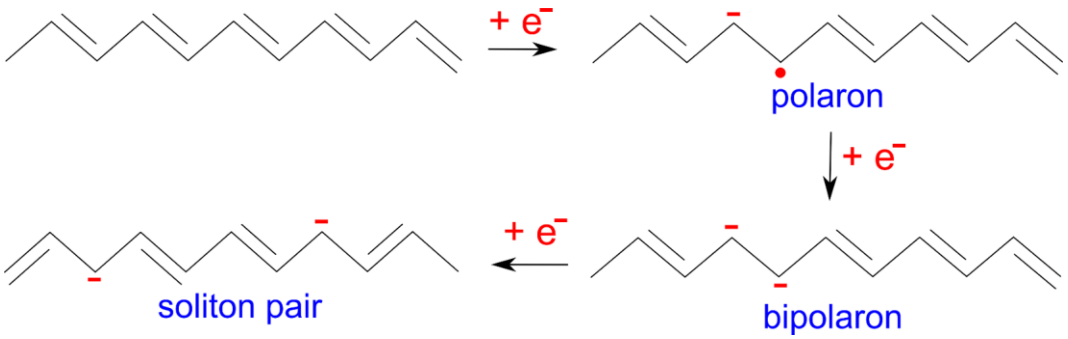

Figure 1.7. Schematic showing the formation of polaron, bipolaron, soliton pair on a *trans*-polyacetylene chain by doping.

Doping can be performed in conjugated polymers in several ways as discussed below

Chemical Doping: Conjugated Polymers can be either partially oxidized (reduced) by electron acceptors (donors).[13]

Electrochemical Doping: Conjugated Polymers can be Owing to the extensive conjugation of π-electrons, conjugated polymers can also be easily oxidized (*p*-doping) or reduced (*n*-doping) electrochemically with the conjugated polymer acting as either an electron source or an electron sink. In particular, the doping reaction can be accomplished by applying a DC power source.[14]

Photo-doping: Conjugated Polymers can be also doped by the irradiation with a light beam of energy greater than their EG could promote electrons from the valence band into the conduction band.[15]

Charge-injection Doping: Charge carriers can be injected into the bandgap of conjugated polymers can be applying an appropriate potential on the metal/insulator/conjugated polymer multilayered structure.[16] This will be discussed in detail in the following section 1.5.

1.3 Background Research and Motivation

Importance of the growing interest of the scientific community in the area of organic electronics is to develop low cost organic electronics devices implementing facile and low cost techniques, which could be only feasible when high mobility semiconductors can be solution processed at large scales. In this term the solution processable conjugated polymers (CPs) seems to be a promising candidate to provide next generation electronics as improvement in mobility of CPs seems to be reaching 10 $cm^{-2}/V.s$.[17] Enhancement in the mobility of CPs is highly dependent on the morphology of the CPs owing to their inherent one-dimensionality. The mobility of CPs can be highly improved by aligning the CPs in 3-D space, thereby inducing crystallinity in the 3-D reducing the inter-chain and intra-chain resistances and increasing the π-π stacking. Another intriguing problem lying with the solution processed CPs is towards the fabrication of oriented multilayered architectures without affecting the underlying layers. In recently developed methods for the orientation of CPs, fabrication of multilayered oriented films seems to be highly cumbersome especially towards the protection of underlying layers. To solve these issues, it is highly desired to develop novel low cast, highly efficient solution casting techniques in which large scale oriented thin films of CPs can be prepared by solution procedure and a method where thin films could be independently prepared and then possibly transferred on to the desired substrate.

Previously, our group has proposed and developed a novel method named as Floating Film Transfer Method (FTM),[18] where a floating thin film is first casted on the hydrophilic liquid substrate. This solid thin film is then transferred on to any desired substrate for its characterization as well as for applications in electronic devices with improved device performance.[18] In order to have multilayered thin films of CPs, conventional spin coating and other solution based procedures needs orthogonal solutions to avoid any kind of morphological and compositional damages occurring from the subsequent layer deposition. However, through FTM, it was also demonstrated that such films had least impact of the top layer coating on to the underlying bottom layers which is one of the very important requirements in order to have devices with multilayered architectures.[19] Subsequently in following research it was also found that FTM has the ability to induce unidirectional orientation of liquid crystalline (LC) conjugated polymers.[20] LC polymers, therefore, show the tendency to align their backbone structures along a preferred direction once they meet certain temperature range if they are of thermotropic LC nature and when they (in solvent) meet slow evaporation at certain concentration. Subsequently this method was applied for many conjugated polymers to form oriented film and later applied to electronic devices showing anisotropy in OFET and organic light emitting diodes.[21,22]

In order to have large area implementation of organic electronics, undoubtedly, there is a need for development of solution casting method aiming towards,

1. Solution based procedure
2. Capable of fabricating oriented films
3. Minimum material loss in comparison to other solution based procedures

4. No need of sophisticated instrument
5. Ease of handling
6. Thickness of the film can be easily controlled

Taking the above advantages into the consideration there was huge scope for the development of this novel method to solve the many unknown issues related to this procedure and their ability and application towards the development of anisotropic electronic devices utilizing CPs with improved device performance. Such as the basic factors of casting conditions which influences the orientation of conjugated polymers. Understanding the role of different polymer backbone in orientation intensity and how such orientation can improve the transport characteristics. Therefore the motivation lies to carry out the development of this method and to demonstrate the various features of this procedures and the same has been conveyed in the subsequent chapters.

1.4 Orienting Conjugated Polymer

Controlling the morphology of the conjugated polymers play a key-role in deciding the performance of the Organic electronic devices.[23,24] Owing to inherent 1-dimentionality of conjugated polymers, transport properties can be easily enhanced if the main-chain backbone can be oriented in one direction, which can lead to anisotropic charge transport. In general, large scale orientation of conjugated Polymers can be understood by two way: a) the preferred alignment of main-chain of conjugated polymers from the substrate, b) the length scale of the preferential alignment. The preferred alignment of the conjugated polymers on the substrate is crucial as this impact the transport performance significantly whereas length scale of orientation is highly important for realizing the dense array of devices for practical application.

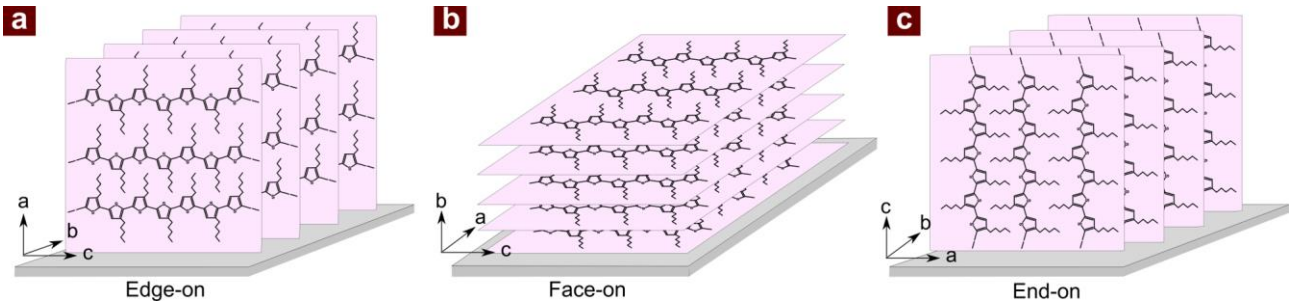

Figure 1.8 Schematic illustration of different types of orientation. (a) Edge-on, (b) Face-on, (c) End-on. The a-axis, b-axis and c-axis represents alkyl stacking, π-stacking and conjugation direction, respectively.

The schematic illustration of different kind of preferential orientation conjugated polymers adopt in their thin film is shown in **Figure 1.8**. The polymer backbone can take three different preferential arrangement edge-on, face-on and end-on. In edge-on orientation, the conjugated

backbone axis and π-stacking axis lie in-plane of the substrate. Whereas alkyl-stacking direction lie normal to the substrate plane. Contrary to this face-on orientation has conjugated backbone axis and alkyl-stacking axis parallel to the substrate having π-stacking axis normal to the substrate. It is well known that high carrier transport is believed to occur along the conjugated backbone direction and in π-stacking direction, whereas alkyl side chains act as insulating barriers leading to lower mobilities in alkyl stacking direction.[25] It has been well understood that in OFET, charge transport takes place at the interface of insulator in few nm of active layer.[26] In this regard, edge-on orientation is highly suitable for OFETs which needs high in-plane transport. On the other hand, face-on orientation is desirable for devices needing high out-of-plane transport such as organic photovoltaics (OPVs). [27,28] In the literature very little is reported about the end-on orientation of conjugated Polymers and their related transport where polymer backbone direction can be normal to the substrate,[29–31] which can give the highest out-of-plane transport properties a promising geometry for OPVs.[32]

A number of methods to induce orientation in conjugated polymers has been demonstrated in recent past. On the basis of these orientation procedure these method can be categorized in to 3 different ways. First way is to use of shear forces to induce orientation by mechanical means, such as mechanical rubbing, friction transfer technique.[33] Second way is to utilize orientation ability of conjugated polymers in solution phase and last. Utilizing the orientation ability of the substrate to align the CPs as guest on these substrate.

The basic quantitative characterization of orientation of conjugated polymers in thin films involve polarized spectroscopic techniques such as polarize absorption spectroscopy, polarized emission spectroscopy. Some other techniques such as polarized Raman spectroscopy, polarized Fourier transform infrared spectroscopy are also suitable. However, for detailed orientation of the crystallite in their thin films involve sophisticated characterization such grazing incidence X-ray diffraction and electron diffraction measurements.

1.5 Organic Field Effect Transistor

Now a days, transistors are the basic element/building block of modern circuitry, and are used as either signal amplifiers or on/off switches. The field effect is a phenomenon in which the conductivity of a semiconductor changes due to the application of an electric field normal to its surface.[34] This is carried out by applying an electric field in a configuration analogues to parallel plate capacitor, where one plate can be considered as gate (metal) and another plate is semiconductor, separated by a dielectric material (insulator). The electric field is applied utilizing gate in the device and the direction of the electric field depend on the kind of potential applied on gate terminal. As shown schematically in **Figure 1.9**, OFETs are composed of three terminals, gate, drain, source with conductor type nature as well as a semiconductor layer (also called active layer) and an insulator layer (working as dielectric layer between semiconductor layer and gate terminal). The dielectric can be made of a variety of dielectric materials, through SiO_2 grown on doped silicon

wafer is a common choice. However, in order to realize pure flexible OFETs there are huge number dielectric materials available now as days.[35]

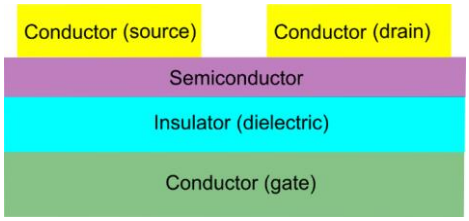

Figure 1.9 Schematic diagram of organic field effect transistor.

As discussed the gate terminal and semiconductor layer is isolated by a insulator serving the purpose of dielectric of the capacitor. The two terminals source and drain are separate but physically connected to the semiconductor layer with separation, and the region between them is called the channel. The geometric region between source and drain terminal "channel" is very important parameter and defined by the channel width (W) and channel length (L). Channel length is the separation between the electrodes and channel width is the width of electrodes.

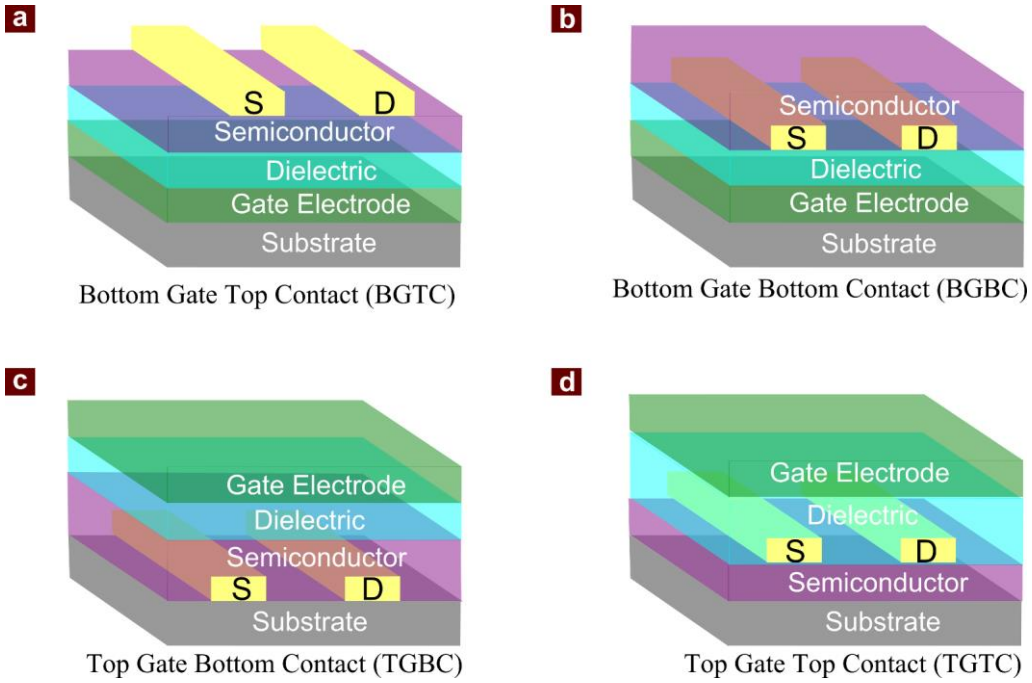

Figure 1.10 Schematic Illustration of four different possible geometry of OFETs.

The geometry of the OFETs usually varies based on the fabrication method, however, in principal it can go under four kind variations as shown in **Figure 1.10**, which meets the above requirements discussed. However, the most commonly used geometry is bottom gated architectures. This

geometry is common, since most of the researchers utilize SiO_2 grown on doped silicon wafers which is easily available for purchasing for preliminary studies related to evaluation of organic semiconductor (OSC) performance.

The gate dielectric layer play an important role since its capacitance, which is actually determined by its thickness permittivity, influence the number of charge carrier to be generated in the semiconductor, concomitantly the operating voltage of the device. To satisfy the need of low voltage operating gate dielectric which can be solution processed, transparent and can be utilized as flexible substrate as well, a number of new organic gate dielectric has been developed in the recent past, simultaneously.[35–38] The advantage of organic dielectric is that it can be solution processed in order to fabricate top gated devices without harming the metal electrodes and semiconductor layer unlikely to other inorganic dielectrics which needed to be deposited using sputtering and thermal evaporation.

The operation of OFET can be explained with the simplified energy level diagram, which involves the Fermi level (E_F) of the source and drain electrodes and the HOMO level of the organic semiconductor as illustrated in **Figure 1.11**. Since the OSC are intrinsically undoped, their E_F lies in between the bandgap and aligned with the E_F of the metallic source and drain, in absence of any applied voltage. Therefore in this state the charge injection is hindered due to potential barrier between the source and energy levels of the OSC.

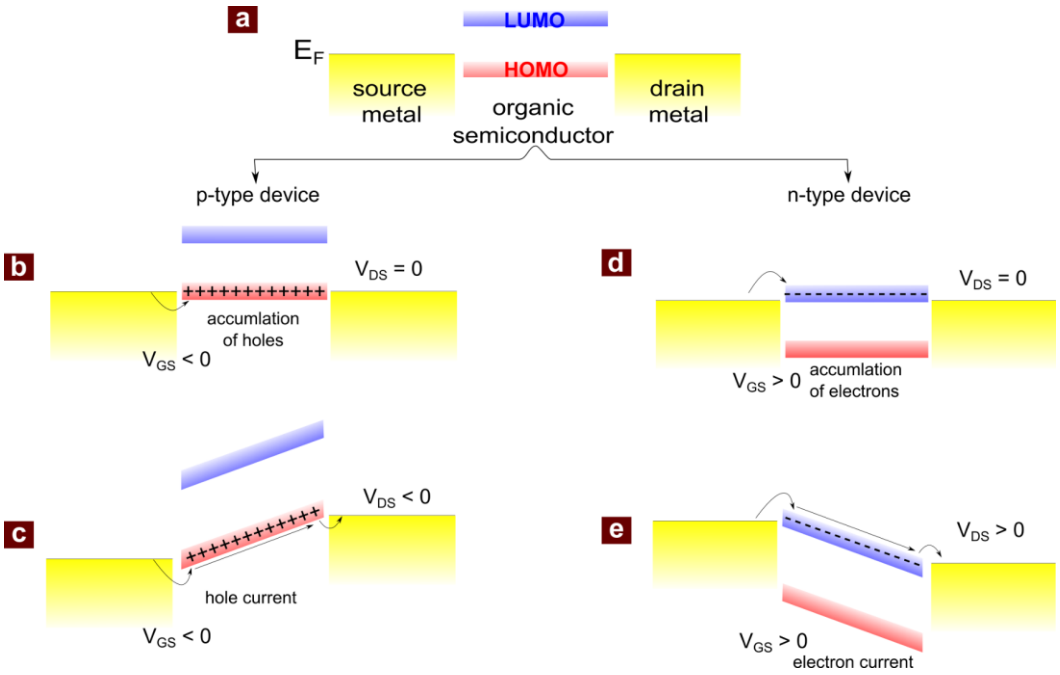

Figure 1.11 Schematic illustration showing simplified energy band diagram of OFET.

Operation: When a negative (positive) voltage VGS between the gate and source terminal is applied, the holes (electrons) are accumulated at the interface of the OSC/dielectric, and the E_F shifts towards the HOMO (LUMO) in case of p-type (n-type) OSC. This accumulation of charge carriers forms a conducting path having the having low resistivity between the source and drain electrodes. Then, holes (electrons) can be transported by applying negative (positive) drain to source voltage to make the transistor in ON state.

OFET Characteristics: As already mentioned, OFET could be simply considered as parallel plate capacitor, where one plate is the conducting gate electrode and the other semiconducting channel physically separated by the dielectric medium, therefore the density of the charge carriers (n) in the semiconducting channel can be easily controlled by applied the appropriate V_{DS}, i.e. negative for p-type and positive for n-type.

The average applied voltage at distance x then given by the difference of the average channel potential with respect to the gate potential acting on the other side of the dielectric, and the total charge carriers density at a distance x is $Q_T(x)$ on capacitor plate is given by Eq. 1.

$$Q(x) = (V_{GS} - V(x) - V_{TH})\, C_i \tag{1}$$

Where C_i is the capacitance of gate insulator per unit area and $V(x)$ is the voltage at distance$x$.

Considering the drift current density (J) in the channel is governed by ohm's law, which is the product if the electrical conductivity (σ) and electric field (E) is given by the Eq. 2.

$$J = \sigma\, C_i \tag{2}$$

Since σ is the product of unit charge (q), change carrier density (n) and mobility (μ), the Eq. 2 can be written as Eq. 3.

$$J = qn\mu E \tag{3}$$

Substituting $E = -\frac{dV}{dx}$, $qn(x) = Q(x) = \left(V_{GS} - V(x)\right) C_i$ in Eq. (3) with neglecting the negative sign, Eq. 3 can be written as Eq. 4.

$$J = (V_{GS} - V(x) - V_{TH})\, C_i \mu \frac{dV}{dx} \tag{4}$$

Eq. (4) can also written as Eq. (5)

$$Jdx = C_i \mu (V_{GS} - V(x) - V_{TH})\, dV \tag{5}$$

Since J is constant we, integrating from source to drain length ($x = 0$ to $x = L$), where L is the channel length.

$$J \int_0^L dx = C_i \mu \int_{V(0)}^{V(L)} (V_{GS} - V(x) - V_{TH})\, dV \tag{6}$$

Since $V\ (0) = 0$ and $V\ (L) = V_{DS}$, on solving the Eq. (6), we get Eq. (7).

$$J = \frac{C_i \mu}{L} (V_{GS} - V_{TH}) V_{DS} - \frac{{V_{DS}}^2}{2} \tag{7}$$

By substituting $J = I_{DS} W$, it should be notes that J for channel is A/cm since $Q(x) = charge/cm^2$

$$I_{DS} = \frac{C_i \mu W}{L} (V_{GS} - V_{TH}) V_{DS} - \frac{{V_{DS}}^2}{2} \tag{8}$$

This Eq. (8) is valid under the two assumptions. First, the transverse electric field in the channel induced by V_{GS} is much larger than the field along the channel due to V_{DS}. This also called Shockley's gradual channel approximation of junction field effect transistor.[39] The validity of this approximation hold true if the thickness of the dielectric is too less than the channel length. Second assumption is that the mobility is constant all over the channel.

Since for linear region $V_{DS} \ll (V_{GS} - V_{TH})$ and $\frac{{V_{DS}}^2}{2}$ in the Eq. (8) will be very small therefore can be neglected and I_{DS} in linear region (I_{DS}^{lin}) can be simplified as Eq. (9).

$$I_{DS}^{lin} = \frac{C_i \mu W}{L} (V_{GS} - V_{TH}) V_{DS} \tag{9}$$

Similarly in saturation where $V_{DS} \geq (V_{GS} - V_{TH})$, the I_{DS} in saturation region (I_{DS}^{sat}) can thus be described by Eq. (10).

$$I_{DS}^{sat} = \frac{C_i \mu W}{2L} (V_{GS} - V_{TH})^2 \tag{9}$$

1.6 Organization of the Thesis

This thesis has been organized as follows by summarizing the research work carried out the total eight chapters.

First chapter provides a brief introduction to the concerns related to the present state-of-art in organic electronics, background problems related to thin film fabrication techniques for conjugated polymers and aim of this present work. Theory dedicated to the basic knowledge of conjugated polymers, merits and demerits of orienting conjugated polymers with existing techniques and working principle of organic field effect transistor.

Second chapter presents brief outline of the conjugated polymers utilized in the present thesis, their film processing with especial emphasis on the introduction to the orientation technique with emphasis on floating film transfer method, various characterization procedures for oriented film, device fabrication and analysis.

Third chapter introduces the basic studies pertaining to fundamental understanding of the orientation characteristics of conjugated polymers taking non-regiocontrolled poly(3-hexylthiophene) (NR-P3HT) as representative example and optimization of floating film transfer method using this conducting polymer.

Fourth chapter of the thesis deals with the characterization of oriented films of widely investigated amorphous conjugated polymer poly(3-hexylthiophene) which was obtained by utilizing the results obtained in 3rd chapter.

Fifth chapter focuses on some more important issues related to orientation of the amorphous NR-P3HT with an aim to further improve their orientation and charge carrier capabilities by blending them with crystalline CP material.

Sixth chapter introduces the orientation characteristics of high performance crystalline thiophene based conjugated polymer pBTTT-C14 and investigation on the charge transport characteristics by fabricating OFETs using this CP as active semiconducting material.

Seventh chapter demonstrates some advantages and potential features of orientating conjugated polymers with floating film transfer method in terms of layer-by-layer coating with parallel and orthogonal architectures using two different CPs.

Finally the eighth and last chapter of this thesis present the brief conclusion of the whole work summarizing main results with guidelines for future work and their perspectives.

Chapter 2: Materials and Methods

2.1 Materials

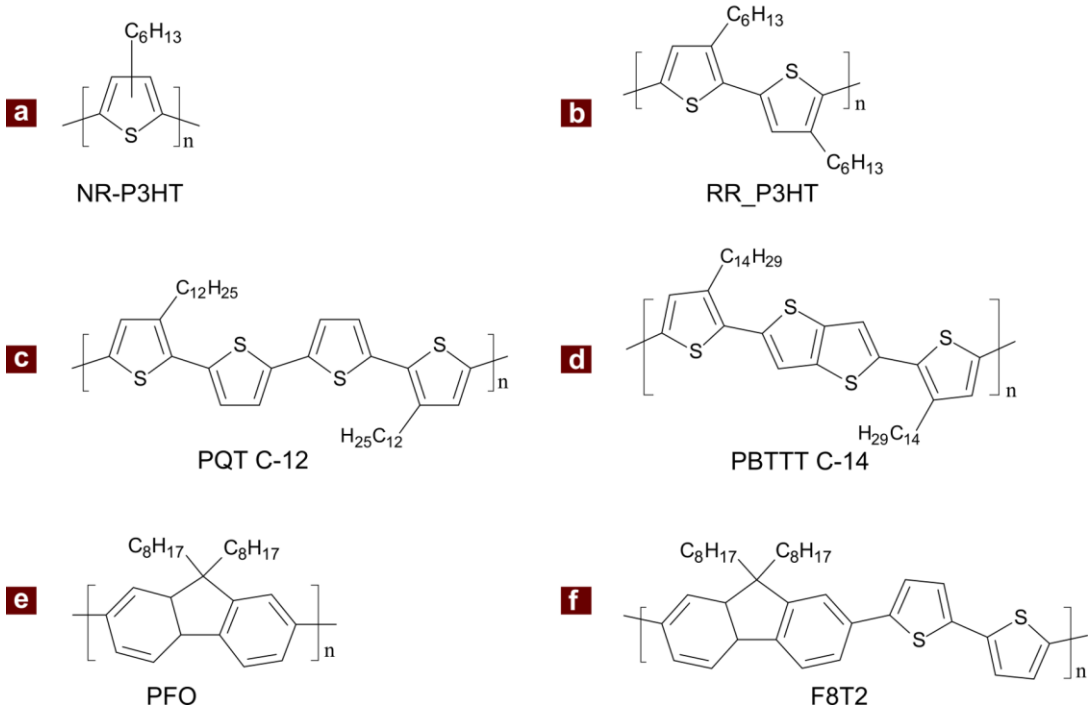

Figure 2.1 Chemical Structure of different π-conjugated semi-conducting polymer with their abbreviation used. (a) Non-regiocontrolled poly(3-hexylthiophene), (b) Regioregular poly(3-hexylthiophene), (c) Poly(3,3‴-didodecyl-quarterthiophene), (d) Poly[2,5-bis(3-tetradecylthiophen-2-yl)thieno[3,2-b]thiophene], (e) Poly(9,9-dioctylfluorene) and (f) Poly(9,9-dioctylfluorene-alt-bithiophene).

Regioregular poly(3-hexylthiophene), (RR-P3HT), non regio-controlled (NR-P3HT) and Poly(3,3‴-didodecyl-quarterthiophene) (PQT-C12) were chemically synthesized according to the literature procedures.[40–42] The synthesized conjugated polymers were purified by Soxhlet extraction as per earlier publications. [43,44]

NR-P3HT was synthesized through $FeCl_3$-mediated oxidative polymerization. In this procedure, NR-P3HT was be synthesized with 3-hexylthophene monomer and $FeCl_3$ as oxidizing agent in chloroform followed by de-doping with aqueous ammonia and treatment with aqueous EDTA in order to remove chloride and Fe^{3+} ions of the catalyst. Finally obtained powder was purified by Soxhlet extraction with hexane in order to remove low molecular weight impurities.[41] Chemical structure of the obtained nR-P3HT was confirmed by ^{1}H-NMR. In particular, the regioregularity of NR-P3HT was estimated by integrated area corresponding to the α-methylene in the ^{1}H-NMR spectra and found to be about 80%.[45] In general when spin coated, it exhibit the field-effect mobility of 10^{-5} cm^2/Vs.[46,47] Owing to the reduced regioregularity, thin films of this polymer exhibits less crystalline which provide flexibility in comparison to regioregular P3HT.

Regioregular (RR) P3HT was synthesized through the reported procedure.[40] In comparison to NR-P3HT, RR-P3HT possesses high mobility due to high interdigitation.[48] Poly(3,3‴-didodecyl-quarterthiophene) PQT C-12 is a liquid crystalline conjugated polymer which offers good stability towards oxygen doping together with high field effect mobility (> 0.1 cm^2/Vs) after annealing it above their liquid crystalline.[42] Poly[2,5-bis(3-tetradecylthiophen-2-yl)thieno[3,2-b]thiophene] (PTTT C-14 or PBTTT) is a liquid crystalline rigid rod polymer widely studied in the last one decade due to its high air stability as well as consistent high mobility (>0.1 cm^2/Vs) after annealing to their phase transition temperatures (also called terrace phase and ribbon phase).[49]

Poly(9,9-dioctylfluorene) (PFO) was synthesized by Suzuki-Miyaura coupling as reported,[22,50] and is a rod-like like in nature, highly used for optoelectronic devices due to its highly efficient photoluminescence, thermal stability, and high solubility in organic solvents. It is also a well knows thermotropic liquid crystalline which exhibit a nematic transition at high temperature. Poly(9,9-dioctylfluorene-alt-bithiophene) (F8T2) is an alternating copolymer and was synthesized by Suzuki coupling as reported,[21,50] This has several favorable properties making it convenient for studying optoelectronic properties.

2.2 Deposition Techniques

2.2.1 Spin coating

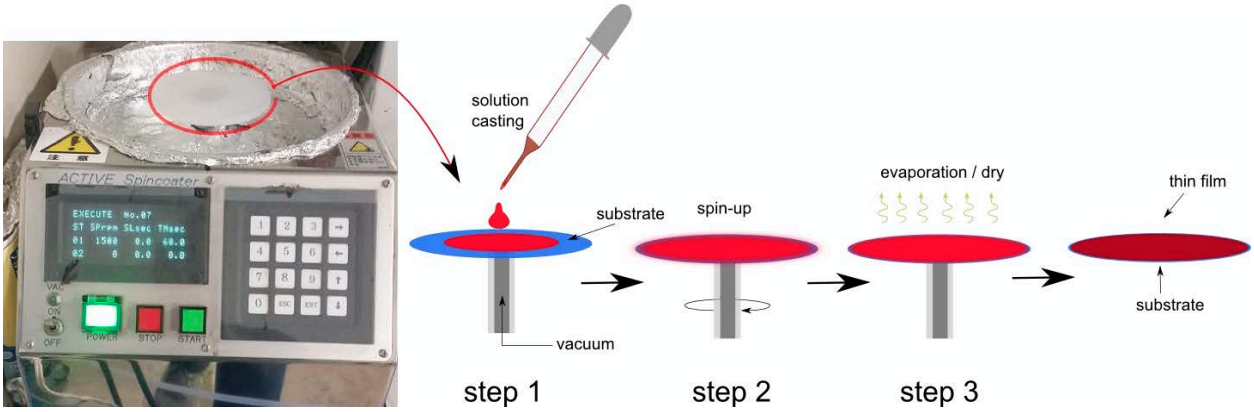

Figure 2.2 Photograph of the spin coater utilized and schematic illustration of related steps.

Spin coating is one of the widely used techniques to deposit thin films of different organic materials such as conducting, semiconducting and insulating. In this procedure, First small amount of solution of organic material is dropped on the different kind of substrates (depending on the requirement) followed by the spinning the substrates are rotated. The rotation speed, acceleration, time can be easily managed by manually programming the spin coated before running it. The

picture of the spin coater utilized for spin coating with the related steps involved in thin film fabrication is shown in **Figure 2.2**.

2.2.2 Floating Film Transfer Method (FTM)

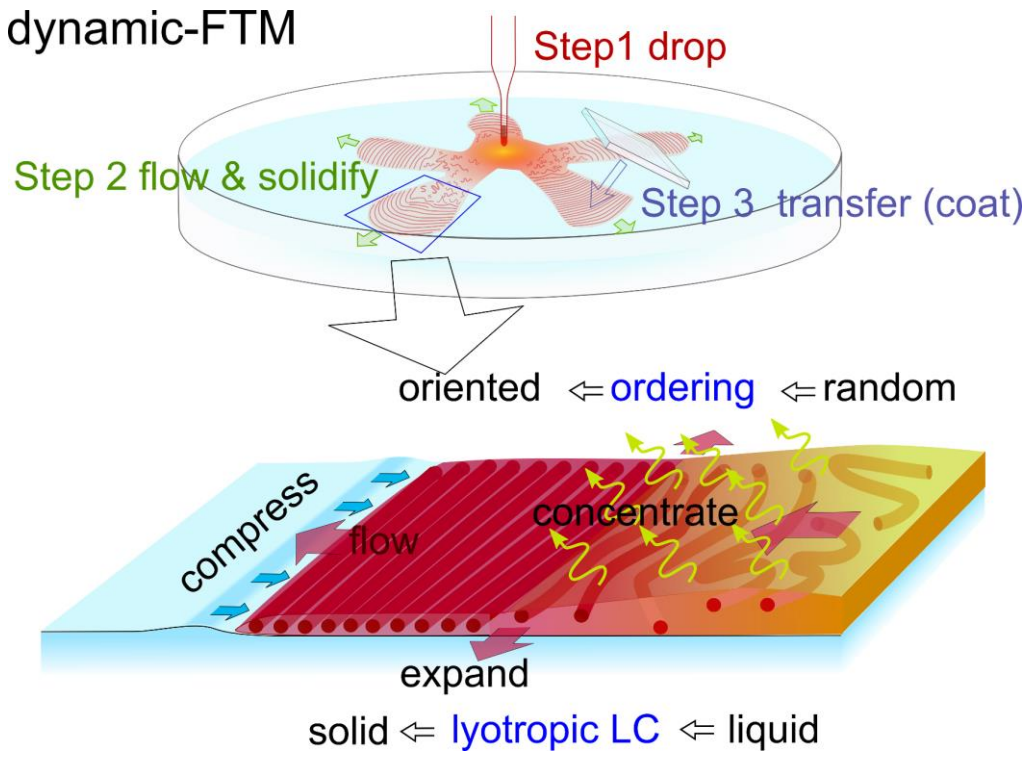

Figure 2.3. Schematic Illustration of Floating Film Transfer Method and associated mechanism.

This deposition method presents a novel strategy to make π-conjugated polymer film utilizing floating-film transfer method (FTM) developed 8 years ago in our laboratory headed by Prof. Keiichi Kaneto and Prof. Wataru Takashima in 2009 , in which we first make thin floating-films on suitable hydrophilic liquid as casting substrate.[18,21] The ensuing floating-film can be effortlessly transferred to the desired solid substrate without harming the surface morphology of the underlying layers. Although this procedure is somewhat similar to Langmuir Blodgett (LB) method, there is no surface pressure application to make a compact and oriented monolayer on the liquid surface. It has been found that on optimizing certain casting parameters this technique ends up being extremely valuable for the orientation of most of the π-conjugated polymers with larger domains in the order of several centimeters by dynamic casting.[51] The detail mechanism for optimization of orientation is described in later section (chapter 3). This dynamic-FTM is highly facile and cost effective method to provide a highly oriented thin film with solution based process,

and this casting method has very less material wastage as compared to other techniques for obtaining oriented thin films. At the same time, multilayer device fabrication with controlled thickness is also possible utilizing multi-coating with dynamic-FTM which is demonstrated in **Chapter 7**. Various process from casting of floating films of conjugated polymers to stamping procedure on the desired substrate is shown schematically in **Figure 2.3**.

In this procedure, Gradually vaporizing solvent after the expansion of dropped semiconductor solution on the liquid-substrate semi-statically provides a floating-film in FTM (represented as static-FTM).[51,52] In contrast, simultaneous solidification of the floating-film along with the expansion of the semiconductor solution is dynamically occurred just after dropped on the liquid surface (represented as dynamic-FTM), leading to a concentric orientation of conjugated polymers. PQT C-12 as well as polyfluorene derivatives can easily oriented by this procedure.[20] The solvent volatility of semiconductor solution, generally, identifies the types of FTM. Namely, under ambient condition static-FTM occurs after the complete expansion of semiconductor solution utilizing high boiling point solvents like chlorobenzene because of their slow evaporation. In contrast, for dynamic-FTM semiconductor solution prepared in the relatively low boiling point solvents (such as chloroform, tetrahydrofuran and dichloro-methane) leads to simultaneous film expansion and solidification as illustrated in **Figure 2.3**.

**Since use of high boiling point solvent is known to provide static floating film, for the rest of the manuscript, wherever FTM is referred is basically dynamic-FTM which is capable of inducing macroscopic orientation.*

2.2.3 Thermal Evaporation in Vacuum

Thermal Evaporation Unit requires a very low pressure of the order of 10^{-6} mbar to deposit metals. Such a low pressure is required in order to have a longer mean free path λ_m. Besides pressure it depends on various other physical parameters as shown in the **Eq. 2.1**.

$$\lambda_m = \frac{RT}{\sqrt{2}\pi d^2 N_A P} \tag{2.1}$$

Where the symbols have the following physical significances.

P = Pressure of the system, R = Gas Constant, T = Temperature, N_A = Avogadro's number and d = diameter of the gas particles in meters.

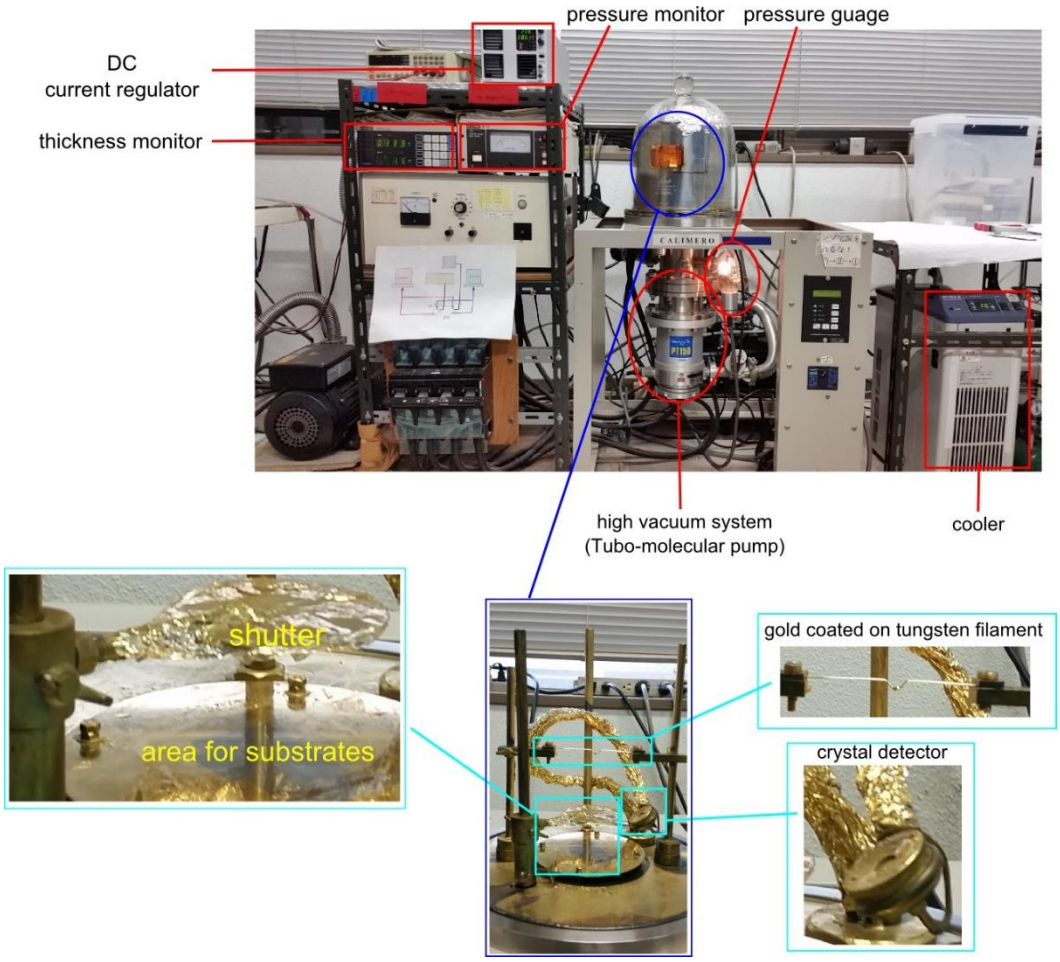

Figure 2.4 Laboratory assembled thermal evaporation system while deposition of metal electrodes.

Eq. 2.1 shows that the mean free path will increase if the pressure inside the thermal evaporation unit chamber will be less. Hence minimum pressure of the chamber is required in order to deposit materials with minimal scattering. A very low pressure of 10^{-6} mbar can be achieved by cascaded evacuation of the deposition chamber. For this, two pumps are utilized, turbo molecular pump backed by a rotary pump. **Figure 2.4** shows the photograph of the high vacuum system with thermal evaporator. The different components which play important role in this deposition if metals are also magnified. As shown gold wire was wrapped in the tungsten filament followed by placing the substrates. The shutter was also used to prevent any direct deposition of any greasy impurity lying on the gold which evaporates prior at lower temperatures. Once the sufficient pressure was reached, the tungsten filament was heated through joule's first law (power of heating $\propto$ [current]^2 $\times$ resistance). Since the temperature to melt the tungsten is too high (~3400 °C) as compared to gold (1064 °C), gold evaporation starts just around the melting point. The current was increased very slowly so that the melted gold wire adhered properly to the tungsten filament before evaporating from the surface. The thickness and rate of deposition was also being monitored by the crystal detector. Once the thickness monitor starts showing the deposition, shutter was opened and thickness measurement was reset to zero and, rate of deposition was slowly increased to the desired

amount depending on the requirement and kept steady at that rate until the thickness reaches to the desired amount. Then the input current was removed and substrates were left in the high vacuum for 15 minutes before taking it out in order to cool them under high vacuum.

2.3 Fabrication and Evaluation of OFET

2.3.1 Substrate Preparation

Highly doped Silicon (Si) wafers with 300nm of silicon dioxide (SiO_2) were utilized to fabricate bottom gate transistors. The wafer was cut into small pieces ~ 1 cm^2. To prevent the formation of any scratch on the insulator side (SiO_2) which serves as the interface for active layer was kept on soft cloth for cutting. The substrates were thoroughly cleaned by ultrasonic baths of Acetone, Isopropanol for 10 minutes each followed by annealing at 100 °C. The SiO_2 as gate dielectric insulator (capacitance = 10 nF/cm^2).

Since depending on the case / requirement the surface of the SiO_2 was made highly hydrophobic depending on the case. The two different kind of hydrophobic preparation of SiO_2 utilized in the coming chapters are CYTOP^{TM} and octadecyl(trichloro)silane (OTS) was carried out. For CYTOP coating on SiO_2, CYTOP was spin coated at 3000 rpm for 120 seconds followed by annealing at 150 °C for 1 hour, resulting in to highly stable hydrophobic surface and the resultant capacitance was found to be 8 nF/cm^2. For OTS preparation, SiO_2 substrates were immersed in closed glass container having freshly prepared 10 mM solution of OTS in octadecene at 100 °C for 3 hours followed by thorough washing in ultrasonic bath with a mixture of dehydrated cyclohexane and chloroform (7:3) twice for 10 minutes. The substrates were annealed at 150 °C for 30 minutes prior to their use.

2.3.2. Deposition of Active Layers and Electrodes

Deposition of the active layer (semiconductor) was carried out with spin coating method for isotropic films and FTM for anisotropic film followed by metal electrode (source and drain) deposition. Masking and deposition procedure of electrodes are shown in the photograph with the schematic flow diagram.

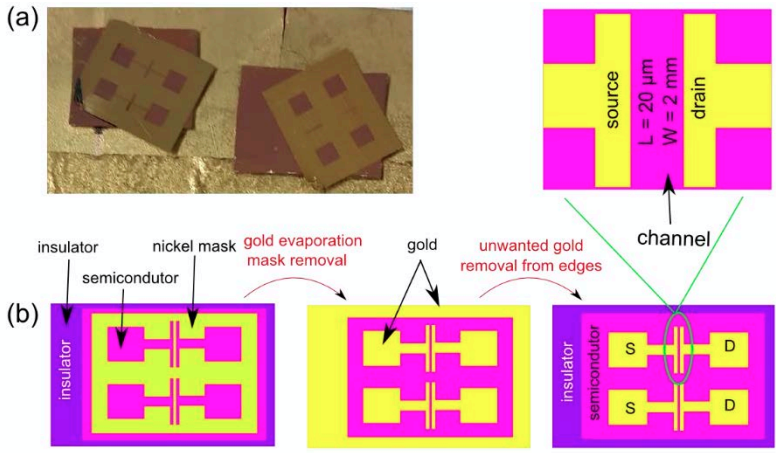

Figure 2.5. (a) Photograph of nickel shadow mask on substrates and (b) schematic flow diagram of the various steps from semiconductor layer to full ready OFET for measurement. The channel length 'L' and width 'W' was 20 µm and 2 mm, respectively.

As shown schematically the unwanted semiconductor and metal layer outside the mask were removed in order to avoid any kind of leakage from the edges while operating the OFETs. The source, drain and gate terminal were connected with 50 µm thick gold wire with the help of silver paste for electrical characterization.

2.3.3 OFET measurement and characterization

The OFET measurement performed in normal vacuum as shown in shown in **Figure 2.6**. The connection to the source, drain and gate electrodes with gold wire (50 µm diameter) was done in an acrylic box as shown. The box was then head of the vacuum chamber followed by evacuating the chamber by pump. Thereafter the OFETs output and transfer characteristics were measured with computer controlled two channel electrometer (Keithley 2612). Saturation field effect mobility (µ), threshold voltage (VTH), on/off ratio was then extracted from the transfer characteristics.

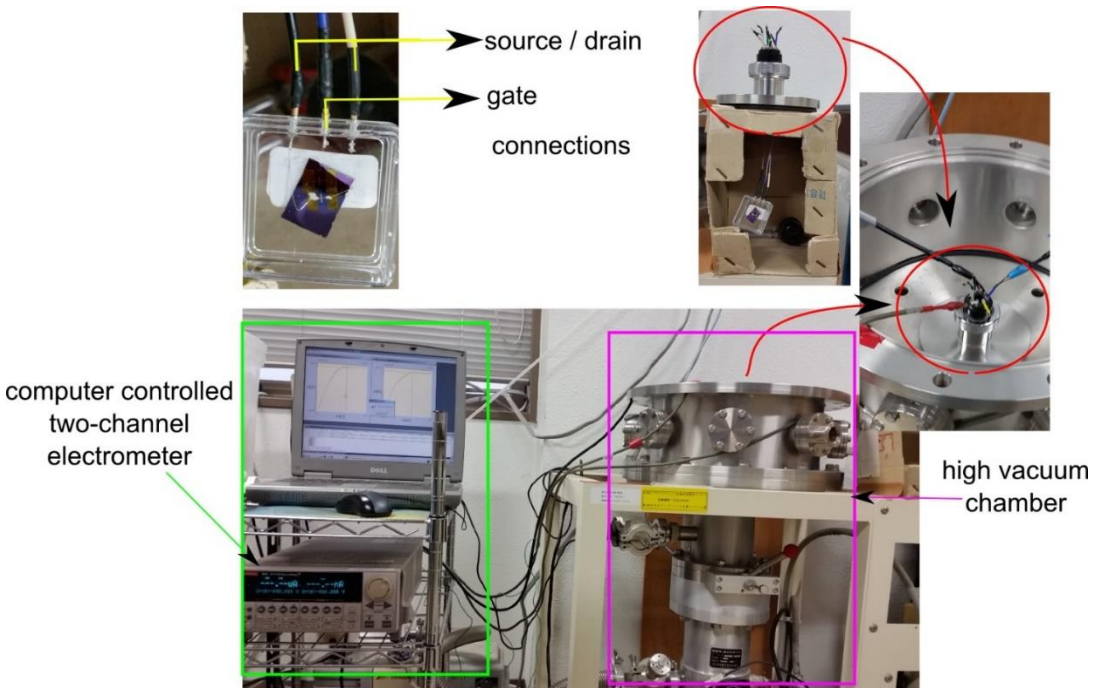

Figure 2.6 Pictures of the OFET measurement system.

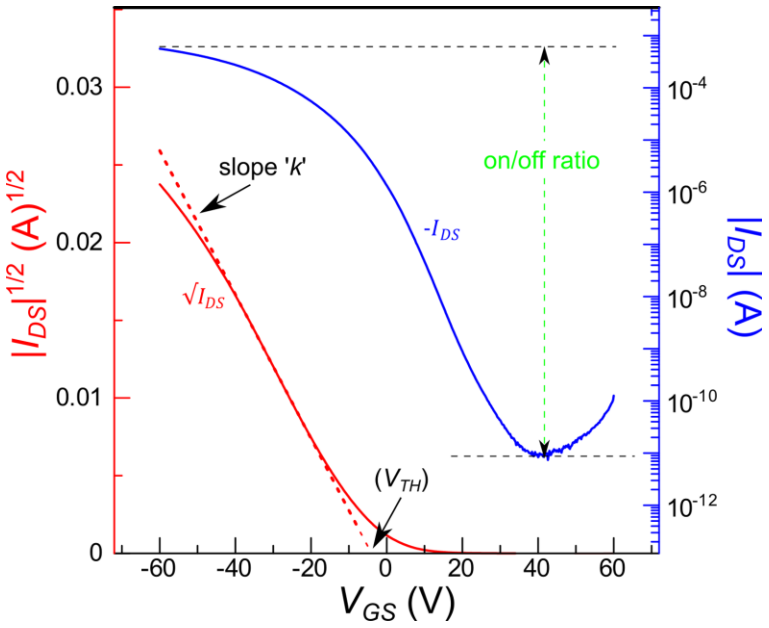

Figure 2.7 An example of transfer characteristics of OFET with PBTTT as active layer.

The graph of transfer characteristics is shown in **Figure 2.7** with $I_{DS}\ vs\ V_{GS}$. Calculation of mobility and threshold can be obtained by the $\sqrt{I_{DS}}\ vs\ V_{GS}$ The Eq. 2.2 represents the value of drain current in saturation regime I_{DS}^{sat}. By solving the equation for mobility 'μ' we get it depends on the slope 'k' of the drain current vs gate voltage. The value μ can be easily obtained by the Eq.

2.5 and the slope can be determined as shown in **Figure 2.7**. Since all the term except slope is constant therefore for a given configuration of transfer characteristics the slope determines the mobility of semiconducting material. The value of the threshold voltage can be determined by the intersection of the line with the V_{GS} axis shown in **Figure 2.7**.

$$I_{DS}^{sat} = \frac{C_i \mu W}{2L} (V_{GS} - V_{TH})^2 \tag{2.2}$$

$$\sqrt{I_{DS}^{sat}} = \sqrt{\frac{C_i \mu W}{2L}} (V_{GS} - V_{TH}) \tag{2.3}$$

$$k = \sqrt{\frac{C_i \mu W}{2L}} \tag{2.4}$$

$$\mu = \frac{2k^2}{C_i \frac{W}{L}} \tag{2.5}$$

2.4 Characterization of Thin Films

2.4.1 Ultraviolet-visible spectroscopy

Ultraviolet-visible (UV-Vis.) spectroscopy relates the absorbance of any solid or liquid samples in the ultraviolet and visible spectral region. Molecules containing π electrons or non-bonding electrons can absorb part of the incoming incident energy to excite these electrons to higher antibonding molecular orbitals. Solution and solid-state electronic absorption spectra provide important information regarding various electronic transitions and has been widely used for the characterization of color bearing molecules in terms of determination of various useful parameters like optical band gap, molecular aggregation and molecular orientation. Schematic illustration of the processes involved in the measurement of electronic absorption spectrum is shown in Figure 2.8 (a). In order to get polarized absorption spectra, A Glan-Thomson polarizer was used in between the incident beam and sample during the measurement. This polarized absorption spectrum was used for the quantitative estimation of optical anisotropy in terms of the optical dichroic ratio (DR).

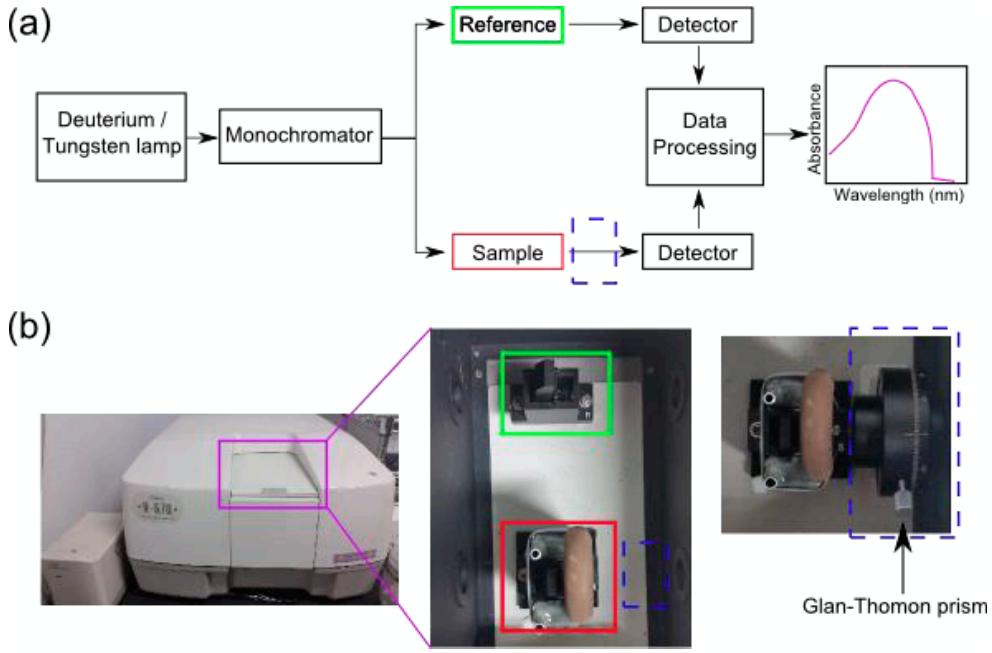

Figure 2.8 (a) Schematic representation of the processes involved in absorption spectroscopy and (b) Photograph of the UV-vis spectrophotometer (JASCO V-750) with magnified chamber. For polarized absorption measurement Glan- Thomson prism is shown in blue-dash square in (a) and (b).

DR was estimated from the polarized electronic absorption spectrum using the Eq. 2.6.

$$DR = \frac{\text{Maximum Absorption}_{\parallel} \text{ at } (\lambda max_{\parallel})}{\text{Absorption}_{\perp} \text{ at } (\lambda max_{\parallel})} \quad (2.6)$$

Where $(\lambda max_{\parallel})$ is the wavelength at which parallel absorption spectrum has the maximum absorption.

2.4.2 X-ray Diffraction (XRD)

X-ray Diffraction is an important measurement tool to determine the microstructural organizations of macromolecules in the polymer films. In order to receive the stacking behavior from the diffracted lattice planes out-of-plane diffraction patterns are enough. Out-of-plane diffractions are in general less surface sensitive owing to large incident angles. The process of Out-of-plane XRD measurement is shown in **Figure 2.9** and was carried out with Rigaku X-ray diffractometer available in Univ. of Kitakyushu (instrumentation center). Since achieving single crystal like films of polymers is difficult and transport properties depends on the organization of macromolecules in space of the thin films. Moreover, since the polymers are highly anisotropic it is of utmost importance to determine the orientation of conjugated polymer in thin film.[53] Such studies needs

to be done with in-plane grazing-incidence XRD (GIXD), in-fact when the incident rays are close just above the critical angle it becomes more surface sensitive and refracted beams are stronger.[53]

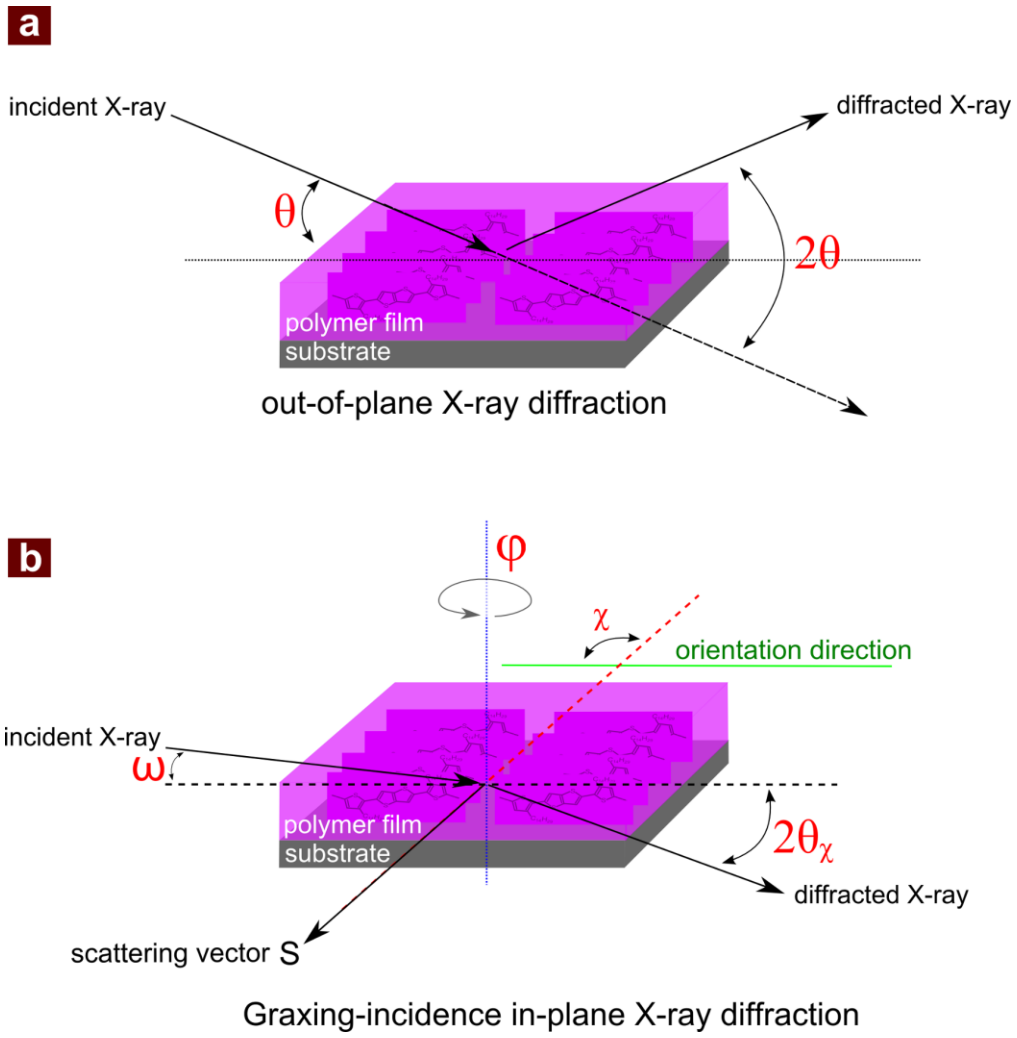

Figure 2.9 Schematic geometry of out-of-plane XRD (a) and in-plane GIXD (b).

In-plane GIXD measurement were carried out with Rigaku smart lab, following the geometry. Since in our case the films were highly anisotropic prepared by FTM, we followed the above geomtery as shown in **Figure 2.9** (b).[54] The incident angle was kept just above the critical angle of the sample. For studying the anisotropic nature arrangements of the molecules was determined by measuring the scattered intensity (χ). The scattering vector 'S' is the the difference between the scattered and incident X-ray vector and positioned in parallel with film surface. The angle between the vector S and orientation direction 'χ' was kept constant throughout the φ – 2θχ scan. In general such measurements usually take place at high intensity synchrotron light sounces, however high crystalinty of the thin films and layer-by-layer films fabrication capability of our FTM method enabled us to carry our these measurements in with our normal laboratory based X-ray source.

2.4.3 Fourier Transform Infrared Spectroscopy

Fourier Transform Infrared Spectroscopy (FT-IR) is an analytical technique used to characterize the materials, where it measures the energy associated with various kind of vibration of the constituent bonds resulting from incident infrared radiations. [55] The characteristic bond vibrations upon infrared radiation identifies structural components with their spatial arrangements based on molecular finger printing.[56,57] FTIR spectroscopy in this thesis was used to characterize the molecular orientation using polarizer and changing the angle of incident beam to record the polarize FTIR spectrum. FTIR spectrum was recorded on a JASCO FT/IR 4100. Here it is important to note that the background measurement must be carried out with the same angle (0° or 90°) at which the intended sample measurement is required. Figure 2.10 represents the set up and its inset exhibit the arrangements used in this work.

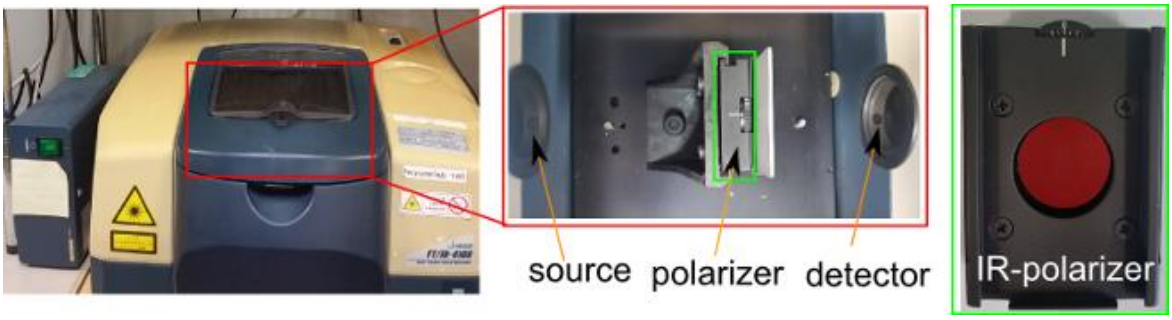

Figure 2.10 Photograph of the polarized FT-IR measurement arrangement for this work.

2.4.5 Atomic Force Microscopy

Figure 2.11 Photograph of the JEOL-SPM used for AFM measurement

Atomic force microscope (AFM) is a very high resolution scanning probe microscope. It is extensively used to see determine the surface topography of any thin films. One of its advantages is that there is no strict need of conducting sample to probe the surface. The basic idea of AFM imaging is mapping the differential force between the tip and the sample. When the of tip of the AFM cantilever is brought near to the sample surface, forces between the tip and the sample lead to a deflection of the cantilever. These forces can be mechanical, electrostatic, van der walls, chemical or capillary forces etc. In order to detect the binding of tip, a laser beam is focused on the back side of the cantilever which reflects it to a position sensitive photo detector. The photo detector converts this change in an electrical signal. Atomic force microscopic (AFM) images were taken under tapping mode by JEOL SPM5200 with Olympus probe (OMCL- AC200TS-C3). The photograph of the AFM measurement set up is shown in the **Figure 2.11**.

2.4.5 Polarized Raman Spectroscopy

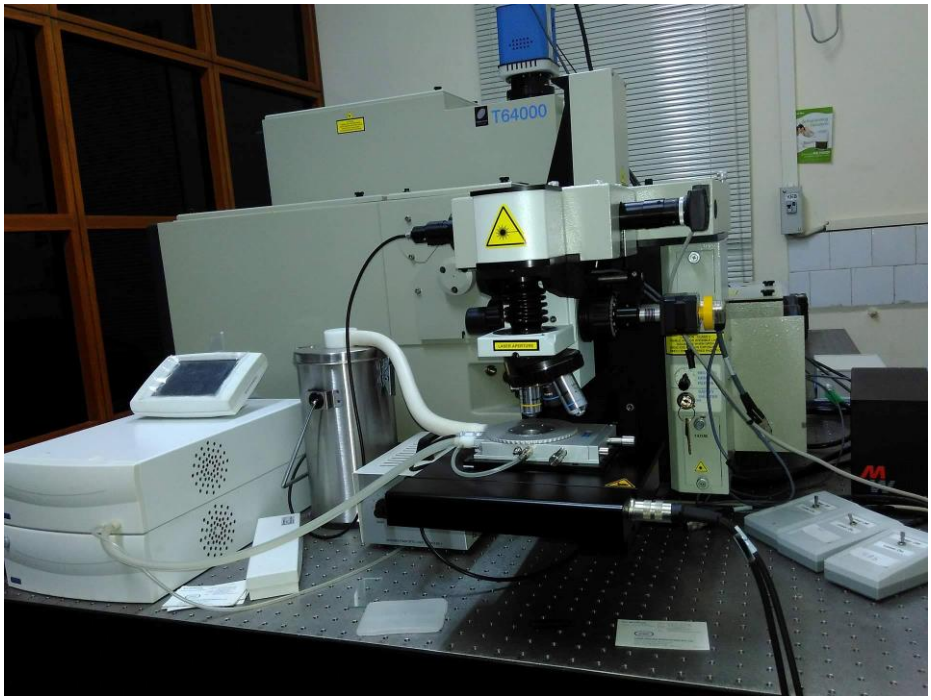

Figure 2.12 Photograph of the Polarized Raman Setup.

Raman spectroscopy is vibrational spectroscopy, like infrared spectroscopy where Raman bands arise from change in polarizability of the molecules. In this sense, When the uni-axially polarized laser beam is incident parallel to the orientation direction the beam passing along the orientation direction will encounter majority of bond vibration resulting in to high interaction between the polarized laser beams.[58,59] Polarized Rama spectrum was measured by inserting a polarizer between the sample and the spectrometer, which allows the Raman polarisation angle to be set by the user. Flexibility in the measurement lies in the sense that polarisation of the laser beam can also be kept in its normal state, rotated by desired angles by inserting polarising optics between the laser

and the sample. Polarized Raman spectra provide information about the molecular orientation as well as symmetry of the bond vibration under consideration. It has been widely used in order to get valuable information pertaining to the molecular shape and molecular orientation in a variety of systems like ordered materials, polymers and liquid crystals. Polarized Raman Spectroscopy was carried at Raman Research Institute Bangalore, India with Horiba Jobin Yvon T64000 Micro Raman using a He–Ne Laser operating at $\lambda = 632.8$ nm and at constant power of 1.8 mW throughout the measurements. The sample stage was rotated against polarization direction of the incident beam and Raman spectra was recorded at every 30º between 00º to 90º.

Chapter 3: Influence of Casting Parameters and Polymer Backbones structures on their Orientation Characteristics in FTM

3.1. Introduction

Uniqueness of organic conducting polymers lies in the aspects like molecular anisotropy, solution processability and fabrication of thin as well as thick films providing them versatile technological potential. Especially, for organic electronic device applications, film morphology has always been of much interest as it affects the overall device performance [60]. In order to fabricate organic electronic devices based on π-conjugated polymers, spin-coating is one of the most preferred techniques because of its ease for the thin film fabrication. On the other hand, it leads to very large (>90 %) material wastage during the thin film fabrication[61,62]. Essentially, semiconducting properties of π-conjugated polymers arise from the π-electrons which are delocalized along the polymer backbone and can adopt the various conformations depending upon processing conditions [63,64]. Therefore, the control of π-conjugated polymer morphology is highly required to attain the improved device performance.

In our group, we have developed a novel strategy for thin film fabrication of π-conjugated polymers utilizing floating-film transfer method (FTM), in which we first make thin floating-films on suitable hydrophilic liquid as casting substrate[18,21]. The ensuing floating-film can be effortlessly transferred to the desired solid substrate without harming the surface morphology of the underlying layers. Although this procedure is somewhat similar to Langmuir Blodgett (LB) method, but there is no application of surface pressure to make an oriented monolayer on the liquid surface. It has been found that this technique ends up being extremely valuable for the orientation of most of the π-conjugated polymers with larger domains in the order of several centimeters by dynamic casting [51]. One dimensional nature in π-conjugated polymer offers the inherent capability of molecular orientation during self-assembly which depends on the number of factors such as their structural feature, solvent, temperature and film processing conditions. It is indeed a matter of in-depth discussion that amongst these which factor plays a dominant role for influencing orientation and mechanistic aspect that how they affect orientation [65]. In order to achieve maximum orientation in π-conjugated polymers, all of the dependent factors for orientation need to be investigated and optimized in detail. However, it was found that in spite of optimization of these film formation conditions in this method, the orientation intensity varies with the nature of conjugated polymers under investigations. Even under tuning the casting conditions, it was found that RR-P3HT shows very weak molecular orientation.

In this chapter, FTM has been used as a versatile method to prepare highly oriented thin films of CPs and orientation mechanism is discussed based on systematic experimental investigations. To accomplish this goal, two different kind of investigations were carried out, since both of the casting parameters and nature of the conjugated polymers plays an important role for getting highly oriented film. In the first part, investigations pertaining to the effect of controlling factors of the casting conditions was studied using non-regiocontrolled poly(3-hexylthiophene) (NR-P3HT) as a representative conducting polymeric material. NR-P3HT was selected for the present investigation owing to its facile solubility in chloroform in the wide range of temperatures. Effects of various controlling parameters such as concentration of the polymer solution, temperature of the liquid-substrate and polymer solution, viscosity of liquid-substrate, post-annealing temperature etc. have been systematically investigated. 2nd half this chapter deals with the investigation pertaining to the role of nature of the polymeric backbone on the orientation characteristics. For this purpose, four different kinds of conducting polymers from the thiophene family namely NR-P3HT, RR-P3HT, PQT C-12, PBTTT C-14 have been employed. The differential behavior in the orientation intensity in the conjugated polymers has been discussed by taking the macromolecular structures in to consideration.

3.2. Experimental Details

In this work, RR-P3HT, NR-P3HT, PQT-C12 and PBTTT-C14 having chemical structure as shown in the Figure 1 have been employed as the target thiophene-based conjugated polymers for investigating orientation characteristics in dynamic-FTM. PBTTT-C14 and dehydrated chloroform ($CHCl_3$) were purchased from Aldrich Co. Ltd. USA. Other conjugated polymers such as polymers, RR-P3HT, NR-P3HT and PQT-C12 were chemically synthesized according to the literature procedures.[41,40,42] All the synthesized conjugated polymers were purified by using EDTA or Soxhlet extraction as per earlier publications. [43,44] Regioregularity of the synthesized polymers have been estimated by 1H-NMR at aryl methylene region. [45,66] Polymer solution 1 % (wt/wt) was prepared by dissolving in dehydrated chloroform at respective temperature corresponding to liquid-substrate in order to fabricate the FTM films. Distilled water, Ethyl Glycol (EG) and Glycerol (GL) was used for preparing the hydrophilic liquid-substrate.

Electronic absorption spectra measurements and dichroic ratio was calculated as per chapter 2. Viscosity of the liquid substrate was tuned by mixing deionized water/ethylene glycol (Wt/EG)) or ethylene glycol/glycerol (EG/GL) in the optimized ratio. For estimating the viscosity of the mixture of hydrophilic liquids was calculated by double-logarithmic equations of Refutas.[67]

3.3. Results and Discussion

3.3.1. Influence of Casting Parameters

FTM is one of the facile casting/coating methods for the fabrication of oriented thin films. In the thus procedure, a thin floating film is first formed by dropping a very small amount (about 15uL) of conjugated polymer solution on a hydrophilic liquid-substrate followed by its transfer to a desired solid substrate. This stamping like procedure is similar to the Langmuir-Schaefer technique. The unique and key-feature in this casting procedure is to form the floating-film during concentration followed by its solidification dynamically. The compressive/expansive force offered by the liquid substrate while spreading the floating film along with the simultaneous solvent evaporation leads to the self-alignment. The compression/expansion behavior on liquid-substrate plays a role as shear force to promote the macromolecules orientation and could be responsible for providing oriented films as shown in schematic **Figure 3.1** (a). The main chain orientation was found tangential to the direction of propagation. The plausible reason for the molecular alignment during film formation can be understood considering the fact that when hydrophobic polymer solution starts propagating, viscosity of the hydrophilic liquid-substrate hinders it to propagate on it which acts as a compressive external force (viscosity) hindering the spreading of polymers, which promotes macromolecules alignment. The synergistic actions by both of the compressive force and the lyotropic liquid-crystal phase in dynamic-FTM should induces the polymer alignment tangential to spreading direction as shown in **Figure 3.1** (a). Moreover, Apart from viscosity, another possibility is the surface energy of components of liquid phase since it deals with the interaction between top molecular layers of hydrophilic liquid with that of hydrophobic polymer molecules which is also supposed to control the propagation of the polymer solution. Since hydrophobic polymer solution is same, therefore, surface energy of liquid phase seems to control the spreading of the polymer. Surface energy is basically surface tension per unit area, thus utilization of liquid phase composition with varying surface tension can also be used to control the spreading and therefore, thickness of FTM films. In this context surface tension varies in the order of water < EG < GL, therefore, binding force between glycerol and polymer will be highest leading to slowest propagation of FTM films. In this procedure, the polymer solution continuously concentrates by the volatilization of solvent leading to appearance of lyotropic liquid-crystal phase,[59] which promotes macromolecules self-alignment.

Oriented NR-P3HT FTM films were transferred on glass by stamping. The films which are tangential to the direction of propagation is parallel (||) whereas the direction of propagation is believed to be perpendicular (⊥) to the main chains. One can easily distinguish the parallel and perpendicular direction by naked eye looking on the FTM film through a linearly polarized film, which show deep colour when FTM films are parallel to polarizer and light colour when perpendicular to polarizer. A perusal of the polarized absorption spectra (**Figure 3.1 (**b))

corroborates a strong optical DR indicating the orientation in parallel and perpendicular directions in FTM film. Apart from the anisotropic optical absorption, there is distinctive spectral behavior for spin-coated and parallel FTM films of NR-P3HT. Spin-coated film shows a featureless absorption spectrum having λ_{max} at 480 nm a typical characteristics of amorphous NR-P3HT and associated with π-π^* electronic transition. On the contrary, parallel FTM film exhibits a red-shifted λ_{max} at 523 nm along with clear shoulder around 550 nm. This oriented assisted red-shift of λ_{max} is associated with extension of π-conjugation of polymeric main chain. The shoulder around 550 nm is has been assigned to be originated from O-O transition and known as vibronic side band. This red-shifted λ_{max} along with the clear vibronic side band very much similar to electronic absorption feature observed for regioregular P3HT.[68,69] This observation of the orientation in FTM film could be attributed to several factors such as concentration of polymer solution, viscosity, casting temperature and annealing temperature. These factors must be addressed amicably in order to obtain further understanding of orientation mechanism and for inducing large orientation reproducibly.

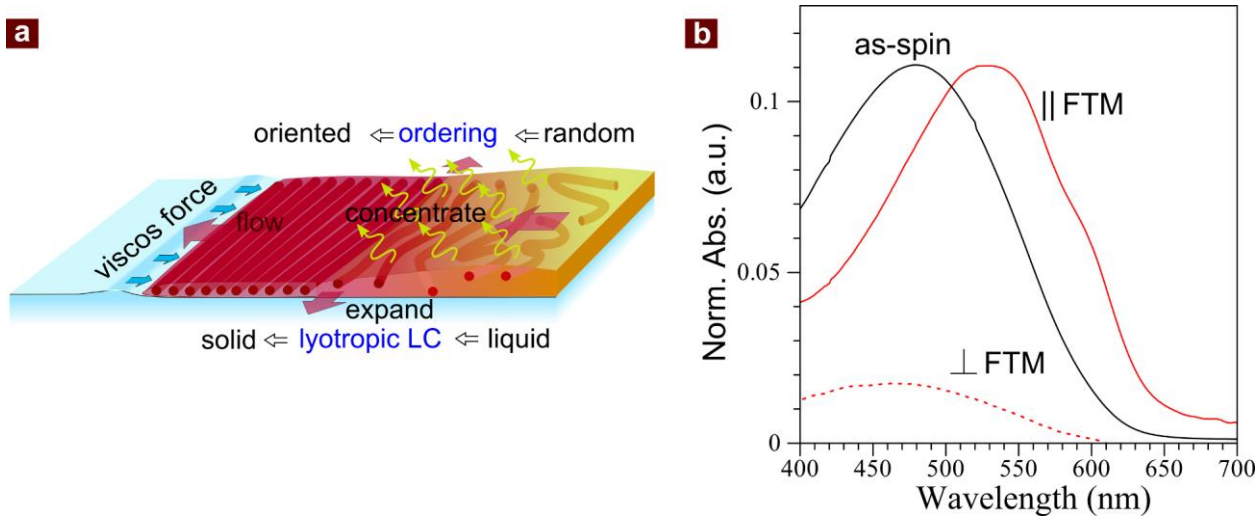

Figure 3.1 (a) Schematic illustration for orientation mechanism of floating-film formation process and (b) Normalized absorption spectra of spin coated (black) and polarized absorption spectra of highly oriented FTM film of NR-P3HT

Concentration of the polymer solution is an important factor for controlling the film orientation in FTM. An optimum concentration is, therefore, highly desired to attain the highest orientation of the polymer for dynamic-FTM. Polarized absorption spectra for different solution concentration as shown in the **Figure 3.2** (a) give the change in the orientation intensity. A red shifted absorption maximum (λ_{max}) along with clear vibronic shoulders can be seen when the concentration of NR-P3HT solution was increased from 0.3 to 1 % (w/w) suggesting the increase in the effective π-conjugation length of the polymer main chains.[68] Further increase in the

concentration up to 5 % (w/w) leads to not only the blue-shifted of λ_{max} but relatively less-defined vibronic shoulder also. The increase in DR of the solution concentration from 0.1 to 1 % (wt/wt) promotes the orientation then turned to decrease the orientation characteristics with further concentration of the polymer solution. These results suggest that, when the polymer concentration is too high, the solvent evaporation and the polymer solidification are too rapid to spread, hindering the polymers to expand and to generate a uniform floating-film on the liquid-substrate. On the other hand, for very low concentration, dropped solution parts easily spread on the whole surface before their solidification. These findings clearly reflects that the solution concentration is an important factor for the orientation of main chain for dynamic-FTM.

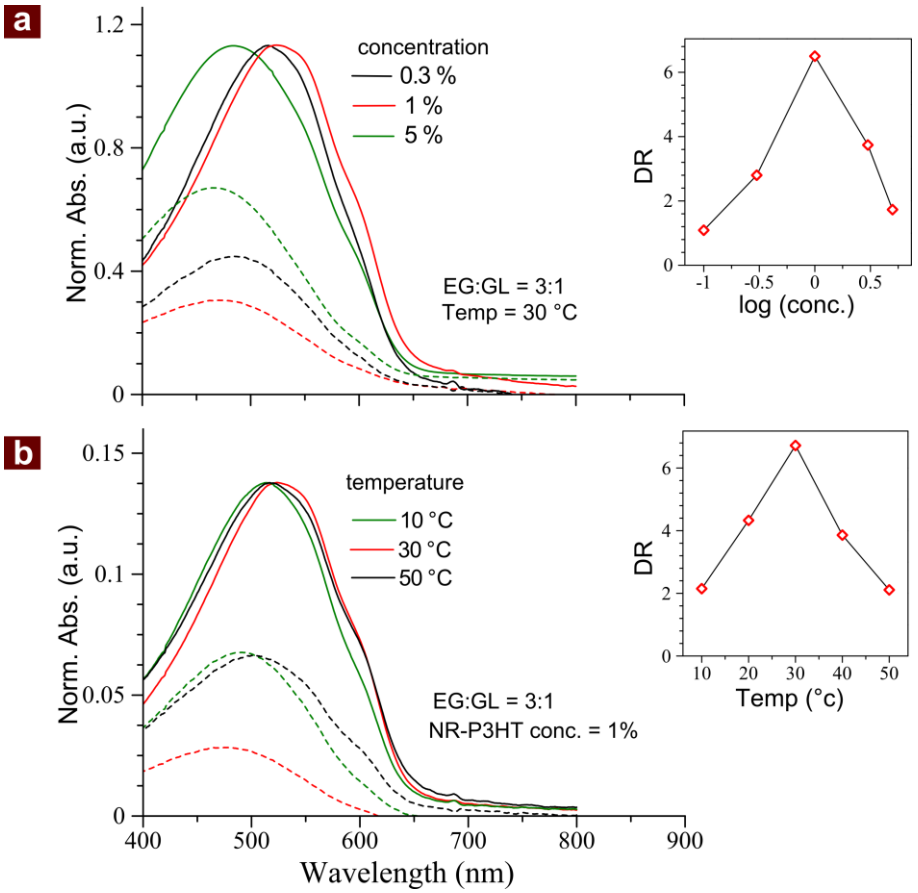

Figure 3.2 Polarized absorption spectra of NR-P3HT as function of polymer concentration (a) and (b) liquid substrate temperature. The insets in (a) and (b) shows the variation of DR. The values other two parameters is listed inside with pink color.

Temperature of the Liquid Substrate changes the evaporation speed of polymer solution as well as the viscosity. Therefore, the temperature of polymer solution and liquid-substrate plays a crucial role in controlling the molecular orientation in FTM. In the case for the polymer solution, at low temperature the polymer solution spreads wider due to take a long time to evaporate the solvent. Against this, at high temperature solvent evaporates rapidly providing a short time for spreading of polymer solution. Temperature of the liquid-substrate also affects the expanding

action of the polymer solution. As similar to the case for polymer solution, low temperature reduces the spreading speed with relative high viscosity, and high temperature provides the rapid expansion. Both the temperatures of polymer solution and liquid-substrate, therefore, are crucial factors for generating the film orientation in dynamic-FTM. Both temperatures should be comparable to attain the maximum possible orientation and the simplicity for analysis. Although, here we control the same temperature of liquid substrate and NR-P3HT solution owing to the high solubility of NR-P3HT at wide range of temperatures. However, it should be noted that controlling the temperature of the all polymer solution is sometimes difficult such as PBTTT C-14 is less solubility at low temperatures. Hence for such cases the temperature of the polymer solution can be ignored also.

Polarized absorption spectra of FTM films at different temperatures were measured in order to elucidate its implication on the molecular orientation of NR-P3HT films (**Figure 3.2** (a)). A perusal of this figure indicates not only the red-shift of λ_{max} but also the pronounced vibronic features in spectral shape upon increase in the temperature. The effect of temperature on molecular orientation is more clearly visible in DR as the orientation index. At 30 °C has been found to be optimum temperature for getting high DR, and lower or higher to this temperature leads to decrease the difference resultant DR value. A maximum DR of 6.8 was obtained on 30 °C liquid-substrate. A similar temperature dependent DR has also been reported in our previous work for π-conjugated polymer PQT C-12.[20] Therefore, molecular orientation can be achieved even in the non-regiocontrolled conjugated polymers like NR-P3HT by optimizing the temperature of polymer solution and liquid-substrate for casting.

Viscosity of the liquid-substrate basically acts as an external dragging force for the propagation of polymer solution, thereby affecting the self-organization of polymer. Viscosity of the liquid-substrate can be easily controlled by changing the mixing ratio of two different liquids with different viscosities. In common, we select three hydrophilic liquids, i.e. Wt, EG and GL as the base liquid. Standard viscosities are known as 0.79, 14.41 and 487.64 centistokes at 30°C for water, EG and GL, respectively. [67,70,71] Binary liquid mixtures, namely water/EG or EG/GL, can provide intermediate viscosities by tuning the mixing ratio for liquid-substrate. It has been observed that viscosity of the liquid substrate affects the spreading of the FTM film on the liquid-substrate and higher viscosity compress the polymer spreading to higher extent and vice versa, resulting in higher thickness of the floating film as shown in **Figure 3.3** (a). In the case of 100 % Wt, NR-P3HT solution spreads instantaneously almost on all over the area, which keeps on decreasing the spread area with increase in viscosity. These characteristics suggest that a dragging force hindering the FTM films to a very confined area resulting in thick films. This gives an approach to tune the viscosity of liquid-substrate for providing the optimum speed to generate the floating-film with higher orientation. Implication of liquid-substrate viscosity on controlling the molecular orientation was investigated by measuring the polarized absorption, The DR in this study was calculated and plotted as a function of viscosity. It was found that, when the viscosity of the liquid-substrates increased up to a certain threshold, it leads to more oriented films and orientation was found to decrease with further increase in the viscosity. At 30 °C as the casting temperature, a mixture of

EG/GL having the dynamic viscosity of 29.56 centistokes provided the maximum DR=6.8 in NR-P3HT film. This result also suggests that the viscosity of liquid-substrate is important factor for orientation in FTM. The optimum viscosity of liquid-substrate should vary with the polymer and possibly the molecular weight as their physicochemical characteristics.

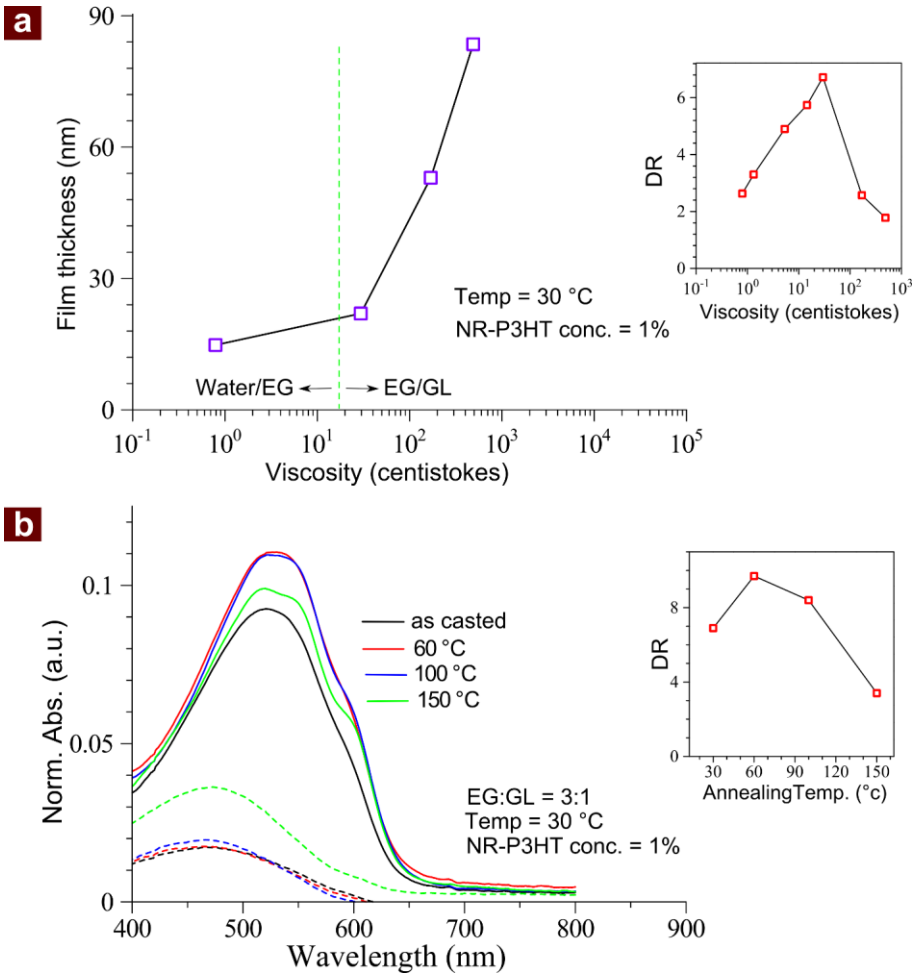

Figure 3.3. (a) Effect on film thickness upon varying viscosities and (b) Polarized absorption spectra of NR-P3HT as function of annealing. The insets in (a) and (b) shows the variation of DR. The annealing was performed on the films with highest orientation obtained from optimizing all the three casting parameters discussed above.

Post-annealing : Effect of temperature on the film morphology of π-conjugated polymers has been widely discussed as it induces red-shifts in optical absorption for P3HT and thiophene based π-conjugated polymers.[20] In spite of the fact that FTM induces molecular orientation in NR-P3HT films casted under ambient conditions, there is still might be the possibility of further molecular rearrangements owing to the rearrangements of macromolecules possibility with thermal conformations in side-chain part. To validate this argument, post-annealing of the oriented films at various temperatures was carried out in inert atmosphere. A perusal of this **Figure 3.3** (b) clearly corroborates that there is considerable increase in absorption coefficient (reflected by increased

absorbance at λ_{max} for film thickness of about 20 nm) for incident light source normal to the substrate. This could be attributed to the tendency of polymeric lamella structure to further orient normal to the glass substrate.[65] It can also be seen that although the NR-P3HT films prepared even at room temperature in dynamic-FTM, absorption spectra show λ_{max} around 523 nm with noticeable vibronic features. This spectral behavior is quite different from that of spin-coated film of NR-P3HT as shown (**Figure 3.1** (b)) but rather similar to the absorption spectrum of regioregular RR-P3HT film.[18] This indicates that FTM is capable to promote self-ordering even in NR-P3HT similar to that commonly observed for RR-P3HT by the post-annealing.[72] As can be seen, there was further enhancement in the molecular orientation when film was annealed at 60 °C. This indicates that conformational changes are still taking place leading to increase the alignment thereby increasing the orientation of P3HT main chain as compared to that as-casted oriented FTM. This can be clearly visible from the dependence of DR as a function of post annealing temperature as shown inset of **Figure 3.3** (b). Upon further increase in the annealing temperature beyond 60 °C, it starts decreasing from 100 °C to higher temperature. This characteristics will be attributed to the conformation change of main chain from rod to coil caused by the thermal stress.[73] The findings in NR-P3HT film suggest that a mild annealing up to certain temperature below 100 °C seems to be optimum for the post-annealing for FTM film. This could be associated with some degrees of freedom to have molecular re-arrangement thereby enhancing the DR up to some extent. A small red-shift from room temperature (λ_{max}=520 nm) to 60 °C (λ_{max}=530 nm) along with more pronounced vibronic features also supports the increase in the effective π-conjugation length on main chain.[68,74]

Anisotropic carrier transport is one inherent feature of organic π-conjugated polymers which is highly required for anisotropic film as active layer in organic electronic devices. It has been reported that there is considerable decrease in anisotropy with increasing the film thickness of π-conjugated polymers offering hindrance towards the fabrication efficient and anisotropic organic electronic devices [21]. Such thickness dependent limitations can be easily circumvented by dynamic-FTM since both of the casting and the coating procedures are isolated. At the same time, multilayer polymers thin films as a multiple of 20 nm can also be easily fabricated followed by their annealing it to enhance the orientation further which is the hindrance for annealing induced orientations.

3.3.2 Influence of Backbone Structures of Conjugated Polymers

In order to analyse and compare the orientation behavior arising from the inherent conformational behavior of the main-chain backbone and side chain of different kind thiophene based polymers, it was necessary to optimize the orientation of individual polymers through individual casting parameters given in the **Table 3.1**, **Figure 3.4** shows the polarized absorption spectra of thin films of NR-P3HT and RR-P3HT prepared by FTM. The non-polarized spectra of respective spin-coated films have also been shown for the comparison. It can be clearly seen that films prepared by dynamic-FTM exhibits clear optical dichroism for both the thiophene-based

conjugated polymers. As shown in **Figure 3.4** (a), large DR of 5.8 has been estimated for NR-P3HT which was collaterally due to the mismatch of λ_{max} for the parallel and the perpendicular-polarized electronic absorption spectra. It is interesting to note that in the perpendicularly polarized spectrum of NR-P3HT there is featureless absorption spectral behavior having λ_{max} around 480 nm which is quite similar to that of spin-coated one. It is reported that NR-P3HT is consisted of the mixture of crystalline as well as amorphous parts.[76] Intensity of the perpendicular absorption possibly correlates with the extent of amorphous region in the oriented NR-P3HT film existing as non-oriented part. Contrary to NR-P3HT, spin-coated films of RR-P3HT typical exhibits main peak in the electronic absorption around 520 nm with well-defined vibronic shoulders around 550 nm and 610 nm. Interesting in the oriented films of RR-P3HT where there is strong molecular ordering and vibronic shoulder appearing around 550 nm becomes more pronounced corresponding to the main π-π^* electronic transition in the polymer main chain.[54,77] To consider the high regioregularity and the high crystallinity of RR-P3HT, the difference in the spectral profile of the perpendicular one is also explained by the essential difference in the perpendicular modes of dipole moments on conjugated main-chain.

Table 3.1. List of the casting condition to obtain optimum DR by dynamic-FTM for polymers under investigation.

Polymer	Concentration of polymer in chloroform (wt/wt)	Temperature	Liquid substrate*
NR-P3HT	1.0	25 °C	Eg:Gl = 3:1
RR-P3HT	1.0	42 °C	Wt:Eg = 1:2
PBTTT-C14	1.0	70 °C	Gl
PQT-C12	1.0	25 °C	Eg:Gl = 2:1

* mixing ratio in volume. Eg, Gl and Wt are ethylene glycol, glycerol and deionized water, respectively.

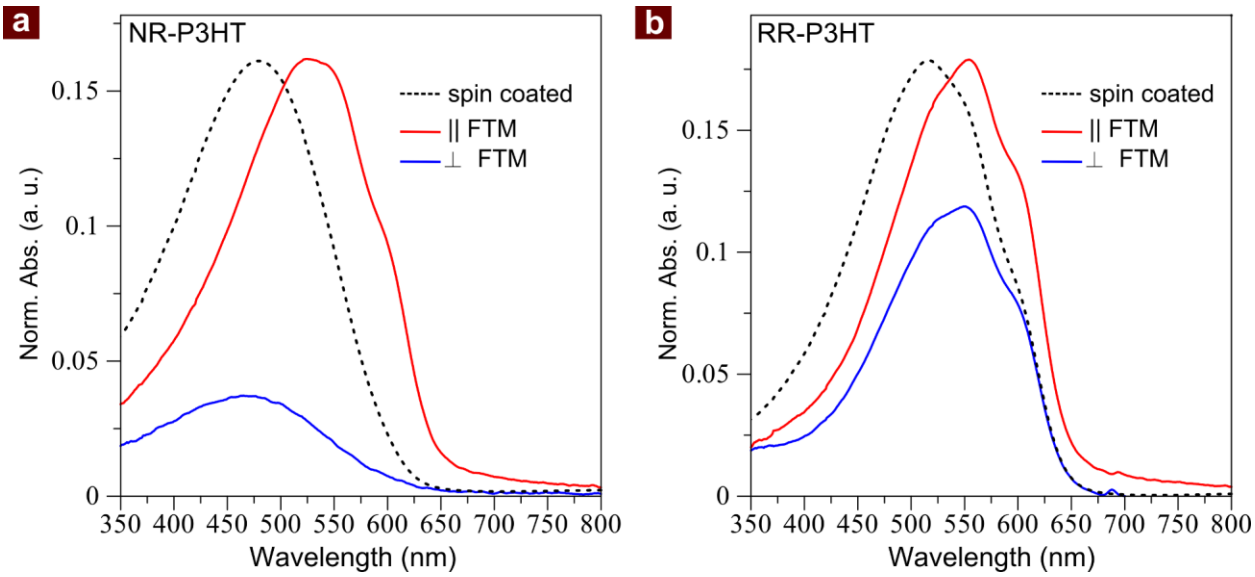

Figure 3.4. Polarized electronic absorption spectra of oriented FTM films (a) NR-P3HT and (b) RR-P3HT. Black dotted absorption represents the spin coated of the same.

A perusal of electronic absorption spectra of spin-coated and FTM films of RR-P3HT reveals that main peak of the spin-coated film appears at 516 nm with vibronic shoulders at 550 nm and 602 nm as shown in **Figure 3.4** (b). Besides this, the parallel polarized absorption peaked at 554 nm with shoulders at 525 nm and 602 nm is similar to that observed for the solution cast films.[77] All the vibronic peaks located at almost the similar wavelength indicates that essentially the same vibronic modes appear by simply change in the Huang-Rhys parameter.[78] Observed red-shift in RR-P3HT films is attributed to the switch of the main-transition mode from 0-2 to 0-1. It is well-known that the slow growth of crystalline domain in RR-P3HT promotes the evolution of lower vibronic modes due to the fibrous crystalline domain formation.[79] In particular the growth of 0-0 modes in RR-P3HT is discussed by Spano model by correlating with the electronic structure of excitonic bandwidth (*W)* with intermolecular coupling transition energy, *Ep*, by Eq. 3.1.[80]

$$\frac{A_{0-0}}{A_{0-1}} \approx \left(\frac{1-0.24\frac{W}{E_p}}{1+0.073\frac{W}{E_p}} \right)^2 \qquad \text{Eq. (3.1)}$$

Where $A_{0\text{-}0}$ and $A_{0\text{-}1}$ represents the corresponding intensities of the 0-0 and 0-1 transitions.

The growth of low vibronic mode essentially represents the extension of conjugation length on the polymer main chain. Observed difference in the absorption profile of RR-P3HT films from those in NR-P3HT is simply explained that RR-P3HT macromolecules maintain rather well-stretched conformation owing to the dynamic-FTM procedure due to its relatively slow casting as compared to spin-coating. It can be seen that vibronic modes in both of the parallel and perpendicularly polarized RR-P3HT, at the same energy level with only differing in their intensity.

This difference in the intensity of vibronic modes is simply due to the changes in the relative conjugation lengths.

Solid-state electronic absorption spectra of spin-coated and FTM-processed thin films of conjugated polymers PQT-C12 and PBTTT-C14 are shown in the **Figure 3.5**. The optical and dichroic parameters are shown in the **Table 3.2.** The polarized absorption spectra in both films exhibit high optical dichroism having a DR of 6.4 and 5.1 for the PQT-C12 and PBTTT-C14, respectively. These DR values are higher as compared to that of RR-P3HT films (1.5). Although there is only a little difference in the chemical structure of polymeric main chain in both of the conjugated polymers, a similar vibronic shoulders were appeared in the thin films prepared by dynamic-FTM. As compared to their spin-coated counterparts, both of these polymers show a bathochromic shift of 7 nm-14 nm which is relatively smaller as compared to those for the RR and NR-P3HT (about 45 nm). In the normalized absorption spectra, it can be seen that vibronic shoulders are more pronounced in the parallel polarized spectra as compared to those of their spin-coated counterparts for both polymers. This could be associated with the consistent expansion of conjugation length by dynamic-FTM. The structural expansion of polymer chain by dynamic-FTM can be assigned as the promotion of conformational expansion owing to the nematic LC phase with appropriate share force during the solidification. It should be noted that both of PBTTT-C14 and PQT-C12 are reported to show a clear thermotropic LC phase transition by differential scanning calorimetry DSC analyses.[42,49] Relatively high performance of carrier transport in these polymers is explained by the good alignment of macromolecules with thermal annealing assisted by the thermotropic LC characteristics in these polymers.[42,49,81]

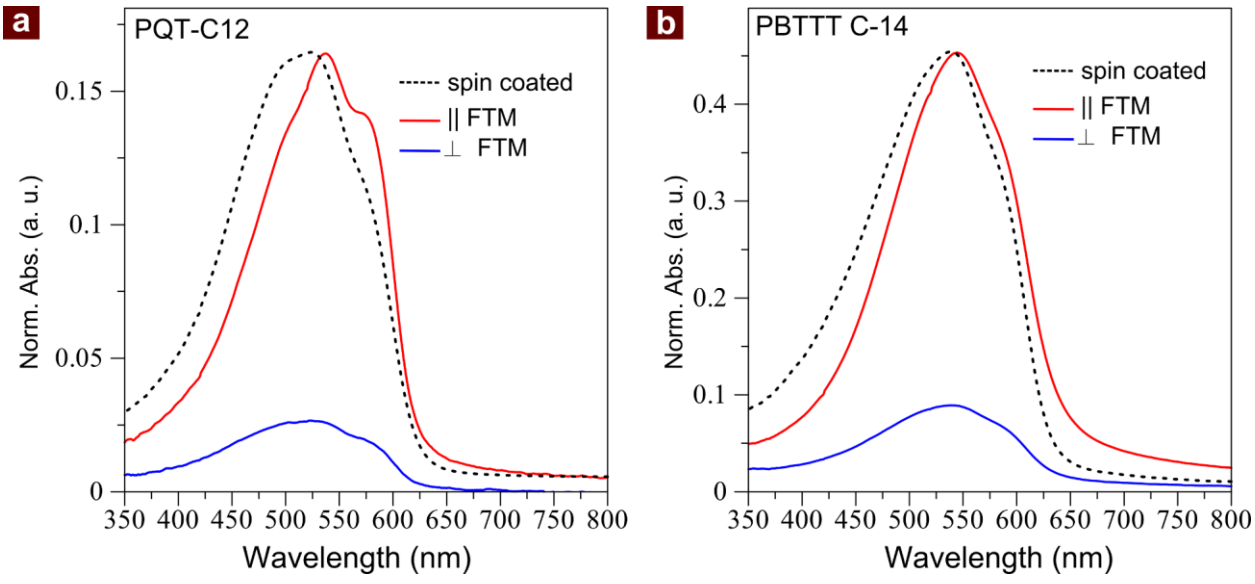

Figure 3.5. Polarized electronic absorption spectra of oriented FTM films (a) PQT C-12 and (b) PBTTT C-14. Black dotted absorption represents the spin coated of the same.

Table 3.2. Optical Parameters for Spin-Coated and FTM Fabricated Thin Films Various Conjugated Polymers used in this work.

Polymer	Conditions	DR	Abs. Max.	Vibronic shoulders
NR-P3HT	Spin-Coated	-	479 nm	-
	FTM- ⊥	5.8	465 nm	-
	FTM- ||		525 nm	602 nm
RR-P3HT	Spin-Coated	-	516 nm	550 nm, 602 nm
	FTM- ⊥	1.5	550 nm	525 nm, 602 nm
	FTM- ||		554 nm	525 nm, 602 nm
PQT-C12	Spin-Coated	-	524 nm	503 nm, 574 nm
	FTM- ⊥	6.4	523 nm	574 nm
	FTM- ||		538 nm	503 nm, 574 nm
PBTTT-C14	Spin-Coated	-	538 nm	592 nm
	FTM- ⊥	5.1	540 nm	592 nm
	FTM- ||		545 nm	592 nm

Orientation intensity varies with the conjugated polymer as well as the casting condition as listed in **Table 3.2.** In order to verify the role of polymeric backbone, it is necessary to compare their relative orientation characteristics under identical casting condition. Taking this point in to consideration we fixed the casting condition utilized for PQT-C12 giving maximum DR and results are shown in the **Figure 3.6**. It can be seen from **Figure 3.6** that DR values for RR-P3HT, NR-P3HT and PBTTT-C14 is much less than that achieved by optimized conditions as already shown in **Figure 3.4**, **Figure 3.5** and **Table 3.2.** Although, these three conjugated polymers have less orientation under similar casting conditions where, PBTTT-C14 exhibits the effective improvement of DR after optimizing the casting parameters under FTM as shown in the **Table 3.2.** For RR-P3HT DR still stays low irrespective of the casting conditions. These results also indicate that basic nature of polymeric backbone and their inherent characteristics seems to play a vital role for orientation, which reflects in differential DR values under the dynamic-FTM.

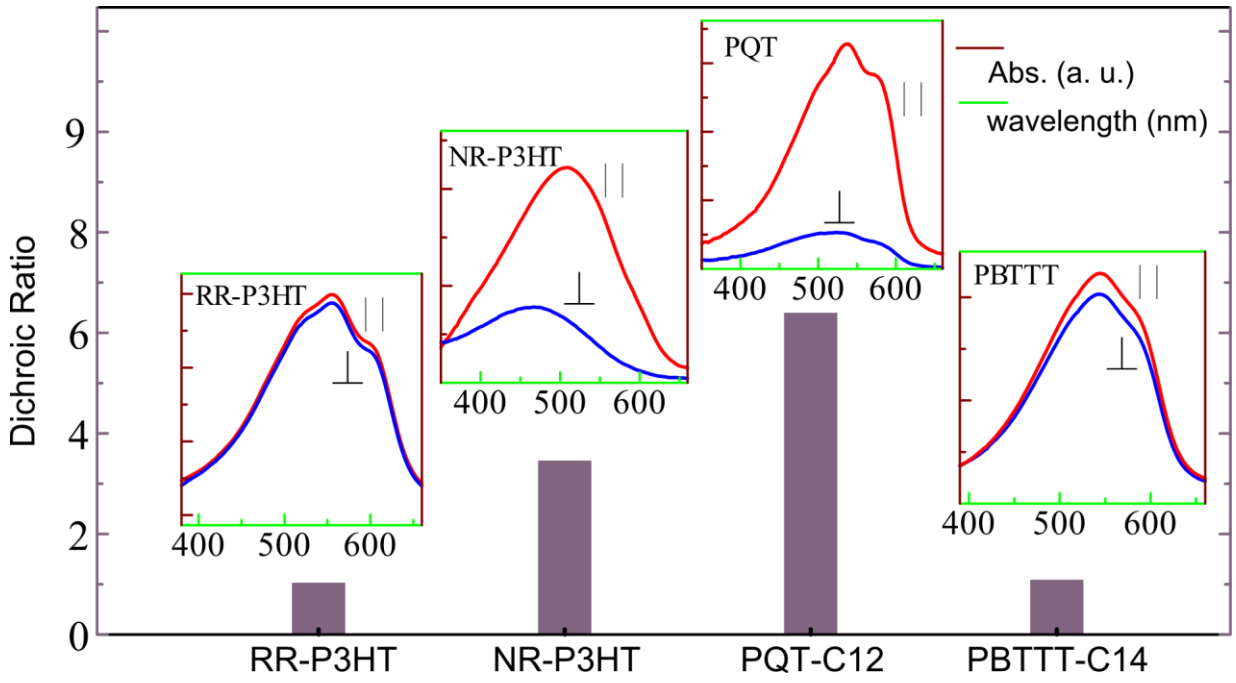

Figure 3.6 Orientation Intensity of all the polymer-films prepared under the identical casting conditions for PQT-C12 to provide highest orientation.

A perusal of **Figure 3.4**, **Figure 3.5** and **Table 3.1** pertaining to the orientation characteristics reveals that orientation strength in RR-P3HT is quite small (DR=1.5) as compared to the other thiophene-based conjugated polymers in this study. In spite of the fact that we attempted dynamic-FTM for RR-P3HT obtained from different commercial sources such as Merck (Iisicon SP001) and Aldrich (Electronic grade), but obtained DRs with all the RR-P3HTs were also found low. It should be noted that the large DR can be obtained with NR-P3HT having the same chemical structure. These facts suggest that the high regioregularity in RR-P3HT inhibits the further promotion of polymer chain orientation. In contrast, completely regioregular conjugated polymers of PBTTT-C14 and PQT-C12 can easily orient in dynamic-FTM as described above. These findings also suggest that structural feature in RR-P3HT resist the promotion of macromolecular alignment into the same direction in dynamic-FTM. The regioregularity in NR-P3HT was estimated to be 80 %, which is lower as compared to that of typical 90-95 % in RR-P3HT.[41,45] This indicates that almost one by 5 units of thiophene ring shows non-regioregular (head-to-head or tail-to-tail) coupling in NR-P3HT. Against this, such mismatch occurs about one by 10-20 units in case for RR-P3HT. This comparison helps us to suggest the orientation mechanism which has been schematically represented in the **Figure 3.7**.

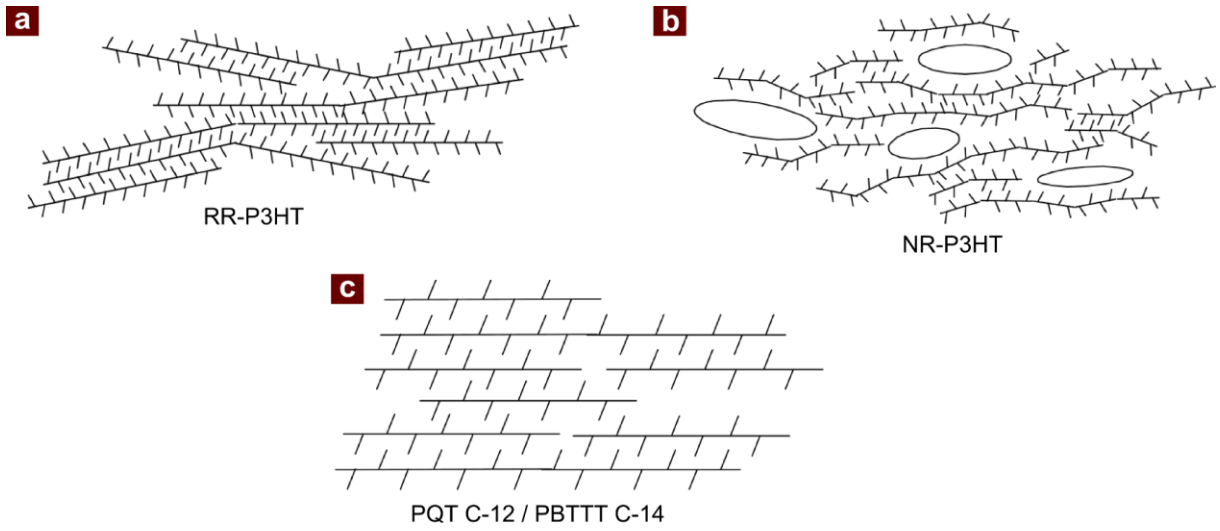

Figure 3.7 Schematic skeletal drawing of possible intermolecular packing for (a) RR-P3HT, (b) NR-P3HT and (c) PQT C-12 / PBTTT C-14. Ovals in (b) represents disordered (amorphous) regions.

In order to explain the differential orientation behaviors for NR-P3HT and RR-P3HT as evident by very large differences in their respective DR, we have to consider their differential inter-molecular interactions associated with the packing of macromolecules in the solid-state. The regioregular part of the P3HT molecular framework attains the fish-bone like structure by the alkyl side chains as schematically shown in **Figure 3.7** (a). These side-chains will interdigitate to the neighbor macromolecules due to the zipper effect.[76,82] The fish-bone structure forces to switch the movable direction of neighboring interdigitated-macromolecules, alternately. This behavior provides the locking force to prevent the sliding action of neighboring macromolecules in highly condensed solution. In particular, the regioregular part of main chain in RR-P3HT strongly forms this interlocking structure by the zipper effect. Against this, for NR-P3HT there are still existing some parts forming amorphous structure. The relative low regioregularity also reduces the interlock formation even in the condensed state as schematically shown in **Figure 3.7** (b). This provides the free sliding motion for NR-P3HT unlike RR-P3HT. In contrast, the base unit in PBTTT-C14 and PQT-C12 forms point-symmetrical substituents unlike the fish-bone structure as shown schematically in **Figure 3.7** (c). This enables no inter-digitation among the individual macromolecules and making the neighboring macromolecules capable for free slide. The higher freedom of sliding motion between the neighboring macromolecules provides effective orientation of macromolecules with strong stretching of main chain into the same direction by shear force in lyotropic LC phase.

It is interesting to note that the thermotropic LC phase transition characteristics in poly(3-alkylthiophene)s has been well discussed till the end of '90s by many researchers.[82–84] After the discovery of the synthetic method to attain very high regioregularity the research for structural and electronic characteristics of NR-P3HT (chemically synthesized with $FeCl_3$) was strongly reduced.[85] This suggests that RR-P3HT seems not to show clear LC phase transition unlikely NR-P3HT.

Against this, PBTTT-C14 and PQT-C12 are focused in their thermotropic LC characteristics and discussed about their contribution for achieving the high carrier transport.[86,87] It should be noted that the correlation between the behaviors for thermotropic LC transition and lyotropic LC transition in conjugated polymers has not been clearly discussed yet. However, PPV derivatives have also been reported to show both of lyotropic and thermotropic LC characteristics.[88,89] Other lyotropic like behaviors in conjugated polymer also have been reported.[59] Interestingly such polymers exhibit clear molecular orientation and optical anisotropy in the films prepared by the dynamic-FTM. Therefore, dynamic-FTM is expected to be one of the important key-technologies for the quick and facile fabrication of oriented thin-film using lyotropic LC phase transition characteristics in conjugated polymers.

3.4. Conclusion

Implications of several factors such as concentration of the polymer solution, temperature of the liquid-substrate and the polymer solution, viscosity of the liquid-substrate and post annealing temperature on the molecular orientation have been investigated in detail using for NR-P3HT films prepared by FTM. It has been successfully demonstrated that degree of orientation in terms of optical anisotropy (DR) in NR-P3HT film can be controlled by optimization of these controlling factors, which has led to the achievement of highly oriented FTM films. A highest DR of 9.3 was obtained when thin films were fabricated using 1.0 % chloroform solution of the NR-P3HT at 30^{o}C of liquid substrate consisted of ethylene glycol and glycerol (3:1) and final post annealing of the FTM film at 60^{o}C. The above results also suggest that highly oriented films of π-conjugated polymers can be obtained by dynamic-FTM if all the parameters can be optimized for a targeted polymer under investigation.

Orientation characteristics of NR-P3HT, RR-P3HT, PBTTT-C14 and PQT-C12 prepared by FTM has been investigated by taking the structure-property correlations into consideration. It has been shown that all of the thiophene-based conjugated polymers show the clear optical anisotropy except RR-P3HT having very small DR of 1.5. This has been explained in terms of the possibility of lyotropic LC phase formation during the solution concentration in dynamic-FTM. The strong zipper effect generated by the highly regioregular conformation with fish-bone structure in RR-P3HT resists the LC phase formation, This tendency of reduced lyotropic LC phase formation hampers the driving force towards its orientation in the dynamic-FTM. Conclusively although dynamic-FTM provides the oriented thin-films of conjugated polymers but their orientation ability depends upon the strength of lyotropic LC characteristics.

Chapter 4: Orientation Characteristics and Charge Transport Anisotropy in Highly Oriented NR-P3HT

4.1 Introduction

Recent past has witnessed the utilization of π-conjugated polymers as active semiconducting materials for the diverse applications in the fast-growing field of organic electronics owing to their facile processability and performance tunability by suitable processing conditions.[90] Amongst various conjugated polymers (CPs), poly (3-alkylthiophene) (P3AT) has been most extensively investigated towards its application as active semiconducting components for various electronic and optoelectronic applications owing to its solution processability along with the facile carrier transport.[91] Intractability of the electro-polymerized P3HT led to the development of $FeCl_3$-mediated polymerization as solution-processable NR-P3HTs (having moderate regioregularity of about 80 %).[41] In this procedure, NR-P3HT can be synthesized with 3-hexylthophene monomer and $FeCl_3$ as oxidizing agent. Synthetic process is very simple and use very cheap reagents. On the other hand, synthesis of regioregular (RR) P3HT, demands, relatively much costly chemicals like 2,5-dibromo-3-hexylthiophene as monomer, air sensitive Grignard reagent as mediator and Ni-based complex as catalyst along with utilization of inert atmosphere. This leads to incur much higher cost of production as compared simple synthesis of NR-P3HT using oxidative polymerization. However, the lower mobility of NR-P3HT (~ 10^{-5} $cm^2/V.s$) was found to be the stumbling-blocks for practical applications.[46] It was found that uncontrolled growth of polymeric chains along with the mixing of various regio-isomers were responsible for the poor carrier transport and hampered device performances. To circumvent this problem, a regio-controlled synthesis with very high head-to-tail coupling (regioregularity > 98 %) was developed,[92] which not only lead to improved field-effect mobility as compared to their pure-regiorandom and non-regiocontrolled (NR) counterparts.[41,92,93] This could be attributed to the fact that this regioregularity promotes the two and three dimensional ordering of polymeric chains via self-assembly in both of the solution as well as solid-states.[79,94]

Owing to the inherent one-dimensionality of π-CPs, development of polymers with high mobility needs comprehensive understanding of the intricate roles played by the molecular structures, their inter molecular packing and molecular orientations which affect and controls the finally achievable transport properties.[27] Various procedures have been reported to align the main chains of the organic CPs in order to fabricate oriented films leading to the enhanced electronic as well as optoelectronic properties.[33] Material wastage, chemo-mechanical damages to the underlying layers and possibility of multilayer coatings are still remaining bottle-necks in the currently employed orientation methods of CPs. Attainment of the facile coating of oriented and multilayer films is desired for the practical realization of highly anisotropic charge transport in electronic devices. In order to provide an amicable solution for such problems, we have proposed

a simple and quick film fabrication method known as floating film transfer method (FTM) to prepare the oriented thin-film with minimal material wastage.[18,95] In this method, an oriented floating film is first casted on to an orthogonal liquid substrate followed by its transfer to a desired substrate by stamping.

In this chapter, we would like to report about the fabrication of OFETs utilizing NR-P3HT as active semiconducting material which is currently considered to be an abandoned conjugated polymer after the discovery of RR-P3HT and our novel FTM for thin film fabrication. It has been demonstrated that NR-P3HT films fabricated by FTM not only exhibits the very high degree of molecular ordering but also leads to the tremendous enhancement (more than two order of magnitude) in the FET mobility as compared to its most commonly utilized spin-coated film counterparts.

4.2 Experimental Details

Spin coated and FTM films were prepared according to chapter 3.10 mg of NR-P3HT was dissolved in 1g of dehydrated chloroform to obtain 1 % (wt/wt) solution. As shown in diagrammatic representation of FTM (Figure1), about 25 µl of NR-P3HT solution was dropped on the optimum hydrophilic liquid mixture of ethylene glycol and glycerol in the ratio of 3:1 resulting in to the formation of oriented floating film on the hydrophilic liquid substrate after the natural evaporation of chloroform under ambient atmospheric conditions [18]. This oriented floating film having thickness of about 20 nm was then transferred on to the glass and SiO_2 substrates for investigation of optical properties and surface morphology, respectively. Films were washed thoroughly with methanol to remove any residual hydrophilic liquid adhered with the hydrophobic substrate prior to the characterization. As a reference, spin-coated films were also prepared from the 0.5 % (w/w) solution of NR-P3HT in chloroform by spin-coating at 3000 rpm for 120 seconds. BG-TC OFETs were fabricated by using a highly p-doped silicon having 300 nm of SiO_2 as gate dielectric insulator (capacitance = 10 nF/cm^2). For FTM deposited OFETs, substrates were spin coated with CYTOP as discussed in Chapter 2 earlier. Owing to the existing fabrication problem of spin coating on CYTOP substrates, it was not possible to fabricate BG-TC by spin coating NR-P3HT solution in chloroform on CYTOP [19]. All the films were annealed at 60 °C for 1 hour in argon chamber prior to electrode deposition. Source and drain electrodes were prepared by thermal evaporation of gold (50 nm) at a base pressure of 10^{-6} Torr using a nickel shadow mask providing the length (L) and width (W) of the channel to be 20 µm and 2 mm, respectively. Transparent white glass and hexamethyldisilazane (HMDS) treated bare Silicon substrates were used for measurements pertaining to the normal/polarized electronic absorption spectra and atomic force microscopy (AFM), respectively. Polarized absorption spectroscopic measurement, sample thickness measurement, and calculation of DR was made similar to as reported in Chapter 2 and Chapter 3.. Atomic force microscopic (AFM) images were taken under tapping mode by JEOL SPM5200 with Olympus probe (OMCL-AC200TS-C3).

4.3 Results and Discussion

Figure 4.1 shows solid-state electronic absorption spectra of spin coated and FTM processed thin films. **Figure 4.1** (a) indicates that spin-coated thin film exhibits a feature-less absorption spectrum with absorption maximum (λ_{max}) at 480 nm.[66] Although this peak has been attributed to π-π^* electronic transition, it is reasonable to be assigned as 0-4 transition of P3HT based on Frank-Condon theory by the spectral analysis.[78,79] Chen et al have reported that the main-peak wavelength of P3HT film exhibits a red-shift with the increase in the regioregularity of main-chain.[93] In the P3HT prepared by oxidative polymerization using $FeCl_3$,[96] vibronic shoulders are very weak and sometime do not appear in the thin film-absorption spectra.[97] In contrast, RR-P3HT (regioregularity > 90 %) clearly shows vibronic modes along with the main π-π^* peak in the absorption spectra.[77,85,93] The relative height of the vibronic shoulder absorption with respect to the main peak changes with the preparation procedure of the film.[77] This is attributed to the Huang-Rhys parameter varying with the conformational states of macromolecules.[78] On the contrary, FTM processed thin films of NR-P3HT shown in **Figure 4.1** (b) exhibits two absorption peaks around 510 nm and 550 nm along with clear vibronic shoulder at 610 nm. This spectral profile is quite similar to those observed in RR-P3HT films prepared by spin-coating.[77] These findings indicate that only employment of NR-P3HT film formation by dynamic FTM instead of spin-coating provides a film with well-defined vibronic features having optical properties very similar to RR-P3HT.

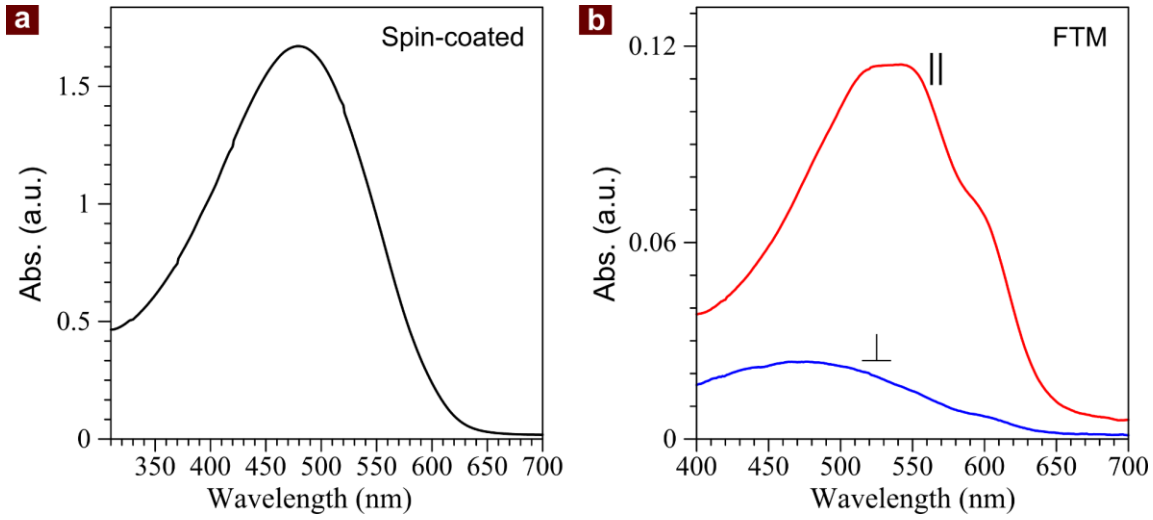

Figure 4.1 (a) Absorption spectra of spin coated NR-P3HT and (b) Polarized absorption spectra of FTM coated oriented NR-P3HT.

FTM processed FTM films also exhibits very good molecular orientation of NR-P3HT having high DR of 8.3 (**Figure 4.1**(b)). The spectral profile in perpendicular polarization is different from that in parallel polarization. Although similar characteristics were reported in the

literatures for P3HT, but there is no clear explanation for this difference [8]. In the case of NR-P3HT, in accordance with the assignment of 480 nm peak in spin-coat film, the absorption spectrum of perpendicular-FTM film can be assigned to non-oriented part present in the film. Strong shrinking or bending form of macromolecules is possibly present in this part which is difficult to align like spin-coated film.

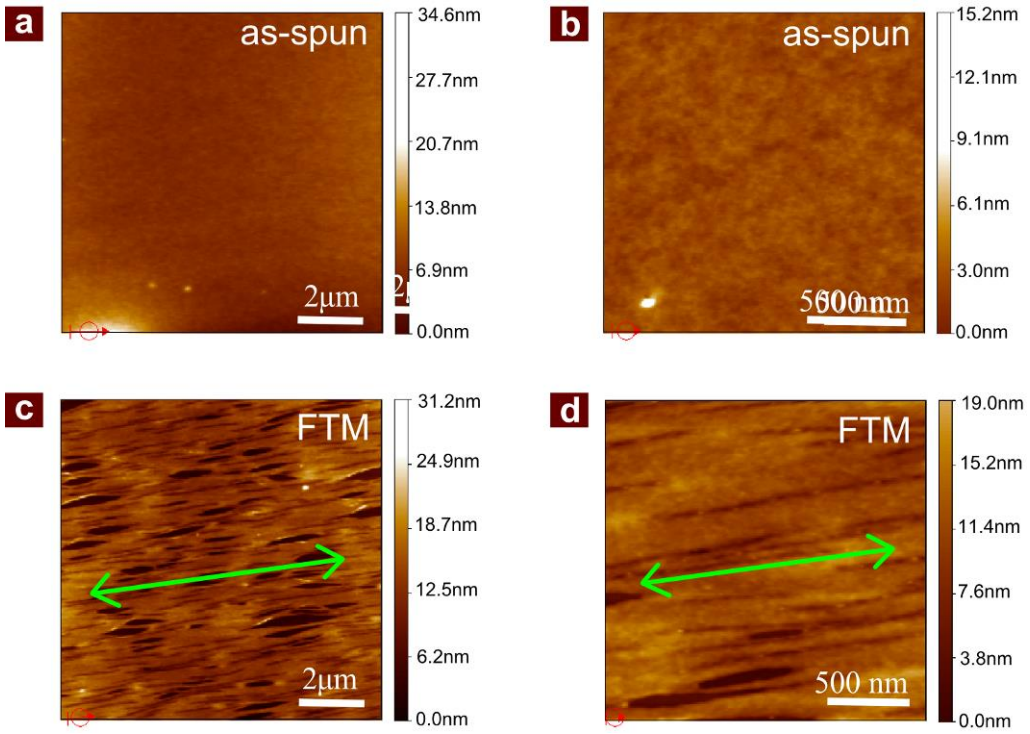

Figure 4.2 AFM topography images. (a), (b) are of spin coated and (c), (d) are of oriented FTM films of NR-P3HT. Green arrow in (c) and (d) represents the direction of orientation.

To verify the high degree of molecular ordering in the FTM films of the NR-P3HT, AFM surface microstructural imaging was also conducted and results are shown in the **Figure 4.2.** Tapping mode AFM image of the spin coated film exhibits highly smooth featureless surface without having any distinguishable surface microstructure (**Figure 4.2** (a), (b)). On the other hand, AFM image of the oriented FTM film clearly exhibits highly aligned polymeric assemblies like fibrous domains which might be responsible for not only to the optical anisotropy but also to the highly aligned polymeric chains with extended π-conjugation and is in the well agreement with the optical absorption spectrum. The observed stretched direction in the AFM images is matched to the orientation direction of main chains visualized optically as well as through polarized absorption spectroscopy.

Figure 4 compares the X-ray diffraction profiles of NR-P3HT films prepared by spin coating (0.70 μm) and multilayer parallel FTM (0.75 μm). In the out-of-plane profiles, the oriented multi-layer film shows clear diffraction peaks at 5.1 (1 0 0), 10.3 (2 0 0) and 15.5° (3 0 0). Contrary

to this, spin-coated film shows only a broad peak at 23.0° (0 2 0). The former three peaks are assigned to lamellar structure attributed to the side-chain stacking, and the later as π-π stacking of P3HT macromolecules, respectively [11, 29]. These differences in the XRD profile indicate that in the oriented multi-layer film, macromolecules stand on the substrate with side-chain as edge-on orientation as also illustrated in **Figure 4** (c). On the other hand, macromolecules lie on the substrate with face-on orientation for the spin-coated films, which is also reported in the literature.[27]

In the in-plane (GIXD) diffraction profiles, all the (h 0 0) peaks disappeared in all the spin-coat, parallel and perpendicular directions. Instead of this, the oriented NR-P3HT film shows only π-π stacking peak-profiles towards parallel direction (red in Figure4 (b)). This π-π stacking peak also disappeared in the perpendicular direction (blue in Figure4 (b)). These in-plane profile characteristics further support that NR-P3HT, macromolecules stands as edge-on structure in oriented FTM films as illustrated schematically in **Figure 4** (c).

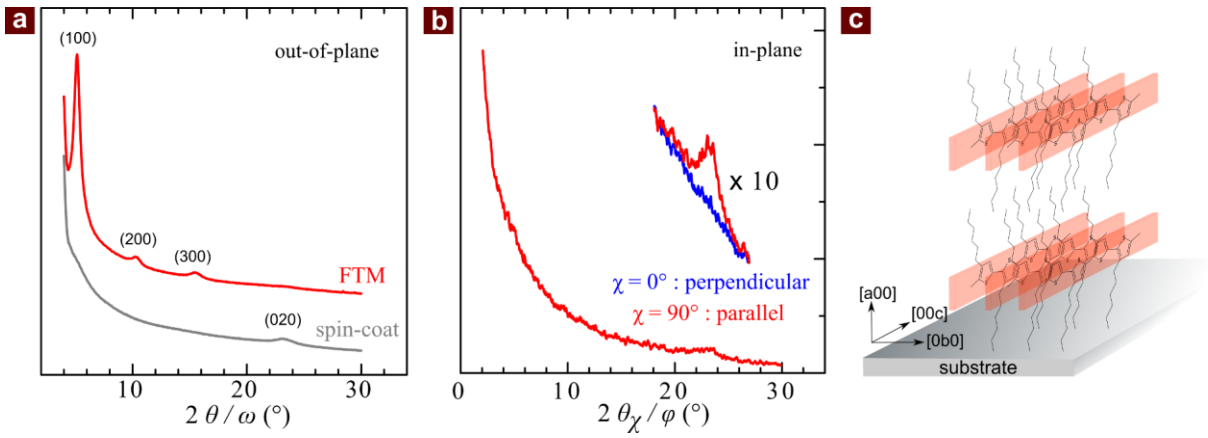

Figure 4.3 X-ray diffraction profiles of spin-coated (gray) and parallel-coated multi-layer (red/blue) films of NR-P3HT. (a) out-of-plane and (b) in-plane (red: parallel; blue: perpendicular) profiles. (c) Schematic drawing of the structural orientation of P3HT macromolecules according with (a) and (c).

Excited by very good molecular alignment and high optical anisotropy in the FTM films of NR-P3HT, efforts were directed to investigate the implication of this striking structural morphology on the electronic characteristics by fabricating the OFETs. **Figure 4.4** shows the transfer curve of different OFETs prepared by FTM as well as spin coating. Various device parameters of the fabricated OFETs estimated from the out-put and transfer curves are summarized in the **Table 4.1**. It can be clearly seen that in the operational regime of the OFETs, there is very low hysteresis in the transfer characteristics. The field effect mobility (μ), in the parallel orientation of FTM films based FETs was 3.4×10^{-3} $cm^2/V.s$ and higher than the FETs having perpendicular oriented films (6.5×10^{-4} $cm^2/V.s$) reflecting the anisotropic transport in the NR-P3HT. Interestingly, measured μ in both of the orientations of FTM films exhibited more than two orders of magnitude increase as compared to the films fabricated by the conventional spin-coating. It can be seen from the **Figure 4.4** that FTM not only improves the μ by > 2 orders of magnitude but also it sharpens

some other features like a clear ON voltage and increase in On/Off ratio which was almost unclear in the spin-coated OFETs.

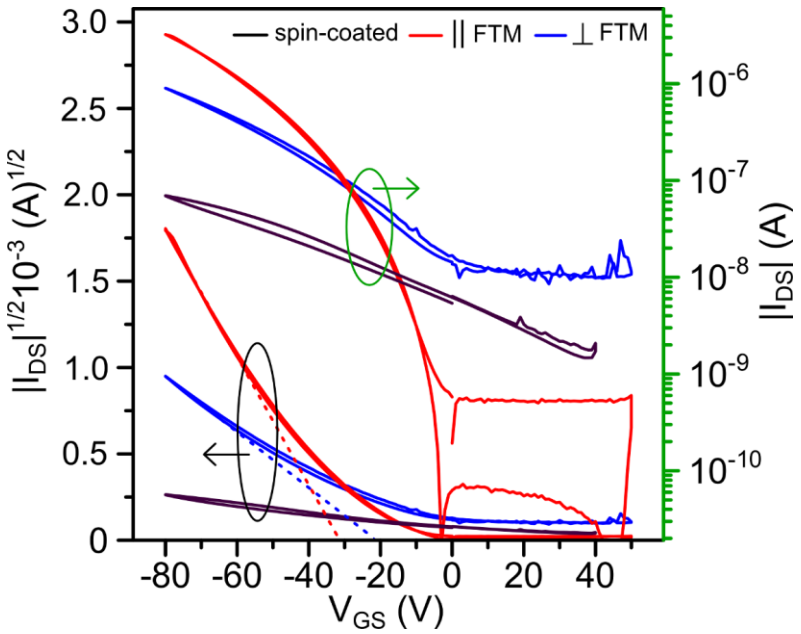

Figure 4.4 Transfer characteristics for the NR-P3HT based field effect transistors fabricated using thin films by spin coating and FTM (at V_{DS} = 80V).

Table 4.1. OFET Characteristics of || and ⊥ Oriented FTM and Spin-coated NR-P3HT Films.

	μ ($cm^2V^{-1}S^{-1}$)	V_{TH}	$V_{on\text{-}set}$ *	I_{on} [A]	I_{off} [A]	On/Off
Parallel	3.4×10^{-3}	-31 V	0 V	3.23×10^{-6}	1.91×10^{-10}	1.69×10^{4}
Perpendicular	6.5×10^{-4}	-21 V	10 V	9.00×10^{-7}	1.26×10^{-8}	7.14×10^{1}
Spin Coat	2.1×10^{-5}	7 V	unclear	6.99×10^{-8}	1.77×10^{-9}	3.94×10^{1}

*on-set voltage was defined as per the reference.[98]

Output characteristics of FETs in all configurations have been compared in **Figure 4.5**. Although every configuration have shown clear p-type transport characteristics but larger currents were observed in case of parallel FTM films as compared to perpendicular FTM and Spin-coated films. These results are in well agreement with the improvement observed in the transfer characteristics of each individual configurations.

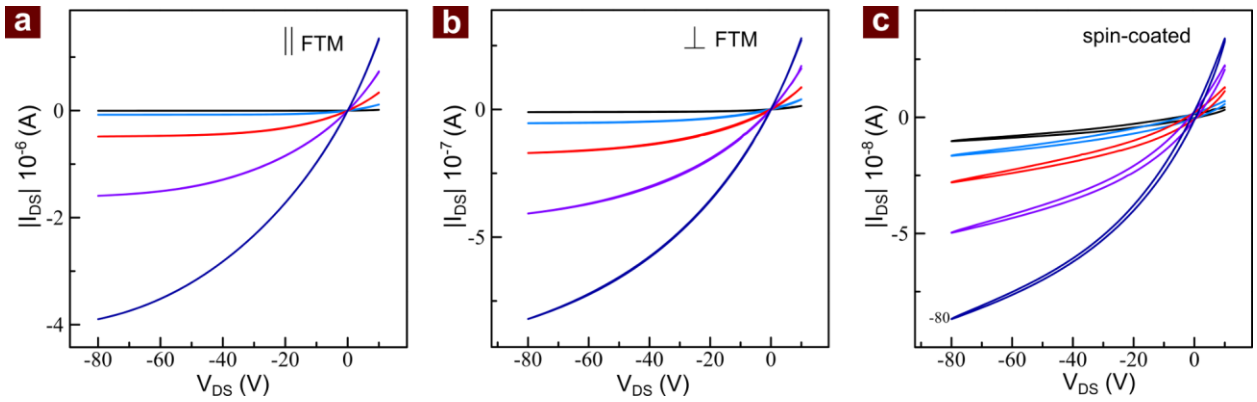

Figure 4.5 Output Characteristics of OFET fabricated NR-P3HT films. (a) ||, (b) ⊥ and (c) spin coated.

Considering the drastic difference in the spectra and the surface morphology of the films by casting methods, uniaxial extended fibrous-domains were formed in the oriented FTM films. In these oriented domains, NR-P3HT macromolecules are expected to be arranged in well-stretched conformation.[78] Charge carriers travel in these domains swiftly, the total carrier flow is limited by the hopping transport at neighboring domain boundaries or amorphous region. This causes relatively larger inter-domain resistance as compared to that at intra-domain region along with electric field. Thus, the electric potential strongly drops at inter-domain and remaining potential contributes to modulate the transport characteristics by the field-effect. This inter-domain number between source and drain, therefore, plays a key-role in the potential ratio of V_{GS} to drive FET.

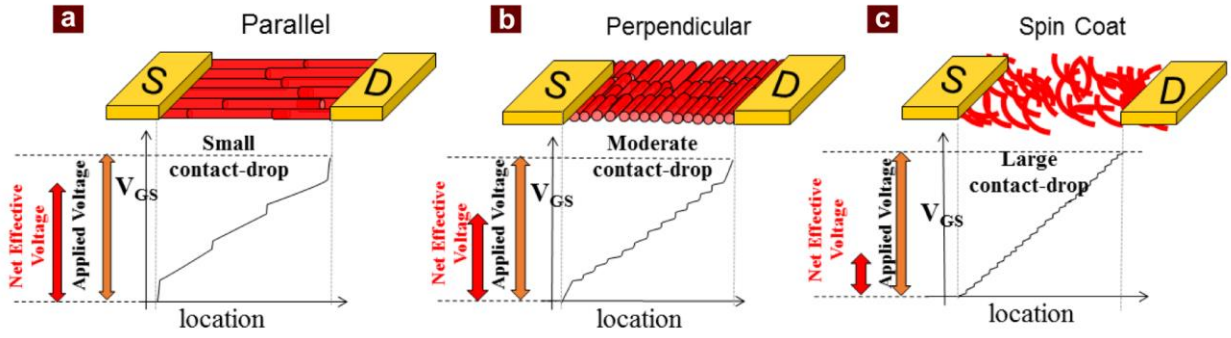

Figure 4.6 Schematic representation showing possible transport mechanism in different orientations of NR-P3HT OFETs and respective voltage distribution for (a) ||, (b) ⊥ and (c) Spin-coated films.

This phenomena has been schematically shown in the **Figure 4.6**. The effective electric potential to drive FET largely applies to the channel of parallel FTM-film. In contrast, the FET with perpendicular FTM-film is consisted of rather more inter-domain rich channels. Since the higher ratio of applied potential is consumed at the inter-domains, the driving potential are reduced in the perpendicular FET. In the case of spin-coated films, domain size is thought to be very small

owing to relatively shorter π-conjugation length as indicated by blue-shifted absorption maximum. In other words, macromolecules are expected to shrink or bend, thus fail to form large domains. In this case, the inter-domain characteristics are likely to be inter-molecular type, resulting in large potential drops while intermolecular hopping. This reduces the effective drive-potential for spin-coated FET. Such difference in V_{GS} distribution for each FET is the cause of different slopes in transfer characteristics, i.e. the field-effect mobility, as listed in Table 1 even in the same potential region. The off-state also characterizes the field-effect modulation of carrier number in the channels. As found in Table 1 as well as in Figure 4 (b), a very small off-current was obtained in the parallel-FET. This directly contributes to improve the on-off ratio of FET. Against this, for the perpendicular-FET, relatively large and constant off-current is persistent in the whole off-state (positive) voltage region. This leads to decrease in the on-off switching performance. In addition, a continuous decrease in the transfer current was observed in the entire gate-voltage region for spin-coated FET, which fails to show any clear off-state region unlike the FTM-based FETs.

One can argue that μ, should also change with the field-effect but extent of this modulation in μ is relative small as compared to the change in carrier numbers (therefore, we can obtain μ as a value of the field-effect mobility). Thus, the modulation of channel conductance in FET is represented by the change in carrier number by the field-effect. Some carriers are stationary and the others are induced/depleted by the field-effect. Whole the carriers are consisted of the sum of the static carriers, n_s, and the field-induced carriers, $n_{fe}(V_{GS})$. Since the field-induced carriers are completely depleted at the ideal off-state region as $n_{fe}(V_{GS}\_off) = 0$, the on-off ratio can be simply represented by the ratio of carrier number as $\{n_{fe}(V_{GS}\_on) + n_s\} / n_s$. The very low off-current observed in parallel-FET indicates that the positive V_{GS} is effectively applied in the whole channel region to deplete the carriers. Against this, the observed large off-current in perpendicular-FET suggests that the perpendicular alignment generates some domains to be isolated from the transverse potential (V_{GS}) application, in which the carrier number is stationary or insensitive to V_{GS} modulation. The former consists of the static conduction and the later relates to the subthreshold traps. These characteristics are in accordance with the drain current in transfer characteristics of perpendicular-FET. Relatively large off-current relates to the static conduction and the large subthreshold swing relates to the existence of various traps in perpendicular-FTM channel as shown in **Figure 4.4**. A clear on-set characteristic in parallel-FET indicates the sharp carrier injections in the whole channel at the same V_{GS}. This is probably due to the well-controlled V_{GS} application into many domains and facilitated by reduced potential drop at inter-domains. These characteristics are still observed but the sharpness of the injection is relatively weak with shifting positive potential of *V*on-set due to increased inter-domain potentials. [98] For spin-coat film, huge and a variety small domains are responsible for carrier transport. The carrier number modulated by a certain V_{GS} also depends upon the carrier path. Such variations in possible carrier path diversify the transport characteristics,[77] which provides indefinite behaviors to switch between on- and off-states along with the negative shift of V_{TH}. As a result, a clear on-set voltage is failed to appear in transfer characteristics for spin-coat film.

4.4 Conclusion

In conclusion, FTM has been used as a novel thin film fabrication method for the preparation of highly oriented thin film of NR-P3HT towards its application as active material for OFET. Implementing this method has resulted in the formation of highly oriented domains of NR-P3HT having high optical dichroic ratio of 8.3. The XRD results has exhibited an edge-on orientation for the FTM films which was contrary to the face on orientation observed for the spin-coated films. OFETs fabricated using FTM processed NR-P3HT film as active semiconducting material exhibited a pronounced enhancement in the field effect mobility along with the anisotropic carrier transport as compared to that of spin-coated films. The anisotropic behavior and highly facile carrier transport in FTM films is attributed to both of the well-organized inter-domain and intra-domain transport characteristics along the FET channel.

Chapter 5: Synergistically Improving the Performance in Blends of NR-P3HT and PBTTT: Interplay of Orientation and Blending

5.1 Introduction

Advent of solution processable conjugated polymers (CPs) and their successful implementation as active semiconducting components have geared the fast development in the area of organic electronics.[99,100] Apart from most acclaimed spin coating there are number of solution based approaches capable of providing high quality thin films towards the realization of improved performances in organic electronic devices.[101,102] Charge transport in CPs has captivated a lot of attentions from the scientific community which can be gauged by their tremendous application potentials in the area of organic field effect transistors.[27,103] Charge transport in CPs are stringently dependent on the overlapping of electron density from their neighboring π-orbitals which in-turn controls the intermolecular associations, molecular stacking, chain alignment etc. Molecular engineering approaches for the in-depth understanding of underlying phenomena have been the center of attention of the research community. Ubiquitous implication of film morphology on controlling the performance of organic field effect transistors (OFETs) make CPs more interesting not only to understand the related transport processes but also efforts towards their control in order to achieve the desired functions.[23,24,51] Molecular orientation in CPs due to their one dimensional character makes them capable of improving their charge carrier mobility, [27,47,48] which has been witnessed by report of a number of methods for their unidirectional orientation in the recent past.[33]

Among CPs, polythiophenes have been most extensively investigated for device application in the area of organic electronics. Intractability of electro-polymerized materials of this family of CPs led to the attraction for solution processable poly (3-hexyl thiophene) (P3HT) prepared by $FeCl_3$ catalyzed chemical synthetic methods but their small field effect mobility (μ) led to its repudiation by majority of the researchers.[41,46,47] In general, they exhibit very small μ ($<10^{-5}$ $cm^2/V.s$) when their thin films are prepared by conventional spin coating due to their low regioregularity,[46,47] uncontrolled growth of polymer chains and presence of various regio-isomers. The presence of regio-randomness in P3HT leads to the mechanical flexibility owing to their low crystallinity.[104] Recently, flexible OFETs utilizing low regioregular and regiorandom P3HT has also been demonstrated by other groups.[105,106] Several attempts has been made to increase the crystallinity of CPs in order to increase the performance of OFETs, however, such problems are irresistible due to their semi crystalline nature.[107] In-fact the high crystallinity affects the mechanical pliancy of film thereby making them inadequate for soft electronics device application.[104] Therefore to solve such issues, many methods have been explored in order to improve the transport properties in low

crystalline systems and is still perpetuating.[105,108] In spite of the that fact reported μ in CPs are breaking their previous records by molecular design and implementation of various film processing techniques,[109,110] however, there is no consensus for a widely acceptable charge transport model in semiconducting CPs.[111]

Furthermore, in P3HT with reduced regioregularity and apart from the presence of head-to-tail (H-T) coupling, there are sufficient head-to-head (H-H) and tail-to-tail (T-T) coupled fractions in the main polymer chain. Such a mismatch in their regioregularity provides large steric interaction leading to increased torsion.[72,112] On the other hand, highly regioregular (RR) P3HT exhibits high crystallinity due to their increased inter-chain interactions assisted by high inter-digitation of alkyl chains between adjacent macromolecules resulting in relatively high μ in their thin films.[48] Microstructures of highly RR-P3HT consists of semi-ordered and amorphous regions where long polymer chains are mainly responsible for the connecting the adjacent crystallites.[111,113] Large scale orientation of CPs is a unique solution for improving the in-plane transport of CPs, however, the resulting performance is governed by the kind of orientation of CPs adopted within their crystallites i.e. edge-on, face-on or mixture of both as shown in chapter 1 (**Figure 1.8**). Although highly oriented films of RR-P3HT with face-on orientation has been demonstrated through some global orientation methods such as mechanical rubbing and friction transfer techniques.[54,94] However, the presence of out-of-plane π-π stacking and in-plain alkyl side-chain impede the inter-molecular transport at the interface of insulator and CPs.[114] The origin of such edge-on and face-on orientation of the film depends on the different film forming methods. Application of mechanical pressure (shear-forces) on the polymer backbone has been reported to adopt the face-on orientation.[54,94] Therefore, this highly face-on oriented films does not serve the purpose of improving the in-plane transport and the problems related to the damage occurring to underlying surface while rubbing and friction transfer cannot be ignored also. In this perspective, such orientation methods are certainly not suitable for devices requiring high in-plane transport like OFETs.[113,115] On the other hand, direct solution casting methods favor slow solvent evaporation, resulting in to thermodynamically favored edge-on orientation with in-plane π-π stacking and π-conjugation favoring facile in-plane charge transport.[24,115] However, preparation of large scale oriented film of RR-P3HT is difficult through solution based approaches. This could be attributed to the stiffness present in the RR-P3HT due to high intermolecular inter-digitation/interaction, concomitantly imparting relatively lower degrees of freedom for adjacent macromolecules to orient freely.[75]

In order to provide an amicable solution for both of the issues like flexibility and orientation in P3HT, recently we have shown that using NR-P3HT with moderate regioregularity of (~80%), it is possible to attain good molecular orientation. To accomplish this goal, we have utilized a facile solution based approach of floating film and transfer method (FTM) which is capable of providing large scale orientation of CPs in single direction. FTM basically involves rapid evaporation of solvent together with orientation and thermodynamically favorable edge-on orientation leading to the remarkably enhanced μ of NR-P3HT by 2-3 order of magnitude reaching ~ 10^{-3} $cm^2/V.s$.[47,95] It has been found that such a large scale unidirectional orientation although leads to high intra-domain

charge transport but they still possesses hampered inter-domain transport due to their relatively low crystallinity or π-π stacking. Therefore, it is of utmost importance to provide a logical solution for the facile inter-domain charge transport while maintaining the inherent flexibility which is expected to be a milestone in the area of high performance flexible electronics. Mixing two CPs of different nature to tune resulting μ by varying their mixing ratio has been a focal point of many researchers and many interesting results have also been reported.[105,116,117] Involving such blending of two CPs with contrasting inherent behaviors by adding a highly crystalline material with pronounced inter-domain transport in the highly oriented domains (with high intra-domain transport) of second polymer would be a prominent approach for solving both flexibility and orientation issues in CPs.

In this chapter, both of the crystallinity as well as the molecular orientation issues have been amicably taken in to the consideration in order to improve the charge carrier transport in the blends of CPs. We have focused on the most widely studied thiophene based CPs like NR-P3HT as amorphous and PBTTT as a crystalline polymeric materials as depicted in chapter 2 (**Figure 2.1**). Using FTM as a highly facile solution based method for the preparation of oriented thin films, the influence of the addition of crystalline CP in the highly oriented NR-P3HT has been investigated together with the charge carrier transport and opto-electrical anisotropy. The orientation in the pristine NR-P3HT is increased drastically by the addition of only 10% of PBTTT and synergistically improved μ with anisotropic charge transport. Transport properties of thin films of different blends and stoichiometry were correlated with the results obtained from various techniques such as polarized absorption spectroscopy, AFM and XRD patterns etc.

5.2 Experimental Details

NR-P3HT has been synthesized by most commonly used $FeCl_3$ assisted oxidative chemical polymerization and purified by Soxhlet extraction as published earlier.[118] Determination of the molecular weight of the synthesized polymer was carried by gel permeation chromatography using polystyrene standards. The molecular weight and polydispersity index (PDI) of the synthesized NR-P3HT was found to be M_w = 102645, M_n = 29849 and 3.4, respectively. On the other hand, its regioregularity was found to be about 80% as confirmed by with ^{1}H-NMR spectroscopic investigations.[45] PBTTT was purchased from Sigma Aldrich having M_w = 40,000 - 80,000 and PDI below 3 and used without any further purification. All of chemicals used in the synthesis were of reagent grade and used without any purification. Anhydrous chloroform was purchased from Sigma Aldrich which was utilized to dissolve all of the above polymers.

1% and 0.2% weight by weight (wt/wt) solutions of CPs were prepared in anhydrous chloroform for the fabrication of thin films by FTM and spin-coating, respectively. FTM was utilized as a casting method used for the preparation of the oriented thin film as per our previous publication.[95] Addition of PBTTT to NR-P3HT has been done in the increasing order of weight percentage in NR-P3HT. All of the solutions were warmed at 60°C to avoid any aggregation and gelation before casting the films on liquid substrate. The Films casting condition was tuned for NR-P3HT and kept constant throughout the experiment according to Chapter 4. The oriented FTM

films from liquid substrate were finally transferred by stamping on the desired solid substrates either for characterization or OFET fabrication.[95] For out-of-plane X-ray diffraction, FTM samples were prepared by multilayer coating on hexamethyldisilazane treated silicon wafers in order to have relatively thicker film (~700 nm) in for getting measurable XRD signal intensity without influencing the film morphology as published earlier.[95] The thicknesses of the all the FTM films were measured by interference microscopy (Nikon Eclipse LV150) and found to be in between 20-25 nm. Polarized electronic absorption spectroscopic. AFM, XRD measurement and DR calculation was carried in similar manner with those of previous chapter.

Heavily p-doped silicon substrates were used as base substrates having 300 nm of SiO_2 as an insulating layer having capacitance $C_i = 10$ nF/cm^2). The SiO_2 surface was spin coated with CYTOP (a highly hydrophobic fluoropolymer) at 3000 rpm for 120 s and baked at 150°C for 1 h to make the surface hydrophobic for better adhesion of the floating films. The resultant C_i after of CYTOP coated substrates were found to be 8 nF/cm^2. The reference spin coated samples were prepared on base SiO_2 substrates owing to existing problem of spin coating on CYTOP due to its high hydrophobicity.[119] The oriented FTM films were stamped on to the prepared substrates. Films were annealed at 80°C prior to electrode deposition. 50 nm thick source and drain were deposited by thermal evaporation of gold (1.5 Å/s) at pressure 10^{-6} Torr using nickel mask with L and W of 20 and 2000 µm, respectively. The μ, V_{TH} and on/off ratio was calculated in saturation regime.

5.3 Results and Discussions

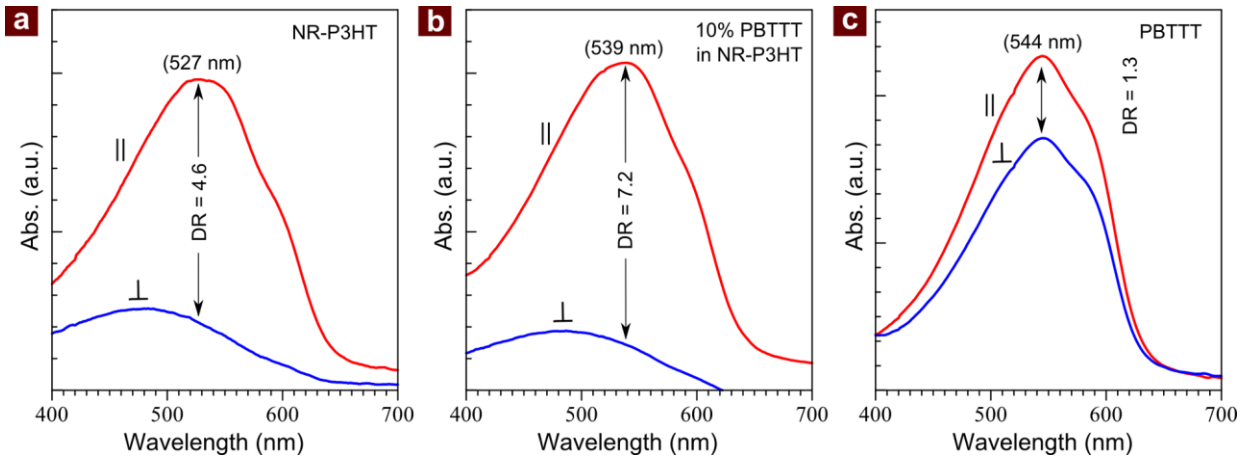

Figure 5.1 Polarized absorption spectra oriented films prepared by FTM. (a) Pristine NR-P3HT, (b) NR-P3HT having 10% PBTTT and (c) Pristine PBTTT.

Solid-state electronic absorption spectrum of P3HT thin film exhibits a pronounced optical absorption in the 400 nm-650 nm associated with the π-π* electronic transition which is parallel to the polymer backbone main-chain axis[120] and the extent of their orientation intensity can be easily monitored by polarized absorption spectroscopy. The ratio of the absorbance at absorption

maximum (λ_{max}) obtained from polarized light parallel and perpendicular to the main chain alignment direction gives with extent of orientation intensity as DR.[121] Spin coated thin films of NR-P3HT exhibits a featureless absorption spectrum having π-π^* transition around 480 nm,[85,95] In contrary to this NR-P3HT film processed with FTM exhibits sharp vibronic features along with red-shifted λ_{max} at 527 nm as shown in the **Figure 5.1 (a)**. The red shifted λ_{max} in the FTM processed film is due to the increased π–conjugation length due to oriented NR-P3HT having the DR of 4.6 which is interestingly higher than that observed for films aligned by mechanical rubbing and almost similar to the observed values for RR-P3HT by strain alignment.[94,121]

Significant works have been done to align the conjugated polymers either by utilizing the nano-confinement during nanoimprinting,[122] assisting the alignment by pre-patterned layers and polyimide layers as host substrates for deposition.[123–125] Such methods utilize the assisted alignment of the guest CP along the in-built direction of the host substrate texture. Unlikely in our case, when we attempted to blend small amount (10%) PBTTT in NR-P3HT there was synergistic improvement in the orientation intensity. It can be clearly seen from the **Figure 5.1 (b)**, that there is a net increase in the intensity of orientation intensity, concomitantly increasing the DR value >7. To the best of our knowledge, this could be the first phenomenon observed where the guest is increasing the orientation of the host. One can argue that increased DR is probably due to the orientation of the guest PBTTT, which can't be distinguished due to the overlapping absorption spectra of constituent polymers. Since in FTM the orientation of individual polymers highly depends on the casting conditions therefore PBTTT has very little orientation (**Figure 5.1 (c)**) under similar casting condition as discussed earlier in Chapter 3. Due to the overlapping wavelength and lack of sharp peaks in the absorption spectra of these individual polymers as can be seen from **Figure 5.1**, it is quite ambiguous to decide and distinguish the role of individual CP in this blends for this surprising increase in the orientation intensity. One of the plausible solutions to clarify this enhanced net orientation intensity in the blend by logically selecting the guest CP having the absorption in higher/lower wavelength region than that of host CP. Taking this point in to consideration, it has been found that by small addition of polyfluorene (PFO) in NR-P3HT, there was an increase in the orientation intensity of the blend similar to that observed for the blend of NR-P3HT and PBTTT as shown in **Figure 5.2.**

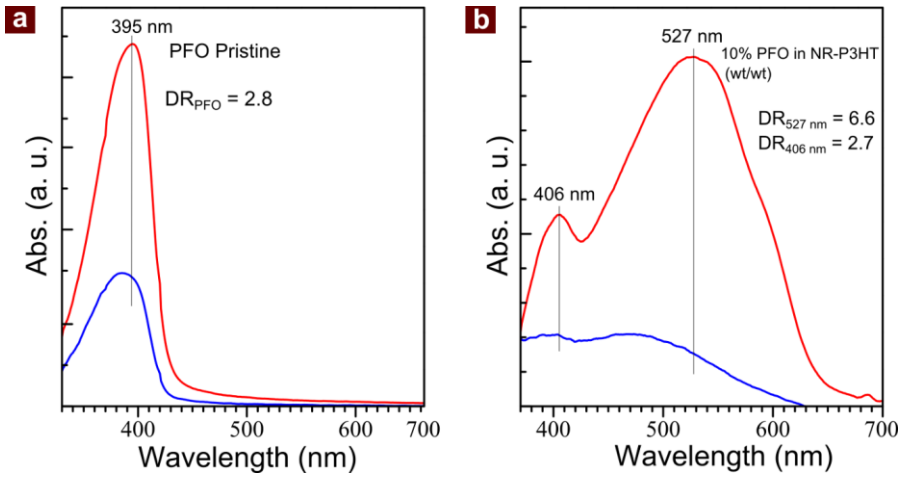

Figure 5.2 Polarized absorption spectra oriented films prepared by FTM. (a) Pristine PFO, (b) NR-P3HT having 10% PFO.

It is reasonable to say that P3HT films having high regioregularity is brittle due to the fish bone structure of their alkyl side chains,[75] concomitantly P3HT with low regioregularity is comparatively flexible due to the entanglement of the polymeric chains, resulting from the discontinuity in head-to-tail configuration.[104] Such materials auspiciously gives the adjacent macromolecules of NR-P3HT to align freely as compared to the highly regioregular P3HT. The possible mechanism for synergistically improved orientation by small addition of PBTTT could be attributed to the fact that the presence of crystalline domains of PBTTT concomitantly reduces the entanglement and provide more freedom to NR-P3HT to align. Such phenomenon related to microstructures rearrangements has been shown schematically in the **Figure 5.3**. As spin coated films consists of amorphous and randomly distributed polymer chain of NR-P3HT while oriented films processed with FTM are consisted of large scale entangled oriented domains, which tends to form more flat aligned structures with the addition of guest material PBTTT. This proposal is in accordance with results revealed by microstructural investigations using AFM and will be discussed in later section.

Figure 5.3 Schematic representation of the thin film microstructures of NR-P3HT coated by (a) as-spun NR-P3HT, (b) FTM coated NR-P3HT and (c) FTM coated NR-P3HT blended with small amount PBTTT (blue stripes).

Effect of post-annealing at 60°C on DR in different blending ratio of PBTTT in NR-P3HT has been shown in **Figure 5.4**. A perusal of this figure clearly reveals that DR of NR-P3HT first increases by 10 % addition of PBTTT followed by a decrease upon further addition. The cause of such gradual decrease in DR upon blending can be easily understood considering the low DR exhibited by pristine PBTTT. Upon annealing the FTM processed films at 60°C, it has been found that net resulting DR of all the blend films increases, however, extent of this change decreases with the increasing PBTTT fraction in the blend. One of the probable reasons could be the evaporation of the remaining solvents but it is of worth to notice that higher changes in DR is observed in NR-P3HT.[67] Such increase in DR is reasonable as macromolecules in the domains of NR-P3HT are less crystalline providing flexibility to the polymeric backbone to reorganize.[104] Such a drastic changes in DR of NR-P3HT is in well agreement with the increment in DR due to small addition of guest polymer.

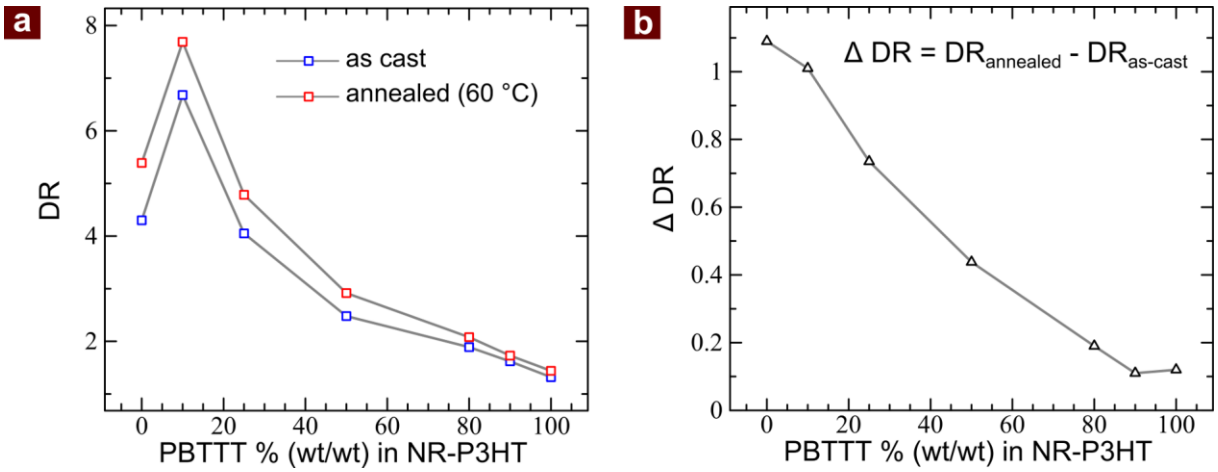

Figure 5.4 (a) Dichroic Ratio (DR) of the as-cast and annealed oriented FTM films, (b) Increase in the DR (Δ) after annealing at 60°C. Δ DR in (b) was calculated from taking the difference of DR of annealed and as-cast film (average of at least 3 films), respectively. Higher changes in Δ DR with higher content of NR-P3HT in the blend fraction shows that the NR-P3HT macromolecules has more tendency to rearrange due to its flexibility.

For spin coated NR-P3HT, the absorption of NR-P3HT at 480 nm represents π-π* transitions with featureless absorption and relatively blue shifted λ_{max} around 480 nm is attributed to the decrease in effective π-conjugation length, concomitantly localizing the wave function of the exciton to higher extent and increasing its energy.[68] The less resolved fine structures in spin coated films can be attributed to wider distribution of the conjugation lengths. However, when the same films of NR-P3HT was prepared by FTM, λ_{max} was found to be red shifted to 527 nm representing the increase in the π-conjugation length with and evolution of 0-0 transitions representing the high degree of inter-chain interaction.[68] In order to visualize the further ordering and increase in the inter-chain interactions by addition of small amount of (PBTTT 10%), Spanos model for the quantitate analysis of inter and intermolecular ordering in CPs was performed.[80] Electronic absorption spectrum of FTM processed NR-P3HT exhibits vibronic structures showing only 0-0

transitions at 602 nm whereas it becomes more resolved and shows the 0-1 vibronic band also appearing at 539 nm upon addition of PBTTT. The amount of the inter-chain coupling can be estimated by the ratio of 0-0 and 0-1 vibronic bands, which corresponds to free exciton bandwidth (W) of the aggregates. The decrease in the value of W can be attributed to the increase in the conjugation length as well as chain ordering. The value of W was calculated from the relation as,

$$\frac{A_{0-0}}{A_{0-1}} \approx \left(\frac{1 - 0.24\frac{W}{E_P}}{1 + 0.073\frac{W}{E_P}} \right)^2 \qquad (2)$$

Where $A_{0\text{-}0}$ and $A_{0\text{-}1}$ represents the corresponding intensities related to 0-0 and 0-1 transitions obtained from the normalized spectra as shown in **Figure 5.5** and E_p denotes the vibrational energy at 0.18 eV. [126,127] The value of W was calculated for both of the pristine FTM coated NR-P3HT film as well as for blend of NR-P3HT having 10 % PBTTT and results are shown in the **Table 5.1**. The value of W in pristine NR-P3HT film was found to be 160 meV which was decreased to 148 meV for NR-P3HT having 10% PBTTT reflecting that slight addition of guest crystalline material leads to promotion of the intermolecular ordering in NR-P3HT macromolecules.

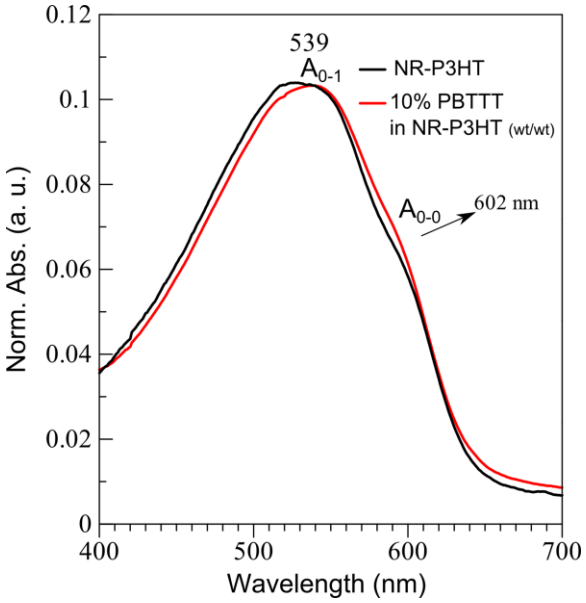

Figure 5.5 Normalized absorption spectra of NR-P3HT, and blend of NR-P3HT and PBTTT.

Table. 5.1 Different Parameters Calculated from Absorption Spectra of Oriented Films of NR-P3HT and Blending Mixture of NR-P3HT and PBTTT.

	DR	$A_{0\text{-}0}$	$A_{0\text{-}1}$	W (eV)
NR-P3HT Pristine	4.6	0.0563	0.1033	0.160
10% PBTTT in NR-P3HT	7.2	0.0591	0.1033	0.148

Previously, we have reported about the formation of aligned fibrous domains like features in NR-P3HT when films were processed with FTM, which were responsible for the optical anisotropy and extended π-conjugation. The nanofibrous domains were well oriented showing clear extended conjugation length confirmed by optical measurement.[47] **Figure 5.6** shows the tapping mode AFM images of the different stoichiometric blends of NR-P3HT and PBTTT. A perusal of the **Figure 5.6 (a)** clearly corroborates the formation of highly aligned fibrous domains in the pristine NR-P3HT films, however, it exhibits higher roughness giving the idea that the domains of NR-P3HT are highly entangled due to their low regioregularity. Addition of only 10 % PBTTT in NR-P3HT is enough to remove such entanglement between the domains and leading to reduced roughness as shown in the **Figure 5.6 (b)**. Pristine PBTTT itself exhibits very less orientation in this casting condition but play a crucial role for controlling the orientation of blend,[75] and increase in molecular orientation upon the addition of PBTTT (10 %) in NR-P3HT has been already discussed by polarized absorption spectroscopy. At the same time, AFM surface topology for blend film with 80 % PBTTT content exhibits relatively smooth texture (roughness 3.8 nm) as compared to the pristine PBTTT (roughness 5.1 nm). This might associated with presence of relatively amorphous and flexible NR-P3HT as a plasticizer occupying the remaining 3-D space existing between the crystalline domains of PBTTT. This proposal has been well correlated with fact that PBTTT exhibits terrace phase morphology as compared to highly flat surfaces observed with NR-P3HT when spin coated.[81,95,128]

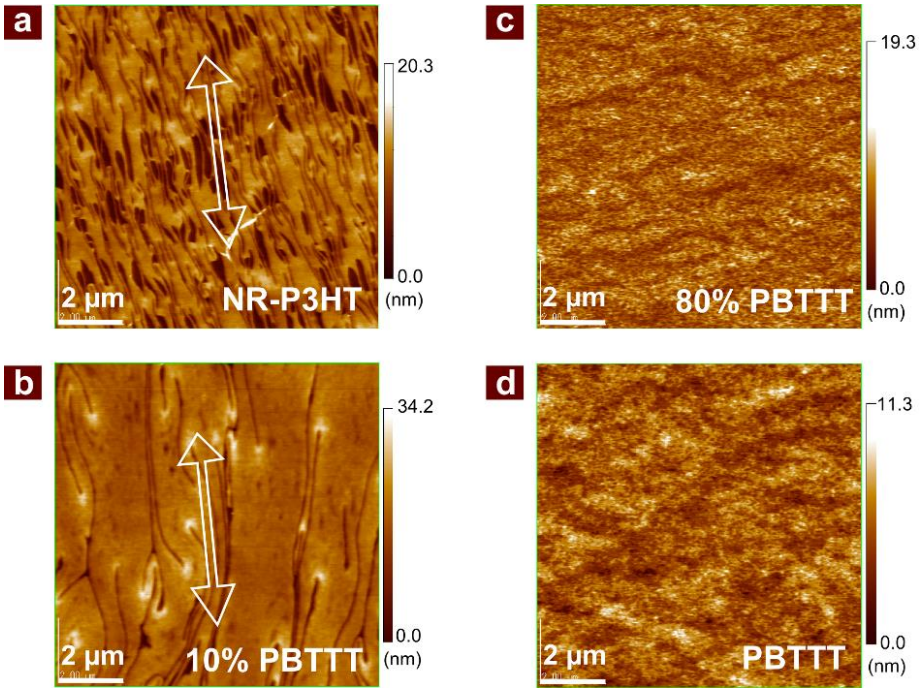

Figure 5.6 AFM images of FTM films. (a) Pristine NR-P3HT, (b) 10 % PBTTT in NR-P3HT, (c) 80 % PBTTT in NR-P3HT and (d) Pristine PBTTT. White arrow represents the direction macromolecule orientation as confirmed by polarized absorption spectroscopy.

FTM processed films of pristine NR-P3HT exhibits edge-on orientation with enhanced crystallinity as compared to that of spin-coated films as demonstrated us in our earlier publication.[95] **Figure 5.7** shows the out of plane X-ray diffraction of the all of the FTM processed blend films with increasing PBTTT contents in the NR-P3HT. It can be clearly seen that NR-P3HT exhibits (100) diffraction peak around at 5.3° corresponding to lamella-stacking of its alkyl-side chains representing the edge-on orientation as shown in Figure 1 (a).[95] The decrease of its intensity upon addition of PBTTT is attributed to the decrease of its relative extent and presence of this diffraction peak is rather more important to decide the microstructure. However, as can be seen that peak at 5.3° still exists in the presence of PBTTT up to 10 %. Disappearance of this peak in the presence of higher extent of PBTTT might be associated with the disruption of the alkyl-stacking of NR-P3HT. On the other hand, diffraction peak (100) at 4.04° starts to appear for PBTTT with the addition of PBTTT (≥ 25%) in NR-P3HT. This clearly represents that films microstructure in these films are governed by the NR-P3HT up to 10% PBTTT and after which peak at 5.3° disappear and only peaks corresponding to the alkyl d-spacing of PBTTT at 4.04° appear prominently[51,81]. Based on the XRD pattern observation of the blend films it could be concluded that majority of crystalline domain formation in microstructures are governed by the PBTTT and NR-P3HT exists as oriented amorphous phase like and play an important role to connect these separated crystalline domains.

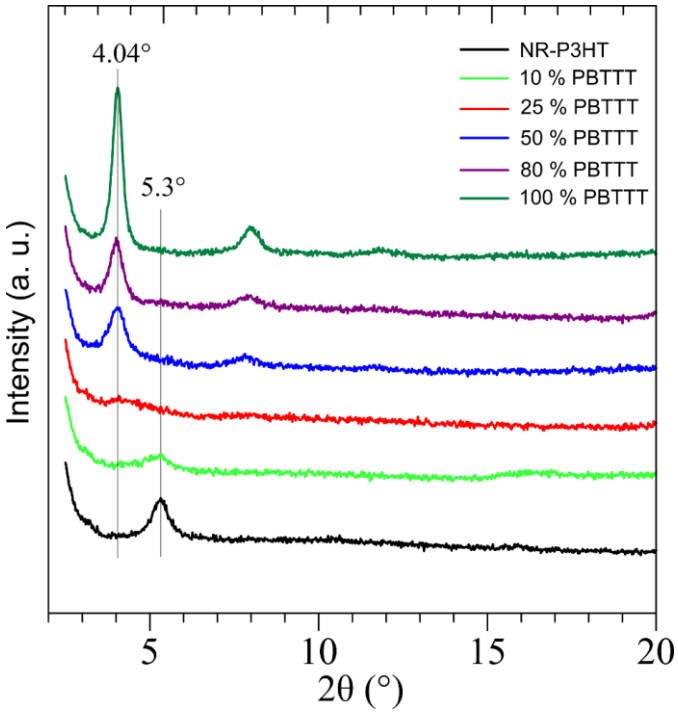

Figure 5.7 Out-of-plane XRD pattern of FTM films with increasing amount of PBTTT in NR-P3HT.

Charge transport properties of NR-P3HT and PBTTT blend thin films were investigated by fabricating OFETs with BGTC geometry. We probed the transport characteristics along the || and ⊥ to the orientation direction of the polymer. Charge transport in isotropic films were also investigated by spin coating the corresponding blend fractions. The evolution of μ in different configurations along || ($\mu_{||}$), ⊥ ($\mu_{\perp}$) and spin coated (μ_{sc}) is shown in **Figure 5.8** (a). As can be seen from **Figure 5.8** (a), FTM films of NR-P3HT exhibits much improved $\mu_{||}$ (> 2 orders of magnitude) as compared to its μ_{sc}, as reported earlier also.[47] At the same time, it has also been reported in the literature that spin-coated thin films of PBTTT exhibits rather low μ in the range of (~ 10^{-3} cm^2/V.s) and get pronounced (~ 0.1 cm^2/V.s) when heated to its liquid crystalline temperature around 150 ^{0}C.[81]

This can be seen from the **Figure 5.8** (a) that addition of small amount (only 10%) of PBTTT increased the $\mu_{||}$ of FTM processed NR-P3HT films up to 0.02 cm^2/V.s, which is nearly similar to the $\mu_{||}$ of pristine PBTTT films fabricated by FTM under ambient conditions without any high temperature annealing. The possible reason for such synergistic improvement in the $\mu_{||}$ due to the enhanced orientation exhibited by NR-P3HT having 10% PBTTT as described in polarized absorption spectroscopic investigation, where the DR of 4.6 of NR-P3HT was increased up to 7.2. This pronounced $\mu_{||}$ is also in well agreement with the AFM image where addition of small amount of PBTTT reduces the roughness present in the oriented NR-P3HT films, concomitantly decreased entanglement between the domains of oriented NR-P3HT film. This approximately 8-fold increment in $\mu_{||}$ also suggests that the fibrous domains in NR-P3HT films are capable of very high intra-domain carrier transport and PBTTT as guest macromolecules further facilitates the transport process owing to its very high inter-domain transport. Interestingly, upon further increase in the fraction of PBTTT (> 25%) there was enhancement in the $\mu_{||}$ and $\mu_{\perp}$ with respect to the pristine PBTTT as well as NR-P3HT. However, it was found that there is uneven distribution of increment in $\mu_{||}$ and $\mu_{\perp}$ as can be seen from the **Figure 5.8** (a). The average $\mu_{||}$ at high percentage of PBTTT continues to increase and at 80% the increment in this is about 2 times higher (0.042 cm^2/V.s) than that of average $\mu_{||}$ of pristine PBTTT. This can be easily understood from the perusal of transfer characteristics of the || OFETs fabricated with the blend films of NR-P3HT and PBTTT with varying stoichiometric contents as shown in the **Figure 5.8** (b).

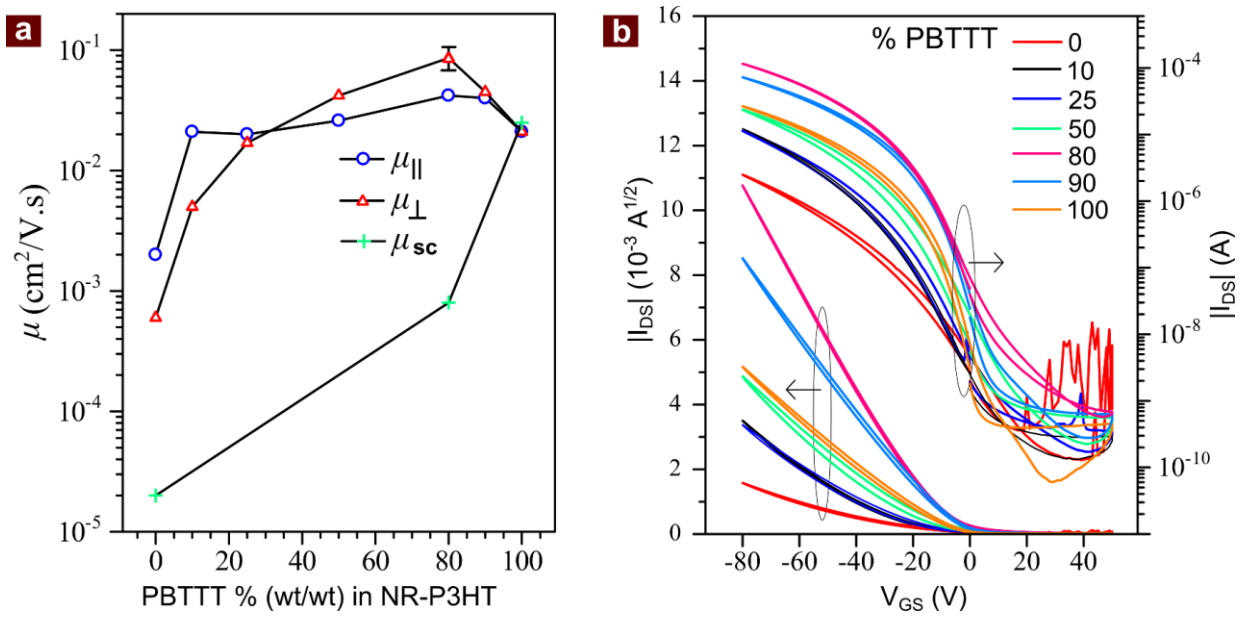

Figure 5.8 (a) Evolution of μ in bottom-gate top-contact OFETs prepared in blending mixture of NR-P3HT and PBTTT. The μ measured along || and ⊥ to the orientation direction of the polymer is $\mu_{||}$ and $\mu_{\perp}$.prepared by FTM. (b) Transfer characteristics of OFETs with increasing amount PBTTT in NR-P3HT having FTM films with orientation || to the channel direction (V_{DS} = -80 V). The μ_{sc} in (a) represents the μ in isotropic films prepared by spin coating.

It is worth to note that unlike RR-P3HT, PBTTT in general exhibits small electrical anisotropy ($\mu_{||}/\mu_{\perp}$) in spite of having high optical anisotropy due to the different structures of grain boundaries and domain boundary limited transport.[25,129] Therefore, origin of $\mu_{||}/\mu_{\perp}$ in blend due to PBTTT must be negligible as the DR exhibited by pristine PBTTT is very less (Figure 2c). As can be seen from **Figure 5.8** (a), for PBTTT rich blends $\mu_{\perp} > \mu_{||}$, blends having 80% contents of PBTTT have shown average $\mu_{\perp}$ of 0.086 cm^2/V.s with maximum value of 0.11 cm^2/V.s exhibiting an increase of almost 5-fold when compared to that of pristine PBTTT. On the other hand, as summarized in **Table 5.2**, when same blend fraction having 80% PBTTT as well as pristine PBTTT were spin coated, they exhibited μ_{sc} of 7.0 x 10^{-4} cm^2/V.s and 0.025 cm^2/V.s as shown in **Figure 5.9** (a). The possible reason for this observed low μ_{sc} in the blends could be attributed to the amorphous and randomly oriented chains of NR-P3HT and connection between the crystalline domains of PBTTT controlling the inter-chain transport as reported previously.[47]

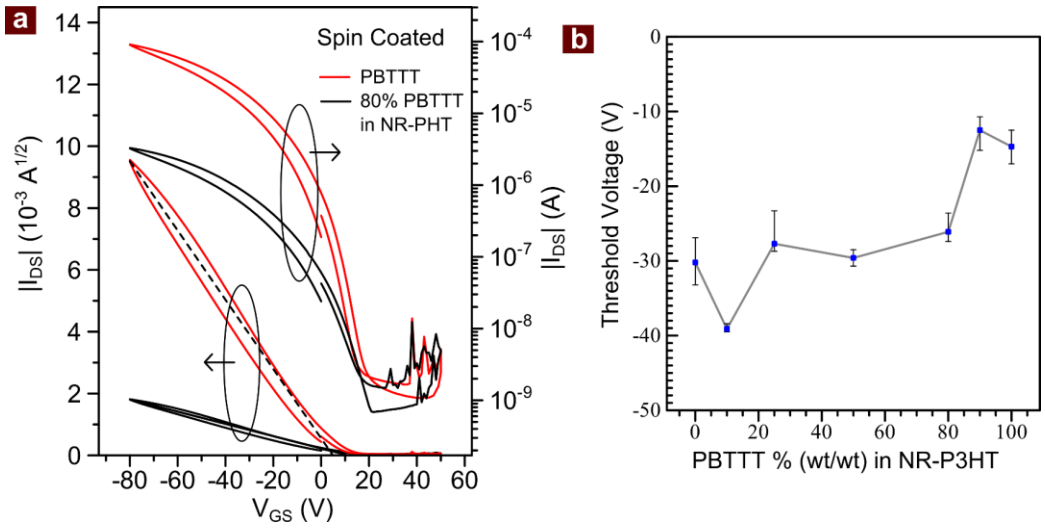

Figure 5.9 (a) Transfer characteristics of spin coated films of pristine PBTTT and 80% PBTTT in NR-P3HT, (b) Variation of threshold voltage in parallel OFETs at different blending mixture of PBTTT and NR-P3HT.

Table 5.2 Device Parameters (Mobility and I_{on}/I_{off}) for Different Blends of NR-P3HT and PBTTT.

	μ (cm^2/V.s)			I_{on}/I_{off}	
	$\mu_{\|\|}$	$\mu_{\perp}$	μ_{sc}	||	$\perp$
Pristine NR-P3HT	0.002	0.0006	0.00002	~10^4	~10^2
10% PBTTT	0.021	0.005	—	~10^5	~10^3
80% PBTTT	0.042	0.086 (Max. 0.11)	0.0008	~10^6	~10^6
Pristine PBTTT	0.021	0.021	0.025	~10^5	~10^5

To the best of our knowledge, this synergistically improved μ in the PBTTT is highest reported so far where no annealing was conducted to their liquid crystalline phase transition temperatures. Reported values of μ_{sc} for PBTTT based OFETs in this range (0.1 cm^2/V.s) have only been reached by processing the substrates with octyltrichlorosilane (OTS) followed by the subsequent annealing of the films to the different phase transition temperatures of around 180 °C and 275 °C.[81,129] Basically OTS treatment of the substrate has been chosen to increase the hydrophobicity of the substrates and when heated on OTS substrates it forms larger domains due to dewetting.[81] Such increase in the grain size due to annealing decreases the inter-domain resistances offered to the charge carriers to travel from source to drain.[81,128] It is also worth to mention here that such an enhancement in the OFET performance is possible without compromising with the off-current characteristics and increase in on-current which increases the on-off ratio.

Evolution of V_{TH} along the || direction with different blends shows similar trends to that of orientation (Figure S5, Supporting Information). It was found that there is slight negative shift in the V_{TH} for 10% PBTTT. The possible reason for such negative shift could be associated with their

increased orientation, since we have previously reported that highly oriented NR-P3HT exhibits negative shift in V_{TH} as compared to the spin coating.[47] Positive shift of V_{TH} observed for further addition of PBTTT can also be correlated with decrease in orientation characteristics as more random film morphology leads to positive shift in V_{TH} which is also reflected in transfer characteristics of spin-coated films too (**Figure 5.9** (b)).[47] Such characteristics of effective control on threshold voltage in blends of spin-coated films have also been published by other research groups.[116] It is worth to note here, that devices were exposed to air atmosphere and their measurements were carried out one by one. Therefore, the possibility of gate bias stress in these OFETs cannot be ignored, which results in undesirable changes in the transistor characteristics associated with charge trapping.[130] However, since the devices were made/measured over the span of months, this obvious trend of V_{TH} observed in this case cannot ignore the role of orientation. However, understanding this behavior more explicitly needs detailed investigation, which is beyond the scope of our present work.

Figure 5.10 shows the output characteristics of || OFETs fabricated utilizing different thin films of the blends consisted of NR-P3HT and PBTTT processed by FTM. Except stoichiometric ratio of NR-P3HT and PBTTT all other device fabrication parameters have been kept constant. A perusal of the output curves clearly reveals p-type charge transport characteristics with well saturated output currents. A Clear higher order of magnitude in output current can be easily seen in the output characteristics in all of the blend system based devices as compared to their corresponding films casted by each of the respective pristine materials.

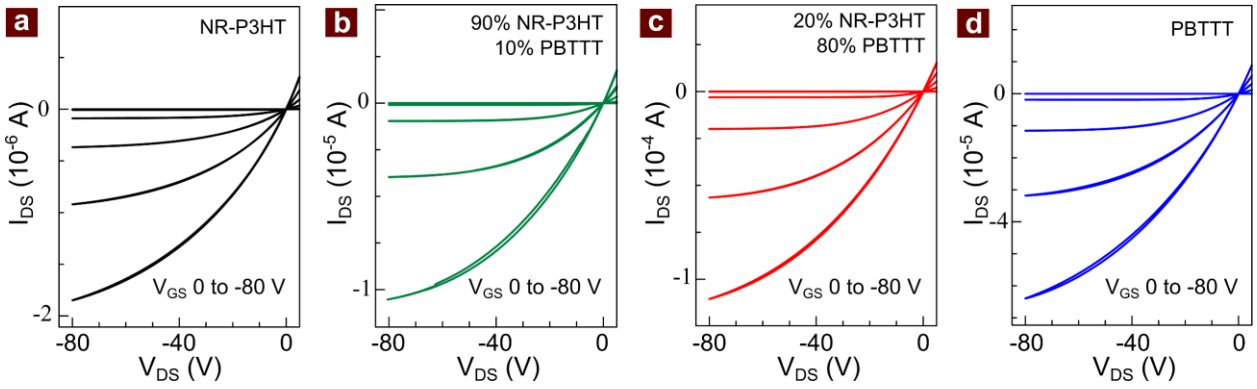

Figure 5.10 Output characteristics of parallel OFETs. (a) Pristine NR-P3HT, (b) 10% PBTTT in NR-P3HT, (c) 80% PBTTT in NR-P3HT and (d) Pristine PBTTT.

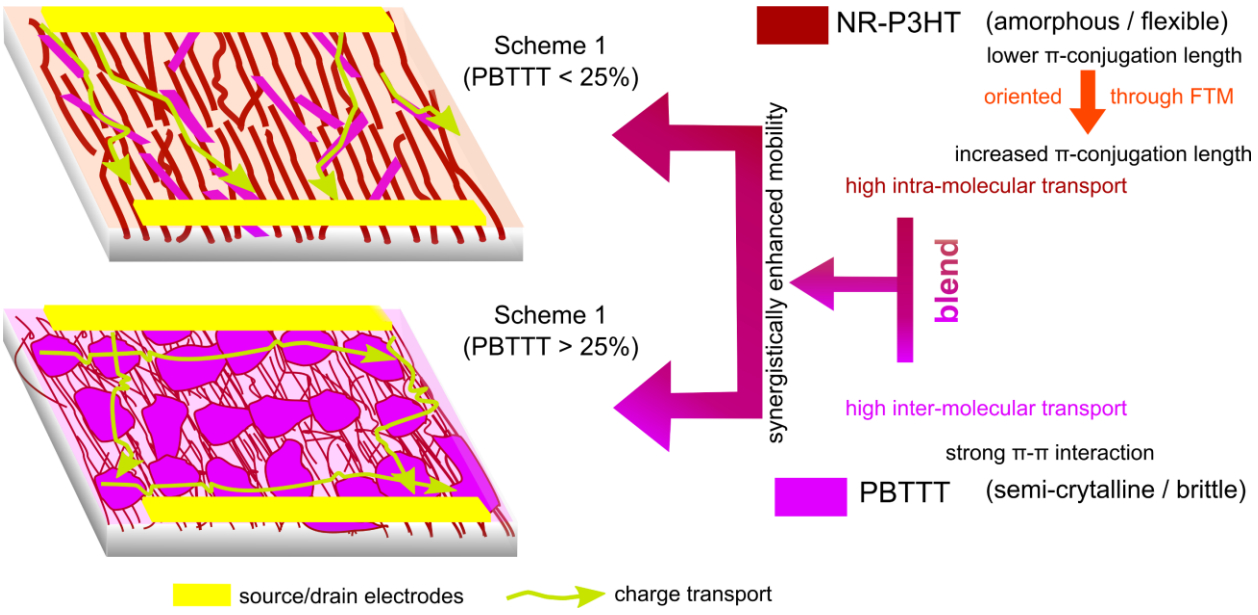

Figure 5.11 Schematic illustration for possible anisotropic charge transport. Scheme 1 is for (PBTTT < 25%) and Scheme 2 is (PBTTT > 25%). Direction of the transport has been shown by green arrows.

Figure 5.11 depicts the schematic representation of two schemes for the synergistic improvement in the OFET characteristics upon blending PBTTT in NR-P3HT. Scheme 1 is related to the improvement of μ when 10% of PBTTT was added in NR-P3HT and this model is well correlated to the above explanation given for improved orientation as shown in **Figure 5.3**. In this case, presence of small fraction of highly crystalline PBTTT decreases the entanglement present in domains of NR-P3HT as reflected in the AFM images (**Figure 5.6**). Firstly, the presence of such crystalline material in amorphous oriented films of NR-P3HT not only leads to increased orientation of NR-P3HT by decreasing entanglement. Secondly, they act like a high transport bridge between the domains of the NR-P3HT owing to the high inter-molecular transport. Scheme 2 is proposed in order to explain the improved transport in blend films consisting of higher PBTTT contents (80%) in NR-P3HT. As shown in polarized absorption spectra and AFM images too, these FTM films of blend do not exhibit relatively higher molecular orientation, therefore, orientation present is mainly contributed by the NR-P3HT domains with extended π-conjugation length. Such macromolecules in the domains exhibit a lot of mechanical flexibility to adjust them in to 3-D space of the FTM film, as it was also well reflected in **Figure 5.4**. Possibly this NR-P3HT domains must be filling the vacant spaces between highly crystalline domains of PBTTT and thereby synergistically improving the μ. It has been well accepted that in the case of oriented conjugated polymers, μ in parallel direction is generally higher as compared to its perpendicularly oriented

counterparts. Interestingly, a perusal of **Figure 5.8** (a) indicates that perpendicular μ or either same or a bit higher than that of their corresponding parallel oriented counterparts especially for the blend films having PBTTT contents in NR-P3HT are > 25%. Although exact reason is not completely clear but this could be associated with the collective effect of inter-domain and intra-domain carrier transport. Since PBTTT is in higher extent, inter-domain transport is expected to play a dominant role. Contrary to this, NR-P3HT has relatively higher tendency of orientation in the parallel direction, therefore, charge transport in this direction should be governed by hopping through both of the PBTTT and NR-P3HT domains as schematically shown in the Figure 9. Since NR-P3HT exhibits relatively lower electrical conductivity, it will offer higher resistance towards the charge carrier transport in parallel direction.

It can be argued that whether the charge transport in this present blend system is energetically favorable or not. It has been be reported that ionization potential (IP) PBTTT (5.1 eV) is about 0.3 eV lower as compared to P3HT under similar experimental conditions.[49] It means holes induced within the channel after negative gate bias application in both of the NR-P3HT as well as PBTTT can be easily injected in to Au electrode. At the same time, holes from PBTTT have another pathway of the transport via NR-P3HT also which is energetically favorable. Device stability is another important criterion for the practical applications. PBTTT has been widely reported as air stable CP owing to its relatively lower IP having stability of 600 h at relative humidity of 4% even for non-encapsulated devices.[49] However, stability can also be enhanced either by encapsulation or adopting the top gate device architecture.[105] Although, we have not evaluated the long term device stability but it is expected that our blend system should exhibit improved device stability as compared to NR-P3HT. This is attributed to the fact that IP of the blend of two materials lies in between the component CPs and varies nearly linearly as a fraction of blending.[116] Therefore, in this present case of blend of NR-P3HT and PBTTT, the IP of the blend should always be lower than NR-P3HT hence device stability should practically be improved.

5.4 Conclusion

In conclusion, utilization of FTM as a facile solution based approach for the fabrication of orientated thin films of blends of CPs have been successfully demonstrated. In order to circumvent the trade-off issues between flexibility and high charge carrier transport, a unique strategy of casting oriented films of blends involving the addition of highly crystalline material (PBTTT) in amorphous NR-P3HT which is susceptible to high molecular orientation has been adopted. An increase in the orientation and effective conjugation length of amorphous NR-P3HT by the incorporation of small (10%) crystalline guest CP is well reflected and supported by optical and microstructural characterization. Addition of only 10% of crystalline PBTTT in the oriented NR-

P3HT resulted in to pronounced (8-fold) FET μ of the blend reaching similar value to that of pristine PBTTT. Employing higher percentage of PBTTT in the blend shows synergistically improved charge carrier transport. Thin films fabricated from the oriented blend of CPs consisting 80% PBTTT led to the improved μ by 5 fold and 33 fold compared to that of pristine PBTTT and NR-P3HT based OFETs, respectively. This field effect μ is 3 order of magnitude higher than that of its corresponding spin-coated device counterparts. Finally, attainment of such a high FET μ (0.11 $cm^2/V.s$) along with high on/off ratio (10^6) for oriented blends of PBTTT (80%) and NR-P3HT (20%) fabricated under ambient conditions without annealing to higher liquid crystalline phase temperature (> 150^oC) provides a novel strategy for fabrication of the room temperature solution processable OFETs towards the potential applications in the area of next generation flexible electronics.

Chapter 6: Orientation and Enhancement of Charge Transport in High Performance Thienothiophene

6.1 Introduction

Although, there exists reports about a number of molecular semiconductors exhibiting a decent value of field effect mobility exceeding the benchmark of amorphous silicon based devices ~1 $cm^2V^{-1}s^{-1}$ for realization of dense array of devices in circuits so that the ultimate resulting production cost can be lowered.[99,100] However, their potential application to large area flexible substrates seems to be difficult in the sense that majority of cases, high device performance was obtained only when thin films were fabricated either by vacuum deposition or using single crystals.[131,132] On the other side, utilizing conjugated polymers for OFETs is expected to enhance the application potentials due to the facile solution processability, flexibility and tailor-made synthetic versatility, which make them a promising candidate for their application in organic FET's as active layer.[133] As already explained in previous chapters, that their morphology dependent performance makes this a critical issue by different deposition techniques.[47,134,135]

In the previous chapter 5 also we have shown that PBTTT is one of the promising semi-crystalline conducting polymers and attracted huge attentions in the last decade owing to its consistent high performance.[49,100,133] Increased device performance due to facile charge transport in the PBTTT can be achieved by orientation; however, in previous chapter we have also shown that the orientation exhibited by the PBTTT was almost negligible as compared to the NR-P3HT. It is also worth to note that oriented films of PBTTT has been only reported utilizing the shear forces at an elevated temperatures utilizing their LC mesophase.[86,129,136] It is also of worth to note here that it exhibits low solubility in all common halogenated organic solvents. This low solubility could be the reason as there exist no reports neither self-assembly on templates nor time-dependent supramolecular fiber formation which are frequently available for other thiophene and fluorene based CPs.[29,79,122,123,137] Therefore, orienting PBTTT by FTM was difficult owing to its relatively lower solubility in chloroform at lower temperatures and majority of the previous reports were included the temperature range between 20 to 50 °C. This has been already demonstrated that used of high boiling point solvent like chlorobenzene results in isotropic films due to the slow solvent evaporation.[51]

In this chapter, we have demonstrated that how by optimizing the conditions as discussed in chapter 3, the orientation in PBTTT can be enhanced using FTM. It has been found that orientation can be further improved by annealing the films at their LC phase transition temperature around (140°C -160°C). The resulted film exhibited high saturation field effect mobility along the

orientation direction reaching up to 1.24 $cm^2V^{-1}s^{-1}$ representing one of the highest field effect mobility as compared to other reports with similar device configurations. The morphological characterization of the oriented film were carried out by polarized absorption spectroscopy, polarized Raman spectroscopy, AFM, out-of-plane XRD, and in-plane GIXD measurements.

6.2 Experimental Details

PBTTT was purchased from Sigma Aldrich and used without any further purification. Dehydrated chloroform, 1, 2 dichlorobenzene were purchased Wako Chemicals and Sigma Aldrich, respectively. The 1% (wt/wt) of PBTTT solutions in chloroform were prepared in dehydrated chloroform. For preparation of FTM films, about 15 µl of solutions were dropped at the center of the large petri-dish (diameter 15 cm) contacting liquid substrate (same as in chapter 5) at 55°C and floating films were stamped on the required substrates for characterization. Spin-coated samples were prepared in mixture of chloroform/1,2 dichlorobenzene (1:1) according to the thickness requirement, 0.25 wt% for OFETs and 2.5 wt% for XRD samples. Bare glass slides were used for all the characterization purpose i.e. Polarized optical microscopy, Absorption Spectroscopy, Raman spectroscopy. Samples were also annealed in argon atmosphere at 180°C for 2 minutes and allowed to cool down slowly to room temperature.

Polarized Optical Microscope images were obtained by using Olympus BX51 polarizing optical microscope (Olympus, Tokyo, Japan) in normal air atmosphere. The images were then obtained by rotating polarizer in from 00º to 90º with respect to orientation direction. UV-Vis Absorption Characterization was carried out with UV-Vis-NIR spectrophotometer (JASCO V-570). For polarized spectra Glan-Thomson Prism were added between the source and detector. Polarized Raman Spectroscopy was carried by Raman Research Institute Bangalore, India with Horiba Jobin Yvon T6400 Micro Raman using a He–Ne Laser operating at λ = 632.8 nm operated at constant power of 1.8 mW throughout the measurements. The sample stage was rotated against polarization direction of the incident beam and Raman spectra was recorded at every 30º between 00º to 90º. Surface topography was probed by AFM (JEOL SPM 5200) under tapping mode. In order to avoid any kind of variation the same OFET samples were utilized. Out-of-plane XRD and in-plane-GIXD patterns recorded with Rigaku X-ray diffractometer having Cu Kα radiations operating at 40KV and 20mA and Rigaku smart lab, respectively. The details of the measurement technique is already described in detail (Chapter 2).

BGTC geometry were adopted to fabricate OFETs. Highly doped silicon substrates having SiO_2 (300 nm) as gate dielectric (C_i = 10 nF). The surface of the SiO_2 was then treated with self-assembled monolayer (SAM) of octadecyl(tricloro)silane (OTS) according to chapter 2. Oriented films were transferred by stamping on Oriented floating films were annealed as previously. Oriented films were transferred by stamping on SAM treated hydrophobic SiO_2 followed by their annealing in argon atmosphere at 180°C for 2 minutes and allowed to cool down slowly to room

temperature. Source and drain electrodes deposition and measurements were carried out with similar method as reported in Chapter 4.

6.3 Results and Discussion

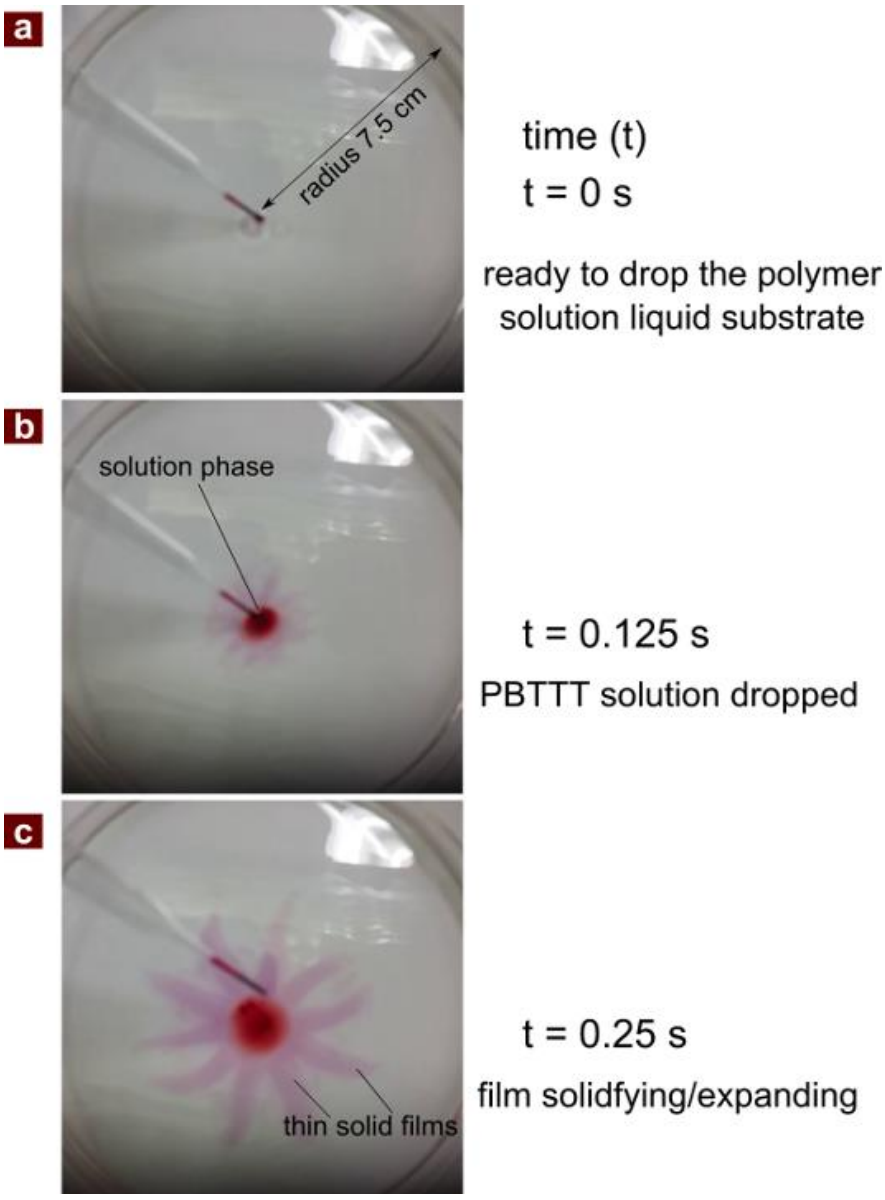

Figure 6.1 Evolution of FTM films of PBTTT with time. (a) t = 0, (b) t = 0.125, (c) t = 0.25 s.

Unlikely to other polythiophenes (P3HT, PQT-C12), the poor solubility of PBTTT can be well understood which arises from the strong interaction among their rigid rod like macromolecules and thereby making them difficult for solution processing at lower temperature of about 50°C. This is why, the choice of high boiling point solvent is required, so that they can resist high temperature

and do not evaporate rapidly. Choice of chlorobenzene, 1,2 dichlobenezene or orthodichlorobeneze is obvious for most of the conventional solution procedures for depositing the films of PBTTT [49,129,138] and is justified also since it induce slow solvent evaporation. This gives an opportunity of self-organization to the macromolecules in their thermodynamically favored state (edge-on-with respect to the surface normal). [23,24] However, casting of thin films with low boiling point solvent leading to quick solvent evaporation which offers macroscopic orientation. Therefore, for casting oriented floating films of PBTTT, PBTTT was dissolved in chloroform and heated to get clear solution before casting it on liquid substrate in similar way as stated in chapter 5, except the temperature of liquid substrate in this case which was 55°C. It should be noted that low temperature of the liquid substrate does not favore the orientation since in chapter 5 we have shown that pristine PBTTT had very little orientation when casted at 30°C. The exact reason for this difference is not clearly known, however, the possible reason could be rapid cooling of solution after dropping on the liquid substrate, thereby inhibiting the freedom of macromolecules originated by heating them. A glimpse of the casting process is shown in **Figure 6.1** (a-c).

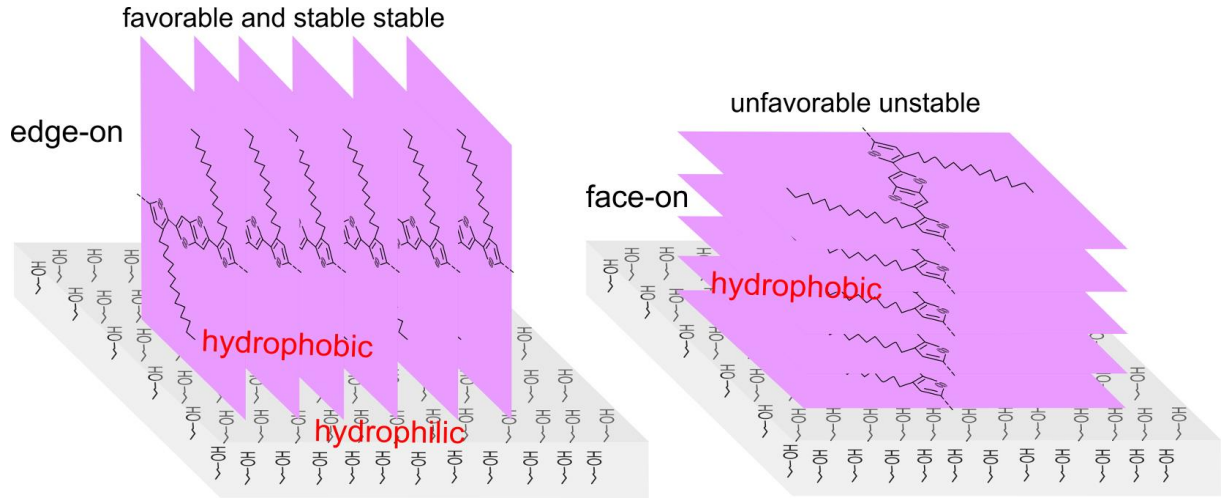

Figure 6.2 Schematic illustration showing the possible arrangement of PBTTT macromolecules on the hydrophilic liquid substrate.

The possible mechanism in detail is illustrated previously in chapter 2 (**Figure 2.3**). where the formation of the film take place by lyotropic assisted self-assembly through simultaneous rapid evaporation and solidification,[59] together with spreading/expansion of the film from the drop point. The high viscosity of the liquid substrate acts as a dragging force hindering the expansion of the film thereby inducing macroscopic orientation in the polymer chains. Furthermore this can be easily understood that viscos liquid substrates utilized in this work possesses high hydrophilicity arising from the presence of hydroxyl groups, on the other hand the PBTTT has long hydrophobic alkyl-chains orthogonal to the main chain as shown in **Figure 6.2**. Therefore the best possible configuration that PBTTT macromolecules can take at the surface is edge-on owing to strong repulsion between the alkyl chains and liquid substrate.

The orientation of the floating film and their direction of the floating film was even visible by naked eye by placing and rotating linearly polarized film. These films were stamped on the glass substrate orientation was confirmed by optical photograph with polarizer and thereafter POM as shown in **Figure 6.3**.

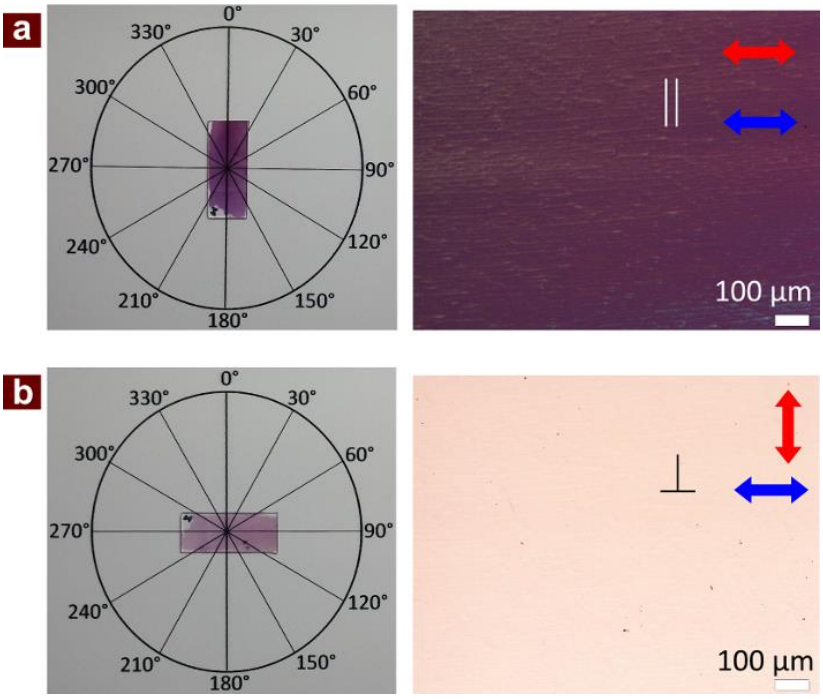

Figure 6.3 Optical photograph (left) and POM image (right) on glass substrate along the parallel and perpendicular direction of the orientation. The blue arrow and red arrow represents the orientation direction of the polymer and polarization direction of the incident light, respectively.

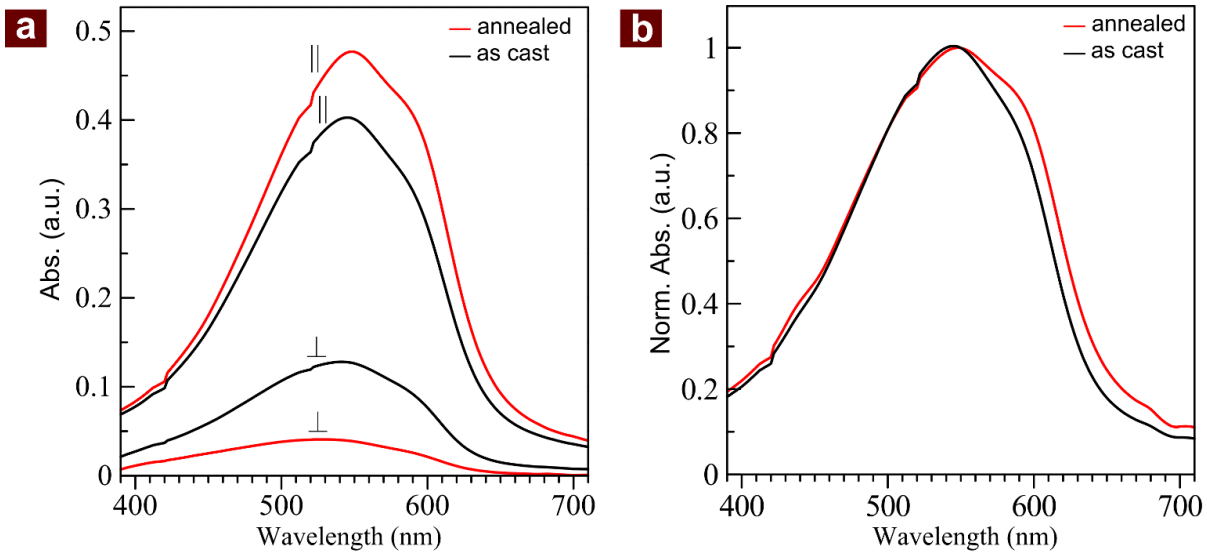

Figure 6.4 Absorption spectra of as cast and annealed FTM films of PBTTT. (a) Polarized and (b) Non-polarized.

This orientation was further quantitatively characterized by polarized absorption spectroscopy for both the as cast and annealed films at as shown in **Figure 6.4** (a). As shown in Figure 6.4 (a), The DR in the as-casted film was 3.2 in the as-cast films, which on annealing above its LC temperature increases the DR more than 10 to 13. A clear blue shifted absorption maximum in perpendicular absorption spectra represent the presence of randomly oriented macromolecules. To the best of our knowledge, this orientation intensity values are the highest till date for PBTTT C-14 both as cast and annealed.[129,136,139,140] Such high orientation was only achieved in analogous of thienothiophene (PBTTT C-12 and C-16), when the casted films were subjected to mechanical rubbing and film compression on ionic liquid respectively, Moreover these orientation processes were carried at elevated temperature near to their LC temperature and relatively less orientation below 100°C were found.[86,140]

From the perusal of the **Figure 6.4** (b), this can be seen that PBTTT films exhibited a weak vibronic structure with absorption maximum at 544 and 548 nm in as-casted and annealed films, respectively. This slight increase in conjugation length is the evidence of increase in the average conjugation length of the backbone in annealed film as compared to the as cast films. On the other hand, a pronounced vibronic shoulder in annealed films is attributed to the high degree of order in the backbones and enhanced π-orbital delocalization due to the formation of terrace phase.[68,129]

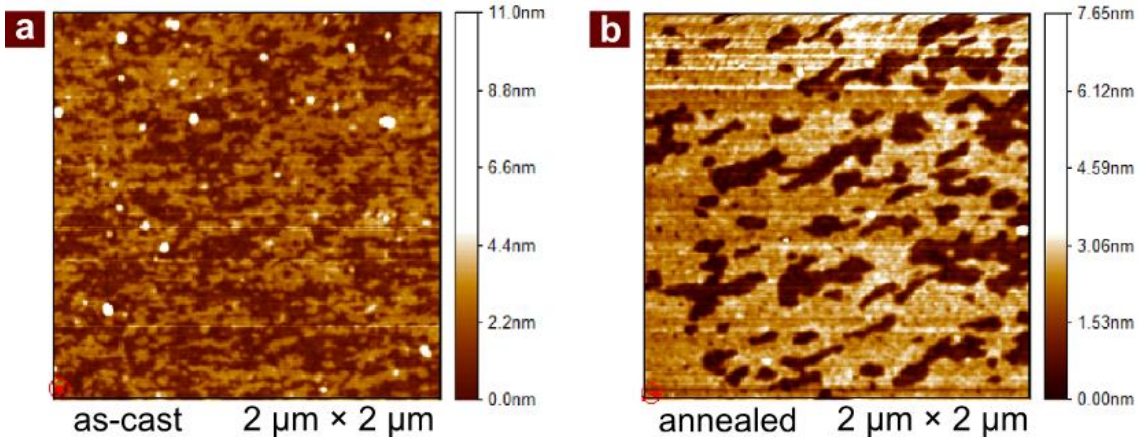

Figure 6.5 AFM image of oriented PBTTT (a) as-cast and (b) annealed on OTS treated SiO_2.

The formation of the terrace phase in PBTTT is attributed to inherent property, in which when annealing above to their LC temperature, the side chains melts and form larger domains. From the perusal of **Figure 6.5**, formation of large terrace phase domains extending up to several hundreds of nanometers can be clearly seen when oriented films were annealed on OTS treated SiO_2 substrates, which is consistent with the previous reports published by other researchers.[81,141]

To further investigate the orientation characteristics of PBTTT macromolecules in annealed oriented FTM films, Polarized Raman spectroscopy was done and spectra was recorded at intervals of 30° from orientation directions to perpendicular direction as shown in **Figure 6.6**. Major Raman peaks of the PBTTT backbone is also given in **Table 6.1**.[142] Considering the majority of PBTTT backbones will be along the orientation direction. When the uni-axially polarized beam was in parallel to the orientation direction the beam passing along the orientation direction will encounter majority of the C–C and C=C bonds resulting high interaction between the polarized laser beams.[59,58] As can be seen in Figure 3, all peaks corresponding to major bonds lying along the PBTTT conjugated backbones, which decreases in intensity while moving from 00° to 90°. The higher peak intensities related 1391 cm^{-1} (thiophene C–C stretch), 1415 cm^{-1} (thienothiophene C=C stretch), 1463 cm^{-1}(interring C–C stretch) and 1491 cm^{-1} (thiophene C=C stretch) in the direction parallel to orientation direction confirms that high PBTTT conjugated backbones are highly aligned with respect to both the other directions (30°, 60°and 90° w. r. t orientation).

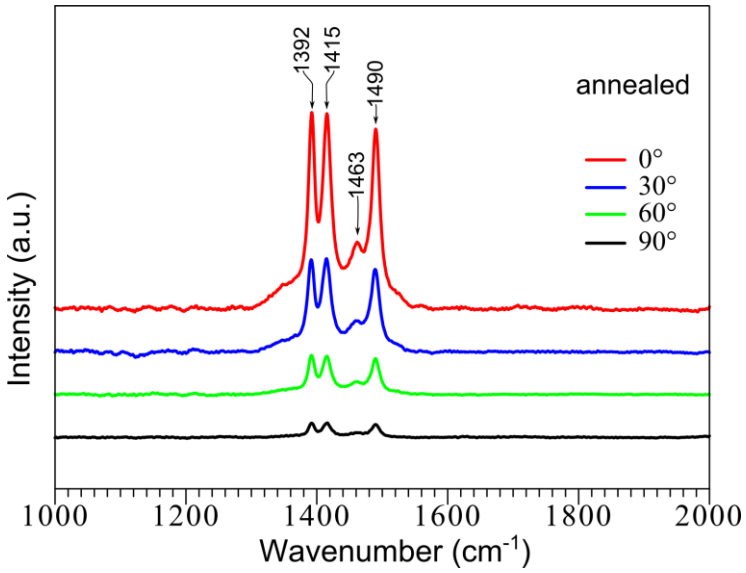

Figure 6.6. Polarized Raman spectra of annealed oriented PBTTT films. The incident angle of beam was rotated from orientation direction (0°) towards (90°) at constant interval of 30°.

Table 6.1 Typical Raman Peaks Assignments of PBTTT (c-14).

peak	frequency (cm^{-1})	assignment[a]
ν_1	1391	thiophene C–C
ν_2	1415	thienothiophene C=C stretch
ν_2	1467	interring C–C stretch
ν_3	1489	thiophene C=C stretch

[a]Peak assignment as determined by the DFT simulation in ref .[142]

Although the vibrational intensities related to thiophene C=C and thienothiophene C=C stretching, which represents the π-electron delocalization in the backbone and is more sharp with decreased full-width half-maximum (FWHM) representing high degree of delocalization along the orientation direction. However no considerable differences in the peak shift of the same was found. One important point is worth to note here that unlikely to anisotropic poly(3-hexylthiophene) (P3HT) case where significant decrease in frequency also take place for significant peak corresponding to C=C stretch as discussed elsewhere.[59,58] We do not understood the possible cause related this and may this could be the attributed to the nature of rigid-rod like behavior of PBTTT, as vibronic position of PBTTT also do not show much changes related to such in their absorption characteristics.[75,128,129] On the other hand, P3HT is well known to show such changes related to the sharp vibronic features while different kind supramolecular assemblies, as well as orientation as discussed by many researchers.[47,68,75,143]

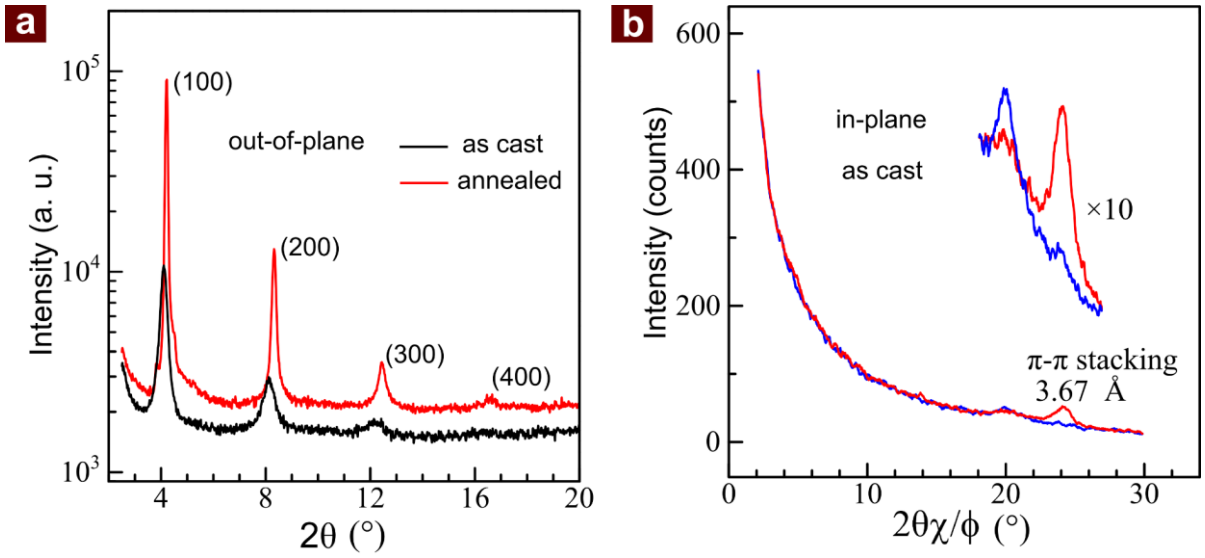

Figure 6.7 (a) Out-of-plane XRD, and (b) GIXD of oriented PBTTT film.

In order to investigate the film crystalline stacking characteristics, out-of-plane and in-plane at grazing angle XRD measurements were carried out as discussed in chapter 2. **Figure 6.7** (a) shows out-of-plane XRD patterns of oriented films on OTS treated Si wafers. A series of (h00) peaks up to 3rd order related to a-axis were observed in oriented film whereas these (h00) peaks becomes more intense after up to 4th order after thermal annealing. The *d*-spacing along the a-axis in the as-casted and annealed oriented films were found to be 21.5 Å (2θ = 4.1°) and 21 Å (2θ = 4.2°), respectively. In general the position of the peak represents the distance of lamellar stacking formation related to the interdigitated alkyl side-chains whereas sharpness relate to its crystallinity and grain size.[53,81,144] A little higher *d*-spacing in the as-cast films must be associated with the high

stretching of the alkyl side chains while the film formation process on the hydrophilic liquid, which further decreases on annealing due to increased inter-digitation due to rearrangement of the alkyl side chains while recrystallization of the melted side chains.[144,145] The possible reason for less inter-digitation in the as-prepared oriented film must be associated with the repulsion of hydrophobic side chains from hydrophilic substrates discussed earlier. Considering the sharpness of the peaks of the oriented films prepared by our method consists of higher intensity as well as sharpness (full width half maximum, FWHM) which is attributed to the film crystallinity, and as prepared and annealed oriented films prepared by this method are more crystalline.

Further in-plane GIXD measurements were carried out for the as-cast oriented films to see the orientation character more precisely (**Figure 6.7** (b)). When the incident X-ray was parallel (red) to the backbone direction peak at $2\theta = 24.2°$ was found which corresponds to face-spacing between the main-chain of PBTTT c-14 representing π-π stacking distance and found to be 3.67 Å similar to reported values.[140] On the other hand when incident X-ray was perpendicular to orientation direction only repeated unit peak was found with no π-π stacking peak. The absence of series of peaks related to the lamella stacking of the alkyl side-chains also represents that these films were edge-on with only backbone and π-π lying in plane of the substrate, which is considered to be the best spatial orientation of the crystallite to have high in-plane transport.[25] The in-plane GIXD clearly indicates that the main chains of PBTTT c-14 were aligned uni-directionally perpendicular to spreading direction of the floating film. It is also worth to note that such characterization are usually take place at with synchrotron light source and these results related to our experiments were carried out at laboratory with limited X-ray source intensity owing to high crystallinity of the films.

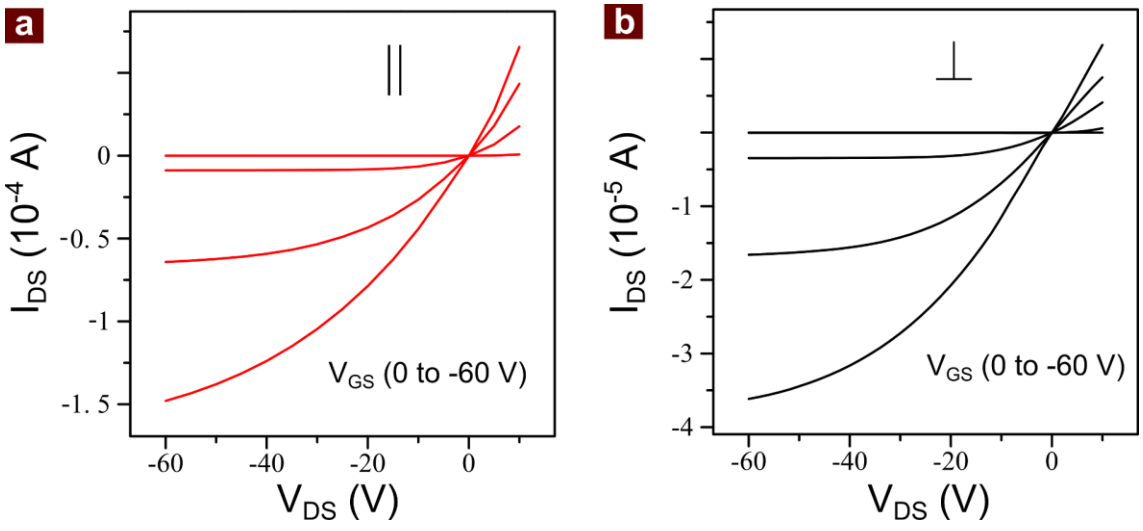

Figure 6.8 Output Characteristics of oriented PBTTT along the orientation direction of the conjugated backbone (||) (a), and perpendicular to the orientation direction (b).

Further the most important was to estimate the impact of these highly oriented film on the in-plane charge transport properties, which was estimated by fabricating OFETs having bottom gate top contact geometry. In order to compare the charge transport capability along the backbone orientation direction and π-π stacking direction, the channel direction was varied with respect to backbone orientation at different angle intervals of 30° from 0° (||) to 90° (⊥). A little variation in mobility was found in between device to device which could have originated due to the fact that charge transport in FET basically take place at the interface of the semi-conductor/insulator and the SAM of OTS at the interface of the SiO_2 treatment play an important role and may have occurred from substrate-to-substrate variation variation,[146,147] and moreover this play even more dominant role in case of PBTTT.[129,144,148] A clear p-type behavior is observed in OFETs, however high output currents were observed in the output characteristics of OFETs with orientation direction || to the substrate as compared to ⊥ same gate bias as shown in **Figure 6.8**.

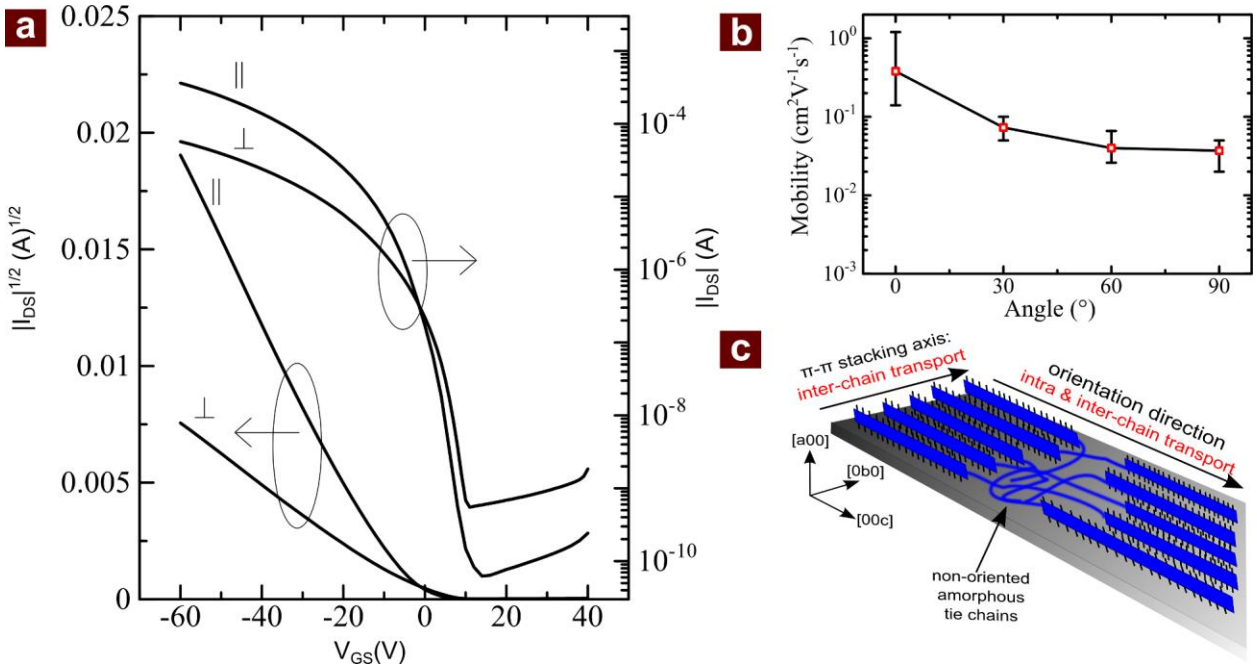

Figure 6.9 (a) Transfer characteristics parallel (||) and perpendicular (⊥) to the orientation direction of the PBTTT (V_{DS} = -80 V), (b) Variation of field effect mobility at different angle with respect to || direction, and (c) schematic illustration showing the possible charge transport in edge-on oriented crystallite. The average mobility was estimated by taking the average of at least 6 to 10 devices.

The average μ measured with channel || to the direction was found to be 0.4 cm^2/Vs with maximum μ of 1.24 cm^2/Vs on the other hand μ in ⊥ direction was found to be 0.04 cm^2/Vs (Maximum 0.05 cm^2/Vs). As shown in **Figure 6.9** (a) the devices typically had a good value of on/off ratio in the range 10^6 to 10^7. It is worth to note here that when the same material was spin coated with identical OTS treated SiO_2 the mobility was considerably low (0.07 -0.09 cm^2/Vs). The observed μ in || is among the highest reported for this material system. Previously, such performance was demonstrated by other groups which was achieved by employing high work function metal (platinum) as source and drain electrodes to decrease the metal/semiconductor

interface and decreasing channel length of 5 μm only.[149] In most of the cases, the transport anisotropy ($\mu_{||}/\mu_{\perp}$) in oriented thiophene based polymer films depends on the orientation of majority crystallite edge-on/face-on and orientation intensity of the polymer backbone. Edge-on favors low transport anisotropy and face-on orientation offers high transport anisotropy, on the other side high orientation favors high transport anisotropy. The X-ray results discussed above shows that these crystallite in oriented film exhibited ideal edge-on orientation. Previously reported edge-on oriented PBTTT films with DR=6.5 with $\mu_{||}/\mu_{\perp}$ ~ 3-5 by Lee et al.,[129] and comparable DR=13 with $\mu_{||}/\mu_{\perp}$ ~ 10 by Biniek et al. reported under similar device configurations.[86] Where as in our case the edge-on oriented films with DR~13 exhibited $\mu_{||}/\mu_{\perp}$ ~ 10, higher than Lee et al. whose thin films were prepared by heating the films above to the second phase transition temperature related to the melting of polymer backbones (ribbon phase) to induce oriented ribbon phase with edge-on crystallites. This conclude that this high mobility along the backbone direction have originated from highly uni-directionally aligned conjugated backbones.

As discussed above, in general the origin of the $\mu_{||}/\mu_{\perp}$ arise from orientation of the crystallite (edge-on, face-on, or both) and as well as the orientation intensity (DR). Previously, Hosokawa et al. have already demonstrated that with in the same thiophene having the same intensity of orientation, edge-on oriented films exhibited less anisotropy (~1 order) in the comparison to face-on (~2-3 order).[150] However, in order to further estimate the dependence of individual role of molecular orientation and π-π stacking on μ more precisely, Orientation direction of the polymer was varied at different angles with respect to the channel direction as shown in **Figure 6.9** (b). In order to avoid any kind of variation originating from device to device variation, efforts were also made to analyze the variation with in the same OFET substrates. As can be seen the there is a sharp decrease in average μ, and significant drops of ~5 times, ~9 times and ~10 times when the polymer orientation direction was at 30°, 60°, 90° with respect to channel direction. It is worth to note here among different thiophene such PBTTT is most favorable material with high μ than P3HT and PQT due to its unique high rigid rod nature, inter-digitation and ordering.[145,151] These results suggest charge carrier mobility along the backbone direction (0°) dominates due the orientation of the majority of the polymer main chains and some randomly aligned polymers (tie-chains) much be acting as transport bridge to connect the crystallite domains as illustrated in (**Figure 6.9** (c)). On the other hand, when measured at other angles the transport capability depends on π-π staking, which play an important role. This results concludes that the charge transport along the along the π-π staking direction exhibits ~1 order less in magnitude as compared to main chain direction.

It should be noted that we have not optimized the device fabrication conditions as the μ in PBTTT show increased performance on the decreasing the interfacial roughness of the dielectric,[128] precise surface treatment,[148,152] molecular weights and polydispersity index,[153] decreased channel length,[149] use of high work function electrodes,[149] and all the OFETs prepared in our case was fabricated in normal air atmosphere with PBTTT purchased and used without any purification. This can also be interpreted that when PBTTT C-14 was spin coated they showed less that the average μ (0.07 - 0.09 cm^2/Vs) achieved by optimizing these parameters (0.2 - 0.4 cm^2/Vs).[128,129]

Optimization of such parameters is beyond the scope of our present work and no effort were made to consider these parameters individually to achieve high device performance.

6.4 Conclusion

In conclusion, fabrication of highly oriented thin films of PBTTT was successfully carried out by utilization and optimization of film casting parameters during dynamic FTM as discussed in detail in the chapter 3. Under optimized condition of 1 % solution of PBTTT in chloroform, ethylene-glycol and glycerol (3:1) as liquid substrate at 55^{o}C under dynamic FTM, fabrication of thin films PBTTT led to the achievement of an appreciable DR of 3.6 which was further enhanced to >10 after its post annealing at its liquid crystalline phase transition temperature of 180^{o}C for 5 min. The orientation characteristics were further characterized by polarized Raman spectroscopy and GIXD, where results supported the uniaxial orientation of the backbone along the orientation direction. The measured μ along the orientation direction arising from the uni-axial alignment of the conjugated backbone showed very high μ of 1.24 $cm^2.V^{-1}.\ s^{-1}$ which is one of the best reported values for this conducting polymer.

Chapter 7: Layer-by-Layer Parallel and Orthogonal Coating of Oriented Conjugated Polymers

7.1 Introduction

Solution processed semiconductor thin film is one of the important features for organic electronics which enables us for large scale and facile fabrication of thin film photonic and electronic devices. Device performance strongly changes with the film morphology of the semiconductor layer.[23,24,52] Casting procedure of semiconductor layer from solution is, therefore, the key-technology to fabricate organic electronic devices. Drastic change in the organic device performance is essentially caused by the anisotropic structure of conjugated molecules and polymers.[47,51,136,154] Molecular alignment is, therefore, very important to induce the potential performance for organic semiconductors. Conjugated polymers are structurally the most anisotropic organic semiconductors due to their one-dimensional expansion of conjugation on main-chain. In the recent past, amorphous film formation has been favored for reproducible electronic performance due to its uniform characteristics.[155] Currently, however, it has been realized that high transport performance is required in semiconductor even with the existence of anisotropy in carrier transport.[47,51,136] This offers a strong urge for suitable thin film fabrication processes capable of promoting the alignment of macromolecules in order to attain enhanced device functionality.

Molecular ordering is essentially required to improve the intermolecular transport for organic semiconductors, where drop-casting is thermodynamically favorable to attain this goal.[27] Drop-casting of semiconductor-solution directly onto the device substrates, however, sometimes results in to partial bumps (islands) or non-uniform thickness, which is supposed to be originated from pinning effect or coffee-ring effect by the solution-solid substrate interactions. Due to the large volumetric reduction during solvent vaporization, discrete solidification results in to the failure of uniform thin-film formation on the solid substrate. In such process, if the substrate surface can move to provide the chance for joining the solidifying parts together it will promote to cast a uniform thin-film. This indicates the importance of utilization of "liquid- or fluid-substrate" for drop-casting process. In the case of hydrophobic semiconductor solution, hydrophilic materials such as water, ethylene glycol and/or glycerol can be utilized as the liquid-substrate for the casting. On liquid-substrates, we obtain the organic semiconductor thin-film as a floating-film after the solvent evaporation, which can be easily transferred on a desired substrate by stamping. The procedure for casting a thin floating-film followed by its transfer on desired substrate can be expressed as floating-film transfer method (FTM).[18]

Gradually vaporizing solvent after the expansion of dropped semiconductor solution on the liquid-substrate semi-statically provides a floating-film in FTM (represented as static-FTM). In contrast, simultaneous solidification of the floating-film along with the expansion of the semiconductor solution is dynamically occurred just after dropped on the liquid surface (represented as dynamic-FTM), leading to a concentric orientation of conjugated polymers. PQT as well as polyfluorene derivatives can easily oriented by this procedure.[20] The solvent volatility of semiconductor solution, generally, identifies the types of FTM. Namely, under ambient condition static-FTM occurs after the complete expansion of semiconductor solution utilizing high boiling point solvents like chlorobenzene because of their slow evaporation. In contrast, for dynamic-FTM semiconductor solution prepared in the relatively low boiling point solvents (such as chloroform, tetrahydrofuran and dichloromethane) leads to simultaneous film expansion and solidification.[75]

Casting of thin-films at the air-liquid interface proceeds under isothermal condition like Langmuir-type methods have been studied and developed by many researchers.[156] Introduction of liquid-crystal molecules with conjugated polymer successfully forms transversally oriented films where thin-film is formed by applying surface pressure in Langmuir isotherm.[157] In contrast, in the dynamic-FTM self-caused motion of liquid substrate and/or semiconductor solution spreading on the liquid-substrate, casts a thin floating-film automatically. These differences suggest that FTM process should be characterized little apart from the Langmuir process in spite of their methodological analogy.

Transverse orientation methods of conjugated polymers also have been developed and investigated by many researchers.[33] In these reports, fine orientation of conjugated polymers at micrometer-scale along with the demonstration of high optical and electronic dichroism. Most of these methods prepare oriented films directly on the device substrate, for example, mechanical rubbing, friction transfer and flow-coating with post-annealing.[54,86,138]

These methods essentially require various chemical, mechanical or thermal stimuli for the promotion of macromolecular orientation. At the same time, these stimuli provide mechanical and/or chemical damages on the coated-surface, in particular, the surface consisted of soluble or soft organic materials. This makes it impossible to build up organic multi-layered fine structure, which is a bottleneck for the application of in particular oriented functional layers into organic electronic devices. FTM is essentially consisted of the two-step processes, namely to pre-cast an oriented thin-film as solution process followed by the post-transfer of the film on the solid substrate like a dry process. The isolation of the orientation process from the coating process enables us to overcoat the oriented film on any surface without chemical or mechanical damages. In particular, conjugated polymer acts as active layer for photonic and electronic devices. As already mentioned above the device performance is sensitive to the film morphology as well as the film purity. Thus, a mild coating procedure of organic semiconductor-layer with conserving the oriented film-

morphology and without the mixture of organic semiconductor with under-lying other materials is strongly required for fabricating organic devices consisted of multi-layered fine structure. In this context, FTM as the solution-based casting procedure provides a mild coating while maintaining the purity as well as the morphology both in the under-coated and the over-coating layers as previously shown in chapter 2 (**Figure 2.3**). Recent past has witnessed the design and development a variety of conjugated polymers in order to provide the tailored functionality.[158,159,4]

For analyzing newly synthesized materials, spectroscopic characterizations are very powerful way to clarify the chemical structure at molecular level. The polarized analyses of the oriented film provide further details about the structural information together with non-polarized spectra. A quick casting method to prepare the oriented thin-film with minimal materials wastage is, therefore, very useful for the material characterization utilizing polarized spectroscopy. In this chapter, we propose dynamic-FTM as one of the candidates to prepare the multi-layered films consisted of oriented polymeric materials. The oriented multi-layer formation renders the realization of anisotropic electronics into the practical devices.[19,22] The proposed dynamic-FTM is not only simple and quick oriented film casting procedure but also leads to the utilization of small amount of the materials with minimum wastage. In this study, we investigated the orientation characteristics of dynamic-FTM films with conjugated polymers. Efforts have also been directed towards the preparation and characterization of multi-layered oriented films of conjugated polymers fabricated using dynamic-FTM.

7.2 Experimental Details

All of the chemicals and the reagents employed in this work are used without further purification. Three types of conjugated polymers, viz. NR-P3HT, PQT and F8T2 were synthesized as per the reported procedures.[41,42,50] Major emphasis in this study has been directed with NR-P3HT as the main polymer due to the fact that it is easy to prepare well-oriented floating-film and to check the orientation intensity simply by the naked eyes through a polarizer-film easily.[47] Typically, 10 mg of polymer powder was dissolved in 1 ml of dehydrated chloroform to obtain a uniform 1 % (wt/wt) semiconductor solution.

Hydrophilic liquids such as water, ethylene-glycol and glycerol were chosen for the materials of liquid-substrate to cast floating-films. Solvents were well-mixed at an appropriate mixing ratio in order to tune the viscosity of the liquid substrate and temperature was also optimized for obtaining the high orientation.[67] The mixture was poured in a 15 cm-diameter petri-dish, stirred and controlled at a suitable temperature. The dynamic-FTM was carried out by putting single droplet (about 10-20 μl) of semiconductor solution at the center of liquid-substrate without touching the pipette on the liquid-surface. After the semiconductor solution quickly spread and formed a floating-film, it kept drying for about 20-30 seconds. A fairly oriented part of the floating-

film was selected and transferred on a solid substrate by stamping similar to Langmuir-Schaefer method. The transferred film-surface was washed with methanol followed by air blowing. Thickness of single layer film was found to be about 20-30 nm as confirmed optical non-contact surface profiler. Spin-coated films of NR-P3HT were also prepared for comparison. Multiple parallel-coatings were conducted for the fabrication uniaxially oriented films in the similar way as described above. For the polarized film characterizations about 50 times parallel-coatings have been done in order to obtain a thick-oriented film of about 0.75 μm for analysis. A thick spin-coated film was also prepared from the 2.5 % (wt/wt) semiconductor solution at 1500 rpm for 120 second to obtain 0.70 μm thick film for the comparison.

Transparent white-glasses were used for polarized absorption spectroscopy. Suitable size of pure Si-wafer pieces were coated NR-P3HT by FTM and subjected to thickness measurement, Fourier transform infra-red (FT-IR) spectroscopy and atomic force microscopy analyses, Si-wafer surface was treated with hexamethyldisilazane for the good adhesion of floating-films. Polarized absorption spectra were measured through a Glan-Thomson polarizing prism with Jasco V-570 spectrophotometer. FT-IR spectra were measured through a polarizer unit with Jasco FTIR-4100. Film thickness was estimated with Nikon Eclipse LV150. Dichroic ratio (DR) has been taken as the index of orientation intensity and estimated by the ratio of absorption maxima in the case of parallel and perpendicular-polarized absorption spectra as per our earlier publication.[67]

7.3 Results and Discussion

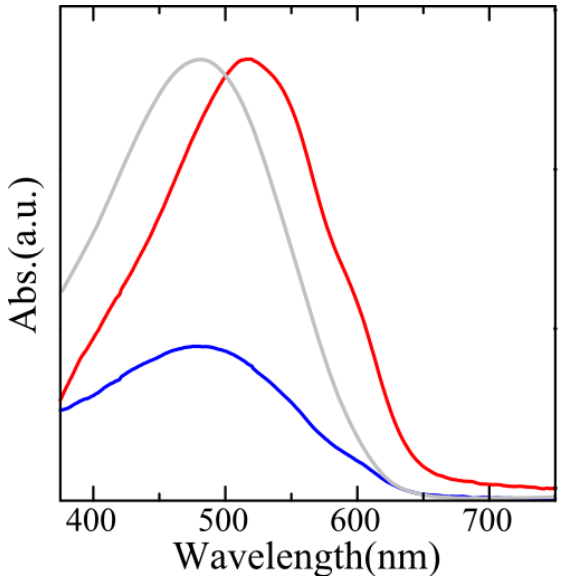

Figure 7.1 Polarized Absorption spectra of NR-P3HT film oriented FTM (red: ||), (blue:⊥). Gray lines represents the absorption spectra of spin coated NR-P3HT.

Figure 7.1 shows the polarized electronic absorption spectra of each FTM and spin coated films where spin-coated films of NR-P3HT exhibit a featureless absorption spectrum having

absorption maximum at 480 nm. This main absorption peak has been assigned to the electronic absorption associated with the amorphous phase.[76,93,160] This indicates that the NR-P3HT intrinsically forms an amorphous-rich film by spin-coating. On the contrary, for NR-P3HT parallel-polarized absorption spectrum of oriented film shows the main peak at 525 nm, which is strongly red-shifted as compared to the spin-coated one. Vibronic shoulders were also clearly observed around 550 nm and 600 nm. The absorption spectral profile of parallel oriented FTM films of NR-P3HT is almost similar to that of RR-P3HT films.[93] The vibronic shoulders at 550 nm and 600-610 nm are assigned to the 0-1 and 0-0 vibronic transitions, respectively, and their appearance suggests the presence of well-expansion of π-conjugation length.[161] This indicates that FTM effectively stretches NR-P3HT macromolecules like RR-P3HT in spite of their low regioregularity (~80%).

A different spectral profile was observed in the perpendicular-polarized absorption spectrum of oriented NR-P3HT film similar to chapter 3 and chapter 4. Although week vibronic shoulders are seen in the perpendicular spectra, the mismatch in the spectral shapes between this and the parallel one has been attributed to the still existence of amorphous region in the film as non-oriented part.[67,93] A similar spectral mismatch was also reported in the oriented RR-P3HT films also although the origin of the spectral mismatch has not yet been clearly discussed and clarified.[54,77] It should be noted that PQT as well as other thiophene-based conjugated polymers such as PBTTT also shows similar vibronic spectra.[138]

Characterization of parallel-coated multi-layered NR-P3HT films

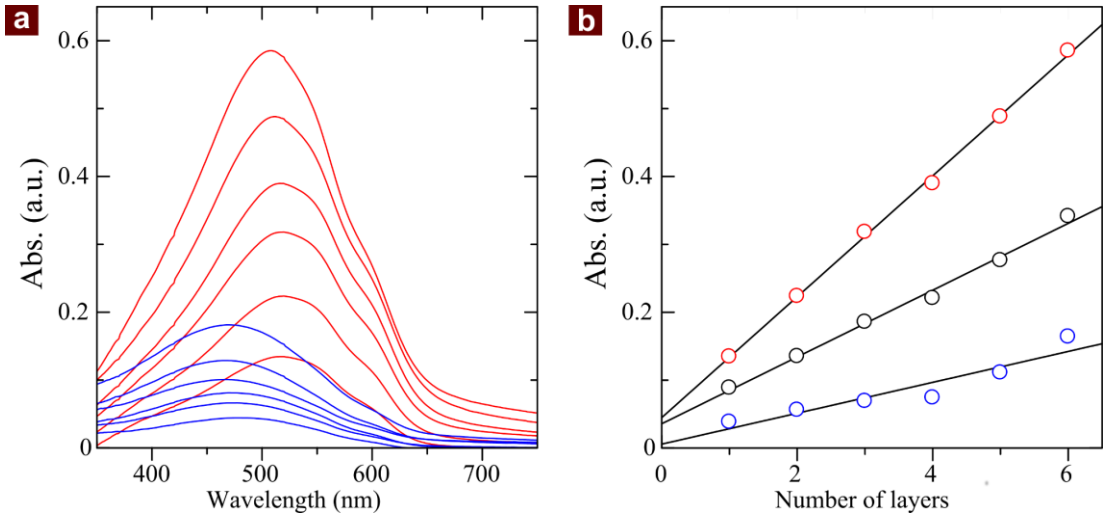

Figure 7.2 (a) Evolution of polarized spectra with layer-by-layer coating in parallel direction and (b) peak height as a function of layer numbers in oriented NR-P3HT films. Red, blue and black colors represent the peak-height of the parallel-, perpendicular- and non-polarized ones at about 520 nm vibronic peak, respectively. Each polarized spectra in (a) can refer the number of layers in (b) adjusted with the peak height of absorption.

Figure 7.2 (a) shows the evolution of polarized absorption spectra of oriented NR-P3HT films with layer-by-layer coating in parallel direction by FTM. As can be seen, the intensities of absorption peak in both the polarized spectra were found to be increased as a function of increasing layer number. In spite of the repetitive manual coating from the oriented region of floating-film, similar DR was maintained for each layer coatings. All of the parallel- or perpendicular-polarized spectra consistently show very similar profiles, indicating that all of the coated layers have similar orientation morphology. The linear relationship of the peak height of non-polarized spectra found as a function of layer number as shown in **Figure 7.2** (b) represents that each layer has a similar thickness and this is similar to that of non-oriented multi-layer coating by Langmuir process. The linear relationships in both of the parallel- and perpendicular-polarized spectra also imply that DRs in all the coated layers are almost the same. This fact enables us to prepare various thickness of oriented film by multiple about 20 nm-thick single layers. At the same time the dynamic-FTM provides over-coating of an oriented film without interlayer-interferences.

It should be noted that there is small blue shift of 1-2 nm in the parallel spectra of NR-P3HT at each layer making the total shift of 8 nm in 6 layers, however there is no such differences were observed in the DR. Although such little differences is possible in spin coated spectra where the increase in thickness caused by high concentration reduces the chances of macromolecules to rearrange while drying. However, since in FTM each individual layer is prepared individually there could be any other possible reason which is not clearly known at present and need further in-depth investigation.

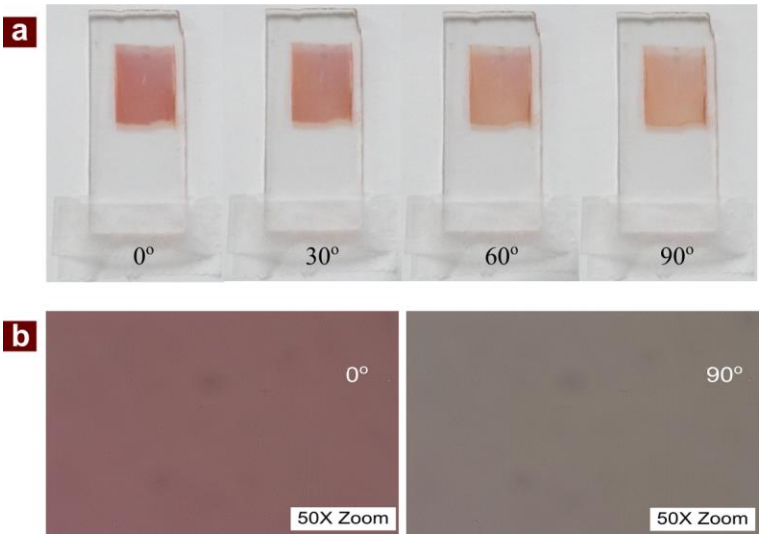

Figure 7.3 (a) Photographs of a 5-layered oriented NR-P3HT film coated on a white glass (1cm width and 2 cm height) taken through a polarizer. Polarized angles based on the oriented axis are 0°, 30°, 60° and 90° from the left to the right ones, respectively. (b) Polarized Microscopic Images at 0° and 90°. The small spot present in the POM images are basically due some stain in the lens.

Figure 7.3 (a) shows the photographs of parallel-coated 5-layer films on glass substrate taken through a polarizer. A perusal of the photographs clearly corroborates that original reddish color of NR-P3HT is faded into orangey color as a function of polarized angle. These photographs represent that whole the coated layer orients almost into the same direction at this macroscopic scale. FTM enables us to cover whole of the centimeter-size substrate with various thicknesses. These facts draw us the quick analysis of anisotropic characteristics of π-conjugated polymer by standard equipment with simple polarizer, and also the easy incorporation of oriented semiconductor layers into organic devices. In addition, to consider both of the surface morphology of the oriented NR-P3HT film observed with AFM (**Figure 4.2** (chapter 4)) and the homogenous polarized color change of the film shown in the **Figure 7.3** (a), the stretched nanoscale objects are continuously aligned throughout up to several centimeters. This means that about 4- or 5-order of magnitude scale orientation of these nano-structures prevails in the whole film. This is also one of the important features of dynamic-FTM to prepare a large (at least centimeter)-scale oriented π-conjugated polymers. This difference in color contrast has been also observed when this was subjected to polarized optical microscopy as shown in **Figure 7.3** (b).

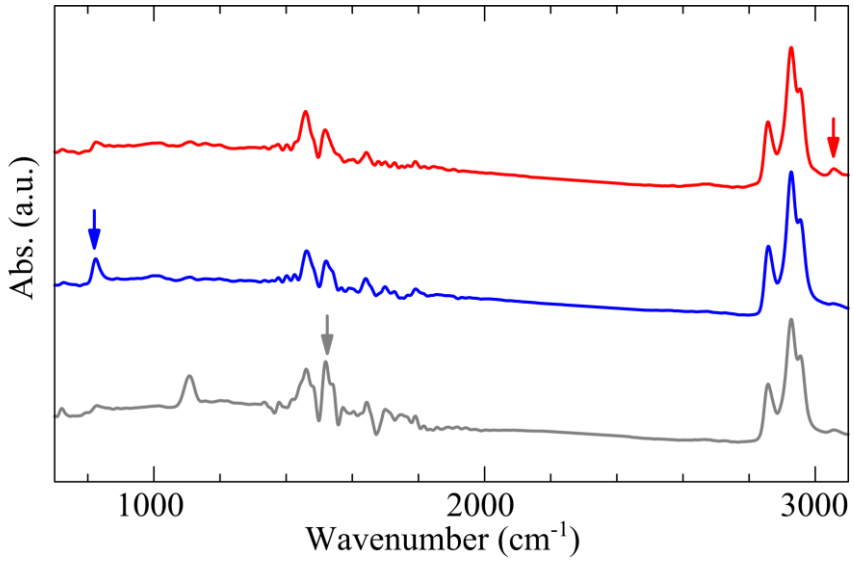

Figure 7.4 FT-IR absorption spectra of NR-P3HT films. Red and blue lines are parallel- and perpendicular-polarized spectra of a parallel-coated multilayer (about 50-layer) film, and gray line is non-polarized spectra of a spin-coat film, respectively. Red-arrow at 3059 cm^{-1}, blue-arrow at 823 cm^{-1} and gray-arrow at 1517 cm^{-1} are guided for the featured peaks in each FTIR spectrum.

Figure 7.4 shows the (polarized) FT-IR absorption spectra for spin-coated and parallel-coated multi-layer NR-P3HT films. Although all the spectra essentially exhibit similar profiles but their detailed comparison clarifies the several differences in absorption band and its intensity. The parallel-polarized spectrum exhibits enhanced intensity at 3059 cm^{-1} (red-arrow) as compared to that of the perpendicular-polarized one.[56] This is assigned as C-H stretching mode in thiophene-ring. In contrast, CH-out-of-plane deformation mode at 823 cm^{-1} (blue-arrow) shows a clear inverse

dichroism.[56] The apparent contrast of these two peaks clearly supports the uniaxial orientation of P3HT main-chain.

It is interesting to note that the stretching vibration at 1517 cm^{-1} (gray arrow) related to antisymmetric modes of thiophene-ring get enhanced in spin-coat (amorphous-rich) film.[162] The perpendicular-polarized spectrum (blue line), intensity of the vibration bands at 1458 cm^{-1} is found to be relatively reduced than that at 1517 cm^{-1} as compared to that in parallel-polarized spectra. These correlations are well-corresponded to the assignment of electronic absorption peaks as already discussed above with **Figure 7.1**. Namely, the amorphous-rich film shows the relatively enhanced absorption at 480 nm in **Figure 7.1** and the 1517 cm^{-1} vibration band in **Figure 7.4**, coincidently. It should be noted that expansion of π-conjugation has been correlated with the intensity of 1517 cm^{-1} against 1458 cm^{-1} based on FT-IR spectral investigations for a series of thiophene oligomers.[56,162,163] This seems to be contradictory compared to the result shown in the **Figure 7.4**. In P3HT, since all the thiophene-rings are connected at both (α- and δ-) sides, strong stresses applied on the thiophene-ring. Amorphous structure enhances these stresses on the ring, which evidences the chemical connection of many thiophene-rings as the extrapolative structure in the series of thiophene-oligomers. Against this, in the crystalline phase of P3HT many thiophene-rings form as the trans-configuration of main-chain. This reduces the double side stresses and rather an isolated mechanical effects for the thiophene-rings. Such effects will increase 1458 cm^{-1} with decreasing 1517 cm^{-1} from amorphous-rich to crystalline rich domains.

It should be noted that in order to obtain the polarized FT-IR spectrum (this chapter **Figure 7.4**) as well as GIXD profiles shown in previous chapters (chapter 4 **Figure 4.3** (b) for NR-P3HT and chapter 6 **Figure 6.7** (b) for PBTTT), a thick film (about 1μm) is commonly required for the orientation analysis by using standard equipment.[82,56,57] FTM can easily provide oriented thick film simply by multiple parallel-coatings with small amount of the materials. For FTM single drop (about 10 μl) of the semiconductor solution casts around 10-25 cm^2 floating-film. Several parts from single floating-film can be transferred for parallel-coating of oriented films. About 5 times of parallel-transfer can be easily done to coat well-oriented layers on the solid substrate from single floating-film. Commonly 1% (wt/wt) semiconductor solution is used for FTM. This indicates that 1 mg of π-conjugated polymer dissolved in 100 mg of chloroform renders coarsely 30 layers for parallel-coating. This layer-number is enough to prepare an oriented thick-film for device fabrication as well as for film characterizations. In addition, these coatings can be carried out with common laboratory apparatus such as pipet, petri-dish, hydrophilic-liquid, solvent and very small amount of target polymer. Therefore, the macroscopic orientation, ease in fabrication, parallel-coatings as a thick uniaxially oriented film prepared by small amount of the materials in FTM becomes the key-technology for polarized characterization of synthetic materials for chemical analysis.

Orthogonal coatings of oriented π-conjugated polymers

Orthogonal coating of conjugated polymers is also the interest counter-process having technological potential in the area of anisotropic optoelectronics. Mismatch of orientation direction consisted of homo-polymer reduces the uniaxial anisotropy. Figure 7.5 shows the distribution of peak absorption intensity of the films as a function of polarized angle mapped on the *x*-*y* plane. Although the orthogonally double-layered film represents circular trace on the *x*-*y* plane like a non-oriented film but it is not a perfect circle.

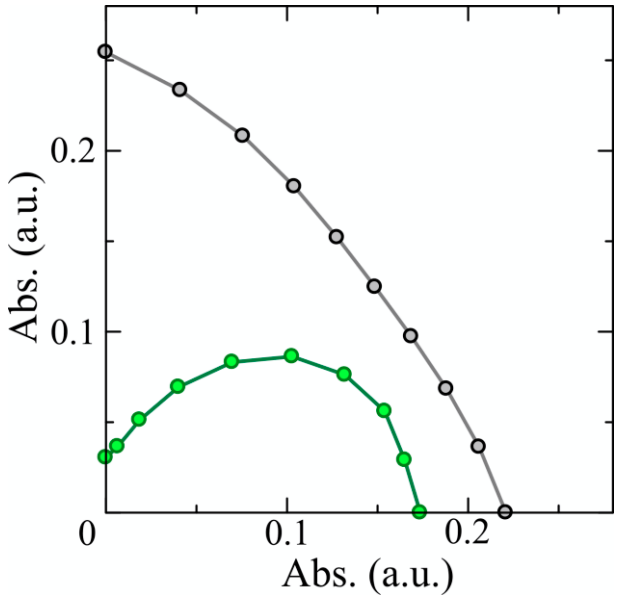

Figure 7.5 Peak intensity distribution as a function of polarized angle plotted on the *x*-*y* plane. *x*-axis is defined as the orientation direction of the bottom layer. Green and gray plots indicate the bottom (single-layer) film and the orthogonally-coated (double-layer) film, respectively.

These characteristics illustrates that both of the over- and under-layers maintains their orientation morphologies. The absorption spectra of this double-layer film still show vibronic profile unlike a spin-coated one. Concerning the good conservation of the film morphologies in orthogonal coating, each layer maintains the vibronic structure as discussed above. This indicates that we can prepare a non-oriented NR-P3HT film consisted of well-stretched polymer main-chains by the oriented multi-layer coatings into various direction. This possibly provides some unique functions to organic devices.

To clarify the orthogonal coatings and its implications on the optical characteristics, we have chosen two different π-conjugated polymers viz. PQT and F8T2. As shown in **Figure 7.6** (a), the main optical absorption-bands of PQT and F8T2 are located around 450-600 nm and 400-500 nm, respectively.[21,164] In addition both of these polymers can be well-oriented by FTM.[20] Orthogonal double-layer has been prepared by over-coating of an oriented F8T2 film onto the oriented PQT film. Owing to the relative mismatch in absorption maxima, we can easily find the changes in the spectral profile as a function of the polarization angle as shown in the **Figure 7.6** (b). Relatively strong vibronic modes were still maintained in both the oriented PQT and F8T2

layer indicating their extended π-conjugation length of both layers. This also represents less-interference on the film-morphologies in both the under- as well as the over-layers even after orthogonal over-coating. Observed polarized-angle dependence in the film spectra implies that the polarized-light can pump a proper inner-layer even though the illuminated surface is covered by a low-bandgap material like as schematically illustrated in **Figure 7.6** (c). The layer-by-layer coating technologies of oriented π-conjugated polymers enable us to explore anisotropic electronics with oriented multi-layer architecture.

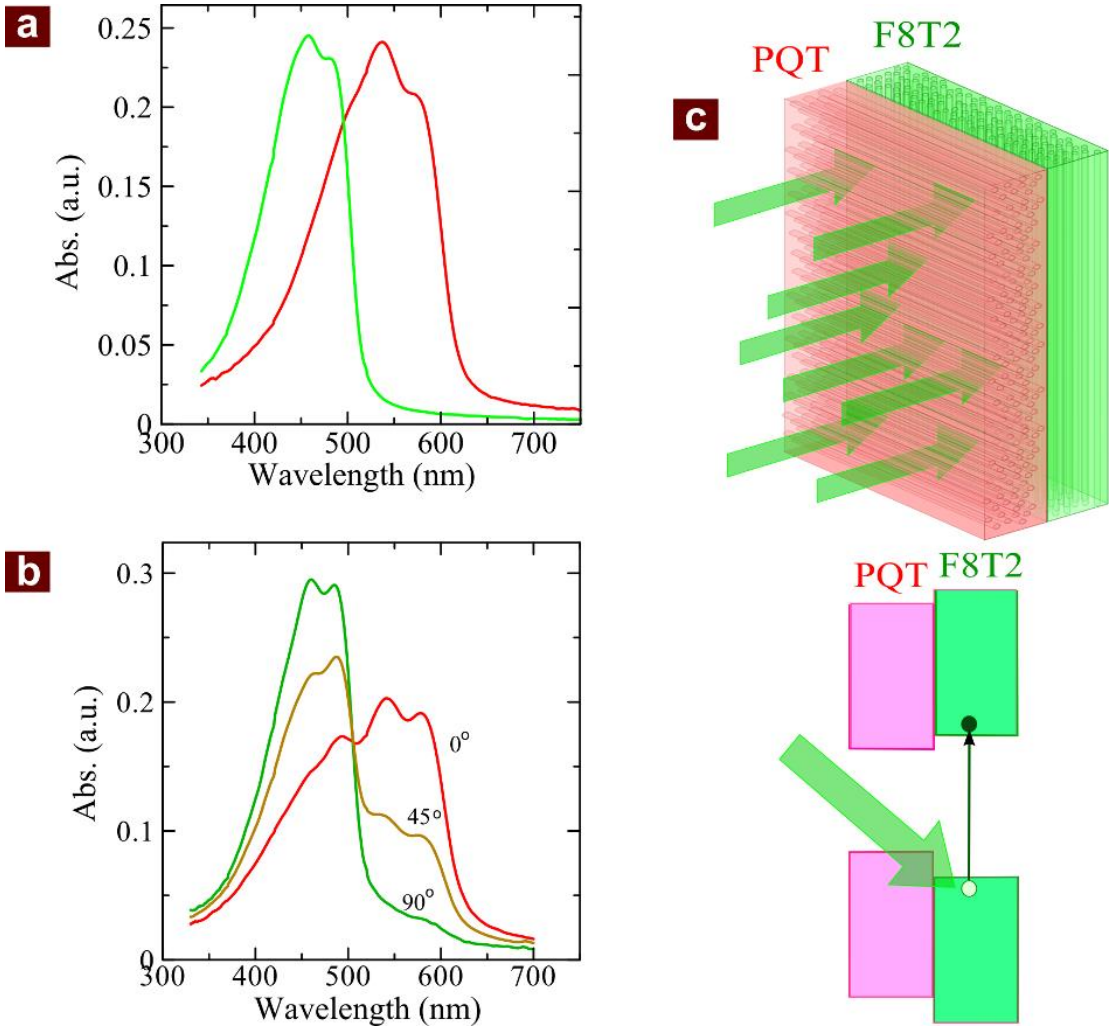

Figure 7.6 (a) Absorption spectra of individual FTM films of PQT (red) and F8T2 (green), (b) Polarized electronic absorption spectra of an orthogonally-coated (double-layer) film consisted of oriented PQT and F8T2. The values inside represents the polarized angle based on the PQT orientation. (c) Schematic illustration of the polarized-monochromatic (about 480 nm) light illumination parallel to the F8T2 orientation.

7.4 Conclusion

Multilayer coating of CPs without having any detrimental effect on the under layer from over layer is one of desired pre-requisite for the versatile application of thin film devices. A variety of multi-layer coatings consisted of oriented conjugated polymer-films by dynamic-FTM have been successfully demonstrated. It has been clearly shown that it is possible to conduct parallel coatings of oriented NR-P3HT films while preserving the macromolecular orientation as well as the anisotropy. Multi-layered parallel-coating enables us to prepare uni-axially oriented films with variable thickness utilizing oriented NR-P3HT films. Polarized FT-IR analysis has been successfully carried out using an oriented thick film prepared by parallel coatings under dynamic FTM. Orthogonal double-coatings consisted of homo-polymer (NR-P3HT) as well as hetero-polymer (PQT/F8T2) has been also demonstrated utilizing polarized electronic absorption spectra. These results suggest unique application of the oriented multi-layer structure functionalized by their anisotropic architecture.

Chapter 8: Conclusion and Future Work

The work presented in this dissertation provides the insights pertaining to the orientation characteristics of conjugated polymers in floating film transfer method and their application towards improving the carrier transport in organic electronic devices with especial emphasis on OFETs.

In the first chapter, understanding the basic role of conjugated polymers for acting as a semiconducting material, role of their morphology for increasing the performance has been emphasized with especial emphasis on the orienting them at macroscopic level has been explained. The problems pertaining to the solution processing techniques together with the techniques utilized for orienting conjugated polymers has been explained. The sole purpose of this chapter is to furnish the basic knowledge required to understand the aim with which this work has been carried out. The second chapter, brief introduction of the materials utilized as conjugated polymers, different experimental methods adopted to characterize the morphology of oriented films and fabrication of OFETs have been presented.

In chapter 3, Taking the consideration of the orientation characteristics of many well-known thiophene based conjugated polymers (NR-P3HT, RR-P3HT, PQT, and PBTTT), basic understanding have been developed in terms, such as 1) What is needed to orient these conjugated polymer in FTM. For this, the obvious two important things were considered, firstly, physical parameters of the casting procedure responsible for orientation and have been investigated in detail through NR-P3HT. It was also demonstrated that optimization of the same physical parameter results in highly oriented thin film. 2) To probe the role of chemical structure (more precisely backbone structure) of the polymers have been taken into the consideration and linking them with their ability to show LC behavior. This chapter provided a basic conclusion that orientation can be easily optimized in a given conjugated polymer provided that conjugated polymer has the ability to orient. For the study originating from the polymer backbone, all the thiophene based polymer was chosen in order to predict the origin of difference and similarity in orientation characteristics. This work was the most crucial part to understand; however, understanding have been established at the end related to casting factors and physical properties related to their liquid crystalline

behavior of the conjugated polymer under investigation related to orientation ability of the polymer was rather more important, because if the any polymer will have the ability, the later part related to the optimization of the casting condition can be easily fixed to achieve their highly oriented thins floating films for characterization and application.

In chapter 4, detailed optoelectronic characterization was carried for the highly oriented NR-P3HT film obtained from optimizing the parameters investigated in chapter 3, interestingly the more pronounced vibronic features with red shift and formation of macroscopic nano-fibrous domains increases the carrier mobility by 2 order of magnitude (~10^{-3} cm^2/Vs) in comparison to isotropic films prepared by spin coating (~10^{-5} cm^2/Vs). This improved results were of significant interest in respect to understand the charge transport in these oriented NR-P3HT more precisely and the reasons were 1) Since NR-P3HT do possesses low interdigitation and are highly amorphous in nature; therefore, the expected origin of such improved mobility could not have originated from the high orientation only of the NR-P3HT, 2) Considering the reason 1 to be true, the improvement might have originated by the formation of oriented macroscopic domains. Moreover, since this NR-P3HT was previously ignored from the scientific community due to their low mobility in spite of their good mechanical flexibility owing to their presence of high entanglement from regio isomers. These results instigated me to think of the perspectives which can promote the charge transport further, and has been discussed in detail in chapter 5. Plans were proposed to increase the performance of in NR-P3HT, First was to decrease the entanglement by incorporating some guest rigid rod like conjugated polymer PBTTT, which can increase the orientation character and they can act like as high performance transport bridge in between the domains of these NR-P3HT which were thought to be capable having high intradomain transport. The detailed optical and microstructural characterization resulted in increased orientation by decreased the entanglement resulted in synergistic improvement of field effect of mobility reaching (~10^{-1} cm^2/Vs) driven by interplay of orientation and blending.

Looking from the perspective of mobility and present interest of the scientific community, PBTTT is one of the promising candidate because of their high charge carrier mobility. In chapter 6, efforts were directed in orienting by FTM, it was found that and initial orientation in PBTTT can be easily enhanced by heating above to their liquid crystalline temperature. The DR achieved was consistent and above 10, and later it was found that the charge carrier mobility along the orientation

direction was considerably high (~0.4 cm^2/Vs) with maximum reaching 1.2 cm^2/Vs which was considerably higher (~ 1 order) if spin coated under similar device conditions. The angle dependent mobility was also carried out to understand that up to what extent this mobility depends on orientation with in the same film.

Chapter 7 was dedicated to interesting advantage of this FTM method where layer-by-layer coating in the same oriented direction as well as in the orthogonal direction have been demonstrated. This work suggested that the coating of succeeding layers do not alter the morphology of the former layers, which was one major achievements. Orthogonal layers between two different kind of conjugated polymers is also demonstrated towards future anisotropic optoelectronic devices.

The future outlooks of the present work includes more detailed analysis of this orientation behavior and how to induce orientation in polymers which don't show any liquid crystalline behavior. Furthermore a parallel research towards orienting n-type of conjugated material are highly desired which can be achieved by either orienting them individually or by assisting their orientation with those which can be easily oriented. Since anisotropy has the only advantage of improving the carrier transport, however the interesting work would be coating different n-type material and p-type materials could lead to the development of flexible high performance inverters. Another interesting work could be realization or orthogonally coated films for the realization of LEDs which shows different color on the changing polarization direction, or in other sense it would be color changing light emitting diode.

References

1. Sun, Y. & Rogers, J. A. Inorganic semiconductors for flexible electronics. *Advanced Materials* **19,** 1897–1916 (2007).
2. Printed electronics. Available at: https://en.wikipedia.org/wiki/Printed_electronics. (Accessed: 21st May 2017)
3. Sirringhaus, H., Tessler, N. & Friend, R. H. Integrated Optoelectronic Devices Based on Conjugated Polymers. *Science* **280,** 1741–1744 (1998).
4. Wang, C., Dong, H., Hu, W., Liu, Y. & Zhu, D. Semiconducting π-conjugated systems in field-effect transistors: A material odyssey of organic electronics. *Chemical Reviews* **112,** 2208–2267 (2012).
5. Jacob, M. & V., M. Organic Semiconductors: Past, Present and Future. *Electronics* **3,** 594–597 (2014).
6. Mühl, S. & Beyer, B. Bio-Organic Electronics—Overview and Prospects for the Future. *Electronics* **3,** 444–461 (2014).
7. Myny, K. *et al.* An 8-bit, 40-instructions-per-second organic microprocessor on plastic foil. *IEEE J. Solid-State Circuits* **47,** 284–291 (2012).
8. What is OLED TV? The tech, the benefits, the best OLED TVs. Available at: https://www.whathifi.com/advice/what-oled-tv-tech-benefits-best-oled-tvs. (Accessed: 20th May 2017)
9. Tseng, H. R. *et al.* High-mobility field-effect transistors fabricated with macroscopic aligned semiconducting polymers. *Adv. Mater.* **26,** 2993–2998 (2014).
10. Liming, D. *Intelligent Macromolecules for Smart Devices*. *Structure* (2004). doi:10.1007/b97517
11. Carlé, J. E. Website. *http://plasticphotovoltaics.org/lc/lc-materials/lc-conjugated.html* date visted 2017 May 10 Available at: http://plasticphotovoltaics.org/lc/lc-materials/lc-conjugated.html.
12. Bredas, J. & Street, G. Polarons, bipolarons, and solitons in conducting polymers. *Acc. Chem. Res.* **1305,** 309–315 (1985).
13. Chiang, C. K. *et al.* Polyacetylene, (CH)x: N-type and p-type doping and compensation. *Appl. Phys. Lett.* **33,** 18–20 (1978).
14. Chien, J. C. *Polyacetylene: Chemistry, physics, and material science*. *British Polymer Journal* **18,** (1984).
15. Heeger, A. J., Kivelson, S., Schrieffer, J. R. & Su, W. P. Solitons in conducting polymers. *Rev. Mod. Phys.* **60,** 781–850 (1988).
16. Garnier, F., Hajlaoui, R., Yassar, A. & Srivastava, P. All-polymer field-effect transistor

realized by printing techniques. *Science* **265,** 1684–6 (1994).

17. Yamashita, Y. *et al.* Mobility exceeding 10 cm ^{2} /Vs in donor-acceptor polymer transistors with band-like charge transport. *Chem. Mater.* acs.chemmater.5b04567 (2015). doi:10.1021/acs.chemmater.5b04567

18. Morita, T. *et al.* Enhancement of transport characteristics in poly(3-hexylthiophene) films deposited with floating film transfer method. *Appl. Phys. Express* **2,** 1–4 (2009).

19. Morita, T. *et al.* Ambipolar transport in bilayer organic field-effect transistor based on poly(3-hexylthiophene) and fullerene derivatives. *Jpn. J. Appl. Phys.* **49,** 0416011–0416015 (2010).

20. Arnaud, D. *et al.* Fabrication of large-scale drop-cast films of π-conjugated polymers with floating-film transfer method. *Trans. Mater. Res. Soc. Japan* **38,** 305–308 (2013).

21. Dauendorffer, A., Nagamatsu, S., Takashima, W. & Kaneto, K. Optical and transport anisotropy in poly(9,9"'-dioctyl-fluorene-alt- bithiophene) films prepared by floating film transfer method. *Jpn. J. Appl. Phys.* **51,** (2012).

22. Dauendorffer, A. *et al.* One-step deposition of self-oriented β-phase polyfluorene thin films for polarized polymer light-emitting diodes. *Appl. Phys. Express* **5,** (2012).

23. Yang, H., Lefevre, S. W., Ryu, C. Y. & Bao, Z. Solubility-driven thin film structures of regioregular poly(3-hexyl thiophene) using volatile solvents. *Appl. Phys. Lett.* **90,** 1–4 (2007).

24. Chang, J. F. *et al.* Enhanced Mobility of poly(3-hexylthiophene) transistors by spin-coating from high-boiling-point solvents. *Chem. Mater.* **16,** 4772–4776 (2004).

25. Jimison, L. H., Toney, M. F., McCulloch, I., Heeney, M. & Salleo, A. Charge-Transport Anisotropy Due to Grain Boundaries in Directionally Crystallized Thin Films of Regioregular Poly(3-hexylthiophene). *Adv. Mater.* **21,** 1568–1572 (2009).

26. Dodabalapur, A., Torsi, L. & Katz, H. E. Organic Transistors - 2-Dimensional Transport and Improved Electrical Characteristics. *Science* **268,** 270–271 (1995).

27. Sirringhaus, H. *et al.* Two-dimensional charge transport in self-organized, high-mobility conjugated polymers. *Nature* **401,** 685–688 (1999).

28. Tumbleston, J. R. *et al.* The influence of molecular orientation on organic bulk heterojunction solar cells. *Nat. Photonics* **8,** 385–391 (2014).

29. Alignment, N. I. C., Defined, H. T. N. & Lithography, N. Nano-Confinement Induced Chain Alignment in Ordered P3HT Nanostructures Defined by Nanoimprint Lithography. *ACS Nano* **3,** 3085–3090 (2009).

30. Liu, J. *et al.* Oriented Poly (3-hexylthiophene) Nanofibril with the π - π Stacking Growth Direction by Solvent Directional Evaporation. *Langmuir* **27,** 4212–4219 (2011).

31. Hashimoto, K., Koganezawa, T. & Tajima, K. End-On Orientation of Semiconducting Polymers in Thin Films Induced by Surface Segregation of Fluoroalkyl Chains. *J. Am. Chem. Soc.* **135,** 9644–9647 (2013).

32. Ma, J., Hashimoto, K., Koganezawa, T. & Tajima, K. Enhanced vertical carrier mobility in poly (3- alkylthiophene) thin films sandwiched between self-assembled monolayers and surface- segregated layers. *Chem. Commun.* **50,** 3627 (2014).

33. Brinkmann, M., Hartmann, L., Biniek, L., Tremel, K. & Kayunkid, N. Orienting semi-conducting pi-conjugated polymers. *Macromol. Rapid Commun.* **35,** 9–26 (2014).

34. Pierret, R. F. Semiconductor Device Fundamentals. *New York* 792 (1996). doi:10.1007/BF00198606

35. Facchetti, A., Yoon, M.-H. & Marks, T. J. Gate Dielectrics for Organic Field-Effect Transistors: New Opportunities for Organic Electronics. *Adv. Mater.* **17,** 1705–1725 (2005).

36. Dimitrakopoulos, C. D. & Shaw, J. M. Low-Voltage Organic Transistors on Plastic Comprising High-Dielectric Constant Gate Insulators. *Science (80-.).* **283,** 822–824 (1999).

37. Noh, Y. Y. & Sirringhaus, H. Ultra-thin polymer gate dielectrics for top-gate polymer field-effect transistors. *Org. Electron. physics, Mater. Appl.* **10,** 174–180 (2009).

38. Liu, P., Wu, Y., Li, Y., Ong, B. S. & Zhu, S. Enabling gate dielectric design for all solution-processed, high-performance, flexible organic thin-film transistors. *J. Am. Chem. Soc.* **128,** 4554–4555 (2006).

39. Borkan, H. & Weimer, P. K. Analysis of characteristics of insulated-gate thin-film transistors. *RCA Rev.* **24,** 153–165 (1963).

40. Lohwasser, R. H. & Thelakkat, M. Toward perfect control of end groups and polydispersity in poly(3-hexylthiophene) via catalyst transfer polymerization. *Macromolecules* **44,** 3388–3397 (2011).

41. Amou, S. *et al.* Head-to-tail regioregularity of poly(3-hexylthiophene) in oxidative coupling polymerization with FeCl3. *J. Polym. Sci. Part A Polym. Chem.* **37,** 1943–1948 (1999).

42. Ong, B. S., Wu, Y., Liu, P. & Gardner, S. High-Performance Semiconducting Polythiophenes for Organic Thin-Film Transistors. *J. Am. Chem. Soc.* **126,** 3378–3379 (2004).

43. Andersson, M. R. *et al.* Regioselective polymerization of 3-(4-octylphenyl)thiophene with FeCl3. *Macromolecules* **27,** 6503–6506 (1994).

44. Trznadel, M., Pron, a, Zagorska, M., Chrzaszcz, R. & Pielichowski, J. Effect of Molecular Weight on Spectroscopic and Spectroelectrochemical Properties of Regioregular Poly(3-hexylthiophene). *Macromolecules* **31,** 5051–5058 (1998).

45. Pandey, M., Nagamatsu, S., Pandey, S. S., Hayase, S. & Takashima, W. Orientation Characteristics of Non-regiocontrolled Poly (3-hexyl-thiophene) Film by FTM on Various Liquid Substrates. *J. Phys. Conf. Ser.* **704,** 12005 (2016).

46. Lim, W. Y. *et al.* Dependencies of field effect mobility on regioregularity and side chain length in poly(alkylthiophene) films. *IEICE Trans. Electron.* **E83C,** 1071–1075 (2000).

47. Pandey, M., Nagamatsu, S., Pandey, S. S., Hayase, S. & Takashima, W. Enhancement of carrier mobility along with anisotropic transport in non-regiocontrolled poly (3-hexylthiophene) films processed by floating film transfer method. *Org. Electron.* **38,** 115–

120 (2016).

48. Bao, Z., Dodabalapur, A. & Lovinger, A. J. Soluble and processable regioregular poly(3-hexylthiophene) for thin film field-effect transistor applications with high mobility. *Appl. Phys. Lett.* **69,** 4108–4110 (1996).

49. McCulloch, I. *et al.* Liquid-crystalline semiconducting polymers with high charge-carrier mobility. *Nat. Mater.* **5,** 328–333 (2006).

50. Lim, E., Jung, B. J. & Shim, H. K. Synthesis and characterization of a new light-emitting fluorene-thieno[3,2-b]thiophene-based conjugated copolymer. *Macromolecules* **36,** 4288–4293 (2003).

51. Pandey, M., Pandey, S. S., Nagamatsu, S., Hayase, S. & Takashima, W. Solvent driven performance in thin floating-films of PBTTT for organic field effect transistor: Role of macroscopic orientation. *Org. Electron.* **43,** 240–246 (2017).

52. Noh, J., Jeong, S. & Lee, J.-Y. Ultrafast formation of air-processable and high-quality polymer films on an aqueous substrate. *Nat. Commun.* **7,** 12374 (2016).

53. Chabinyc, M. L. X-ray Scattering from Films of Semiconducting Polymers. *Polym. Rev.* **48,** 463–492 (2008).

54. Nagamatsu, S. *et al.* Backbone arrangement in 'friction-transferred' regioregular poly(3-alkylthiophene)s. *Macromolecules* **36,** 5252–5257 (2003).

55. Fourier Transform-Infrared Spectroscopy. Available at: http://www.mee-inc.com/hamm/fourier-transform-infrared-spectroscopy-ftir. (Accessed: 28th May 2017)

56. Hotta, S., Soga, M. & Sonoda, N. Infrared dichroic studies of polythiophenes. *J. Phys. Chem.* **93,** 4994–4998 (1989).

57. Gustafsson, G., Inganäs, O., Österholm, H. & Laakso, J. X-ray diffraction and infra-red spectroscopy studies of oriented poly(3-alkylthiophenes). *Polymer (Guildf).* **32,** 1574–1580 (1991).

58. Qu, S. *et al.* Highly anisotropic P3HT films with enhanced thermoelectric performance via organic small molecule epitaxy. *NPG Asia Mater.* **8,** e292 (2016).

59. Park, M. S., Aiyar, A., Park, J. O., Reichmanis, E. & Srinivasarao, M. Solvent evaporation induced liquid crystalline phase in poly(3-hexylthiophene). *J. Am. Chem. Soc.* **133,** 7244–7247 (2011).

60. Tsao, H. N. *et al.* The influence of morphology on high-performance polymer field-effect transistors. *Adv. Mater.* **21,** 209–212 (2009).

61. Licari, J. J. *Coating Materials for Electronic Applications: Polymers, Processing, Reliability, Testing*. *Coating Materials for Electronic Applications: Polymers, Processing, Reliability, Testing* (2003).

62. Aziz, F. & Ismail, A. F. Spray coating methods for polymer solar cells fabrication: A review. *Materials Science in Semiconductor Processing* **39,** 416–425 (2015).

63. Schwartz, B. J. CONJUGATED POLYMERS AS MOLECULAR MATERIALS: How

Chain Conformation and Film Morphology Influence Energy Transfer and Interchain Interactions. *Annu. Rev. Phys. Chem.* **54,** 141–172 (2003).

64. Kim, J. & Swager, T. M. Control of conformational and interpolymer effects in conjugated polymers. *Nature* **411,** 1030–1034 (2001).

65. Zhokhavets, U., Gobsch, G., Hoppe, H. & Sariciftci, N. S. Anisotropic optical properties of thin poly(3-octylthiophene)-films as a function of preparation conditions. *Synth. Met.* **143,** 113–117 (2004).

66. McCullough, R. D., Lowe, R. D., Jayaraman, M. & Anderson, D. L. Design, synthesis, and control of conducting polymer architectures: structurally homogeneous poly(3-alkylthiophenes). *J. Org. Chem* **58,** 904–912 (1993).

67. Pandey, M., Pandey, S. S., Nagamatsu, S., Hayase, S. & Takashima, W. Controlling Factors for Orientation of Conjugated Polymer Films in Dynamic Floating-Film Transfer Method. *J. Nanosci. Nanotechnol.* **17,** 1915–1922 (2017).

68. Brown, P. *et al.* Effect of interchain interactions on the absorption and emission of poly(3-hexylthiophene). *Phys. Rev. B* **67,** 1–16 (2003).

69. Bhargava, K. & Vipul, S. Investigation of Gold and Poly (3-Alkylthiophene) interface in top and bottom contact structures. *Synth. Met.* **211,** 49–57 (2016).

70. Korson, L., Drost-Hansen, W. & Millero, F. J. Viscosity of water at various temperatures. *J. Phys. Chem.* **73,** 34–39 (1969).

71. Segur, J. B. & Oberstar, H. E. Viscosity of Glycerol and Its Aqueous Solutions. *Ind. Eng. Chem.* **43,** 2117–2120 (1951).

72. Kim, Y. *et al.* A strong regioregularity effect in self-organizing conjugated polymer films and high-efficiency polythiophene:fullerene solar cells. *Nat. Mater.* **5,** 197–203 (2006).

73. Olivati, C. A., Gonçalves, V. C. & Balogh, D. T. Optically anisotropic and photoconducting Langmuir-Blodgett films of neat poly(3-hexylthiophene). *Thin Solid Films* **520,** 2208–2210 (2012).

74. Ahlskog, M. *et al.* Thermochromism and optical absorption in Langmuir-Blodgett films of alkyl-substituted polythiophenes. *J. Appl. Phys.* **76,** 893–899 (1994).

75. Pandey, M., Pandey, S. S., Nagamatsu, S., Hayase, S. & Takashima, W. Influence of backbone structure on orientation of conjugated polymers in the dynamic casting of thin floating-films. *Thin Solid Films* **619,** 125–130 (2016).

76. Yang, C., Orfino, F. P. & Holdcroft, S. A Phenomenological Model for Predicting Thermochromism of Regioregular and Nonregioregular Poly(3-alkylthiophenes). *Macromolecules* **29,** 6510–6517 (1996).

77. Takashima, W. *et al.* Photocarrier transports related to the morphology of regioregular poly(3-hexylthiophene) films. in *Thin Solid Films* **393,** 334–342 (2001).

78. Hagler, T. W., Pakbaz, K., Voss, K. F. & Heeger, A. J. Enhanced order and electronic delocalization in conjugated polymers oriented by gel processing in polyethylene. *Phys. Rev. B* **44,** 8652–8666 (1991).

79. Kumar, A., Takashima, W., Kaneto, K. & Prakash, R. Nano-dimensional self assembly of regioregular poly (3-hexylthiophene) in toluene: Structural, optical, and morphological properties. *J. Appl. Polym. Sci.* **131,** (2014).

80. Spano, F. C. Modeling disorder in polymer aggregates: The optical spectroscopy of regioregular poly(3-hexylthiophene) thin films. *J. Chem. Phys.* **122,** 234701 (2005).

81. Chabinyc, M. L., Toney, M. F., Kline, R. J., McCulloch, I. & Heeney, M. X-ray scattering study of thin films of poly(2,5-bis(3-alkylthiophen-2-yl)thieno[3,2-b]thiophene). *J. Am. Chem. Soc.* **129,** 3226–3237 (2007).

82. Tashiro, K. *et al.* Structure and thermochromic solid-state phase transition of poly(3-alkylthiophene): [3] effects of alkyl side chain length on the phase transitional behavior. *Synth. Met.* **55,** 321–328 (1993).

83. Prosa, T. J., Moulton, J., Heeger, A. J. & Winokur, M. J. Diffraction line-shape analysis of poly(3-dodecylthiophene): a study of layer disorder through the liquid crystalline polymer transition. *Macromolecules* **32,** 4000–4009 (1999).

84. Park, K. C. & Levon, K. Order-disorder transition in the electroactive polymer poly(3-dodecylthiophene). *Macromolecules* **30,** 3175–3183 (1997).

85. McCullough, R. D., Tristram-Nagle, S., Williams, S. P., Lowe, R. D. & Jayaraman, M. Self-orienting head-to-tail poly(3-alkylthiophenes): new insights on structure-property relationships in conducting polymers. *J. Am. Chem. Soc.* **115,** 4910–4911 (1993).

86. Biniek, L., Leclerc, N., Heiser, T., Bechara, R. & Brinkmann, M. Large scale alignment and charge transport anisotropy of PBTTT films oriented by high temperature rubbing. *Macromolecules* **46,** 4014–4023 (2013).

87. Wu, Y. *et al.* Controlled orientation of liquid-crystalline polythiophene semiconductors for high-performance organic thin-film transistors. *Appl. Phys. Lett.* **86,** 1–3 (2005).

88. Hamaguchi, M. *et al.* Lyotropic Behavior of Poly (2 , 5-dinonyloxy-p-phenylenevinylene). *Jpn. J. Appl. Phys.* **33,** L1689–L1692 (1994).

89. Hamaguchi, M. & Yoshino, K. Liquid crystalline behavior and optical properties of poly (2, 5-dinonyloxy-p-phenylenevinylene). *Jpn. J. Appl. Phys.* **33,** L1478-1481 (1994).

90. Verilhac, J. M. *et al.* Effect of macromolecular parameters and processing conditions on supramolecular organisation, morphology and electrical transport properties in thin layers of regioregular poly(3-hexylthiophene). *Synth. Met.* **156,** 815–823 (2006).

91. Pethrick, R. a. Applications of electroactive polymers. *React. Polym.* **22,** 91–92 (1994).

92. Yokozawa, T. & Yokoyama, A. Chain-growth condensation polymerization for the synthesis of well-defined condensation polymers and π-conjugated polymers. *Chem. Rev.* **109,** 5595–5619 (2009).

93. Chen, T.-A., Wu, X. & Rieke, R. D. Regiocontrolled Synthesis of Poly(3-alkylthiophenes) Mediated by Rieke Zinc: Their Characterization and Solid-State Properties. *J. Am. Chem. Soc.* **117,** 233–244 (1995).

94. Hartmann, L. *et al.* 2D versus 3D crystalline order in thin films of regioregular poly(3-

hexylthiophene) oriented by mechanical rubbing and epitaxy. *Adv. Funct. Mater.* **21,** 4047–4057 (2011).

95. Pandey, M. *et al.* Layer-by-layer coating of oriented conjugated polymer films towards anisotropic electronics. *Synth. Met.* **227,** 29–36 (2017).

96. Sugimoto, R., Takeda, S., Gu, H. B. & Yoshino, K. Preparation of soluble polythiophene derivatives utilizing transition metal halides as catalysts and their property. *Chem. Express* **1,** 635–638 (1986).

97. Chen, S. & Ni, J. Structure/properties of conjugated conductive polymers. 1. Neutral poly (3-alkythiophene) s. *Macromolecules* **25,** 6081–6089 (1992).

98. Benor, A., Hoppe, A., Wagner, V. & Knipp, D. Electrical stability of pentacene thin film transistors. *Org. Electron. physics, Mater. Appl.* **8,** 749–758 (2007).

99. Forrest, S. R. The path to ubiquitous and low-cost organic electronic appliances on plastic. *Nature* **428,** 911–918 (2004).

100. Sirringhaus, H. 25th anniversary article: Organic field-effect transistors: The path beyond amorphous silicon. *Adv. Mater.* **26,** 1319–1335 (2014).

101. Becerril, H. A., Roberts, M. E., Liu, Z., Locklin, J. & Bao, Z. High-performance organic thin-film transistors through solution-sheared deposition of small-molecule organic semiconductors. *Adv. Mater.* **20,** 2588–2594 (2008).

102. Yamasaki, N., Miyake, Y., Yoshida, H., Fujii, A. & Ozaki, M. Solution flow assisted fabrication method of oriented π-conjugated polymer films by using geometrically-asymmetric sandwich structures. *Jpn. J. Appl. Phys.* **50,** (2011).

103. Coropceanu, V. *et al.* Charge transport in organic semiconductors. *Chem. Rev.* **107,** 926–952 (2007).

104. Kim, J. S. *et al.* Tuning Mechanical and Optoelectrical Properties of Poly(3-hexylthiophene) through Systematic Regioregularity Control. *Macromolecules* **48,** 4339–4346 (2015).

105. Chu, P.-H. *et al.* Synergistic Effect of Regioregular and Regiorandom Poly(3-hexylthiophene) Blends for High Performance Flexible Organic Field Effect Transistors. *Adv. Electron. Mater.* **2,** 1500384 (2015).

106. Kim, H. J. *et al.* Solution-Assembled Blends of Regioregularity-Controlled Polythiophenes for Coexistence of Mechanical Resilience and Electronic Performance. *ACS Appl. Mater. Interfaces* **9,** 14120–14128 (2017).

107. Pascui, O. F. *et al.* High crystallinity and nature of crystal-crystal phase transformations in regioregular poly(3-hexylthiophene). *Macromolecules* **43,** 9401–9410 (2010).

108. Son, S. Y. *et al.* High Field-Effect Mobility of Low-Crystallinity Conjugated Polymers with Localized Aggregates High Field-Effect Mobility of Low-Crystallinity Conjugated Polymers with Localized Aggregates. *J. Am. Chem. Soc.* **138,** 8096–8103 (2016).

109. Kim, B.-G. *et al.* A molecular design principle of lyotropic liquid-crystalline conjugated polymers with directed alignment capability for plastic electronics. *Nat. Mater.* **12,** 659–64 (2013).

110. Chang, M., Lee, J., Kleinhenz, N., Fu, B. & Reichmanis, E. Photoinduced anisotropic supramolecular assembly and enhanced charge transport of poly(3-hexylthiophene) thin films. *Adv. Funct. Mater.* **24,** 4457–4465 (2014).

111. Noriega, R. *et al.* A general relationship between disorder, aggregation and charge transport in conjugated polymers. *Nat. Mater.* **12,** 1038–44 (2013).

112. Snyder, C. R., Henry, J. S. & Delongchamp, D. M. Effect of regioregularity on the semicrystalline structure of poly(3-hexylthiophene). *Macromolecules* **44,** 7088–7091 (2011).

113. Crossland, E. J. W. *et al.* Anisotropic charge transport in spherulitic Poly(3-hexylthiophene) films. *Adv. Mater.* **24,** 839–844 (2012).

114. Heil, H., Finnberg, T., Von Malm, N., Schmechel, R. & Von Seggern, H. The influence of mechanical rubbing on the field-effect mobility in polyhexylthiophene. *J. Appl. Phys.* **93,** 1636–1641 (2003).

115. Tremel, K. & Ludwigs, S. in *P3HT Revisited - From Molecular Scale to Solar Cell Devices From Molecular Scale to Solar Cell Devices* (ed. Ludwigs, S.) 39–82 (Springer Berlin Heidelberg, 2012). doi:10.1007/12_2014_288

116. Chu, P. H. *et al.* Enhanced mobility and effective control of threshold voltage in P3HT-based field-effect transistors via inclusion of oligothiophenes. *ACS Appl. Mater. Interfaces* **7,** 6652–6660 (2015).

117. Zhao, Y. *et al.* Complementary Semiconducting Polymer Blends for Efficient Charge Transport. *Chem. Mater.* **27,** 7164–7170 (2015).

118. Pandey, S. S., Takashima, W., Nagamatsu, S. & Kaneto, K. Effect of Synthetic Impurities on Photocarrier Transport in Poly (3-Hexylthiophene). *IEICE Trans. Electron.* **39,** 1088–1093 (2000).

119. Diemer, P. J. *et al.* Quantitative analysis of the density of trap states at the semiconductor-dielectric interface in organic field-effect transistors. *Appl. Phys. Lett.* **107,** (2015).

120. Gurau, M. C. *et al.* Measuring molecular order in poly(3-alkylthiophene) thin films with polarizing spectroscopies. *Langmuir* **23,** 834–842 (2007).

121. O'Connor, B. *et al.* Anisotropic structure and charge transport in highly strain-aligned regioregular poly(3-hexylthiophene). *Adv. Funct. Mater.* **21,** 3697–3705 (2011).

122. Zheng, Z. *et al.* Uniaxial alignment of liquid-crystalline conjugated polymers by nanoconfinement. *Nano Lett.* **7,** 987–992 (2007).

123. Sirringhaus, H. *et al.* Mobility enhancement in conjugated polymer field-effect transistors through chain alignment in a liquid-crystalline phase. *Appl Phys Lett* **77,** 406–408 (2000).

124. Grell, B. M. *et al.* Blue Polarized Electroluminescence from a Liquid Crystalline Polyfluorene. *Adv. Mater.* **11,** 671–675 (1999).

125. Kinder, L., Kanicki, J. & Petroff, P. Structural ordering and enhanced carrier mobility in organic polymer thin film transistors. *Synth. Met.* **146,** 181–185 (2004).

126. Clark, J., Silva, C., Friend, R. H. & Spano, F. C. Role of intermolecular coupling in the

photophysics of disordered organic semiconductors: Aggregate emission in regioregular polythiophene. *Phys. Rev. Lett.* **98,** 206406 (2007).

127. Clark, J., Chang, J. F., Spano, F. C., Friend, R. H. & Silva, C. Determining exciton bandwidth and film microstructure in polythiophene films using linear absorption spectroscopy. *Appl. Phys. Lett.* **94,** 163306 (2009).

128. Jung, Y. *et al.* The effect of interfacial roughness on the thin film morphology and charge transport of high-performance polythiophenes. *Adv. Funct. Mater.* **18,** 742–750 (2008).

129. Lee, M. J. *et al.* Anisotropy of charge transport in a uniaxially aligned and chain-extended, high-mobility, conjugated polymer semiconductor. *Adv. Funct. Mater.* **21,** 932–940 (2011).

130. Husermann, R. & Batlogg, B. Gate bias stress in pentacene field-effect-transistors: Charge trapping in the dielectric or semiconductor. *Appl. Phys. Lett.* **99,** 83303 (2011).

131. Briseno, A. L. *et al.* High-performance organic single-crystal transistors on flexible substrates. *Adv. Mater.* **18,** 2320–2324 (2006).

132. Briseno, A. L. *et al.* Patterned growth of large oriented organic semiconductor single crystals on self-assembled monolayer templates. *J. Am. Chem. Soc.* **127,** 12164–12165 (2005).

133. Mcculloch, I. *et al.* Semiconducting thienothiophene copolymers: Design, synthesis, morphology, and performance in thin-film Organic transistors. *Adv. Mater.* **21,** 1091–1109 (2009).

134. Janasz, L. *et al.* Improved charge carrier transport in ultrathin poly(3-hexylthiophene) films via solution aggregation. *J. Mater. Chem. C* **4,** 11488–11498 (2016).

135. Persson, N. E., Chu, P.-H., McBride, M., Grover, M. & Reichmanis, E. Nucleation, Growth, and Alignment of Poly(3-hexylthiophene) Nanofibers for High-Performance OFETs. *Acc. Chem. Res.* **(In Press),** (2017).

136. Xue, X. *et al.* Oriented Liquid Crystalline Polymer Semiconductor Films with Large Ordered Domains. *ACS Appl. Mater. Interfaces* **7,** 26726–26734 (2015).

137. Singh, M. K., Kumar, A. & Prakash, R. Self-assembly of regioregular poly (3,3‴-didodecylquarterthiophene) in chloroform and study of its junction properties. *Mater. Sci. Eng. B* **217,** 12–17 (2017).

138. Delongchamp, D. M. *et al.* Controlling the orientation of terraced nanoscale 'ribbons' of a poly(thiophene) semiconductor. *ACS Nano* **3,** 780–787 (2009).

139. Higashi, T. *et al.* Anisotropic properties of aligned ??-conjugated polymer films fabricated by capillary action and their post-annealing effects. *Appl. Phys. Express* **4,** 91602 (2011).

140. Soeda, J. *et al.* Highly Oriented Polymer Semiconductor Films Compressed at the Surface of Ionic Liquids for High-Performance Polymeric Organic Field-Effect Transistors. *Adv. Mater.* **26,** 6430–6435 (2014).

141. Schuettfort, T. *et al.* Microstructure of polycrystalline PBTTT films: Domain mapping and structure formation. *ACS Nano* **6,** 1849–1864 (2012).

142. Gao, J., Thomas, A. K., Johnson, R., Guo, H. & Grey, J. K. Spatially Resolving Ordered and

Disordered Conformers and Photocurrent Generation in Intercalating Conjugated Polymer / Fullerene Blend Solar Cells. *Chem. Mater.* **26,** 4395–4404 (2014).

143. Hamidi-Sakr, A., Biniek, L., Fall, S. & Brinkmann, M. Precise Control of Lamellar Thickness in Highly Oriented Regioregular Poly(3-Hexylthiophene) Thin Films Prepared by High-Temperature Rubbing: Correlations with Optical Properties and Charge Transport. *Adv. Funct. Mater.* **26,** 408–420 (2016).

144. Kline, R. J. *et al.* Critical role of side-chain attachment density on the order and device performance of polythiophenes. *Macromolecules* **40,** 7960–7965 (2007).

145. Delongchamp, D. M. *et al.* Molecular basis of mesophase ordering in a thiophene-based copolymer. *Macromolecules* **41,** 5709–5715 (2008).

146. Salleo, A., Chabinyc, M. L., Yang, M. S. & Street, R. A. Polymer thin-film transistors with chemically modified dielectric interfaces. *Appl. Phys. Lett.* **81,** 4383–4385 (2002).

147. Kushida, T., Nagase, T. & Naito, H. Angular distribution of field-effect mobility in oriented poly[5,5'-bis(3-dodecyl-2-thienyl)-2,2'-bithiophene] fabricated by roll-transfer printing. *Appl. Phys. Lett.* **104,** (2014).

148. Umeda, T., Kumaki, D. & Tokito, S. Surface-energy-dependent field-effect mobilities up to 1 cm2 /V s for polymer thin-film transistor. *J. Appl. Phys.* **105,** (2009).

149. Hamadani, B. H., Gundlach, D. J., McCulloch, I. & Heeney, M. Undoped polythiophene field-effect transistors with mobility of 1 cm2 V-1 s-1. *Appl. Phys. Lett.* **91,** 1–4 (2007).

150. Hosokawa, Y. *et al.* Molecular orientation and anisotropic carrier mobility in poorly soluble polythiophene thin films. *Appl. Phys. Lett.* **100,** 203305 (2012).

151. DeLongchamp, D. M. *et al.* High carrier mobility polythiophene thin films: Structure determination by experiment and theory. *Adv. Mater.* **19,** 833–837 (2007).

152. Umeda, T., Tokito, S. & Kumaki, D. High-mobility and air-stable organic thin-film transistors with highly ordered semiconducting polymer films. *J. Appl. Phys.* **101,** 54517 (2007).

153. Gasperini, A. & Sivula, K. Effects of Molecular Weight on Microstructure and Carrier Transport in a Semicrystalline Poly (thieno) thiophene. *Macromolecules* **46,** 9349–9358 (2013).

154. Chen, X. L., Lovinger, A. J., Bao, Z. & Sapjeta, J. Morphological and transistor studies of organic molecular semiconductors with anisotropic electrical characteristics. *Chem. Mater.* **13,** 1341–1348 (2001).

155. Shirota, Y. Photo- and electroactive amorphous molecular materials—molecular design, syntheses, reactions, properties, and applications. *J. Mater. Chem.* **15,** 75–93 (2005).

156. Zhu, H., Mitsuishi, M. & Miyashita, T. Facile preparation of highly oriented poly(vinylidene fluoride) Langmuir-Blodgett nanofilms assisted by amphiphilic polymer nanosheets. *Macromolecules* **45,** 9076–9084 (2012).

157. Nagano, S., Kodama, S. & Seki, T. Ideal spread monolayer and multilayer formation of fully hydrophobic polythiophenes via liquid crystal hybridization on water. *Langmuir* **24,** 10498–

10504 (2008).

158. Cheng, Y.-J., Yang, S.-H. & Hsu, C.-S. Synthesis of Conjugated Polymers for Organic Solar Cell Applications. *Chem. Rev.* **109,** 5868–5923 (2009).

159. Facchetti, A. π-Conjugated polymers for organic electronics and photovoltaic cell applications. *Chem. Mater.* **23,** 733–758 (2011).

160. Kline, R. J. *et al.* Dependence of regioregular poly(3-hexylthiophene) film morphology and field-effect mobility on molecular weight. *Macromolecules* **38,** 3312–3319 (2005).

161. Pandey, S. S. *et al.* Regioregularity vs Regiorandomness: Effect on Photocarrier Transport in Poly(3-hexylthiophene). *Jpn. J. Appl. Phys.* **39,** L94–L97 (2000).

162. Louarn, G. *et al.* Raman Spectroscopic Studies of Regioregular Poly(3-alkylthiophenes). *J. Phys. Chem.* **100,** 12532–12539 (1996).

163. Furukawa, Y., Akimoto, M. & Harada, I. Vibrational key bands and electrical conductivity of polythiophene. *Synth. Met.* **18,** 151–156 (1987).

164. Ong, B. S., Wu, Y., Liu, P. & Gardner, S. Structurally ordered polythiophene nanoparticles for high-performance organic thin-film transistors. *Adv. Mater.* **17,** 1141–1144 (2005).

Achievements

Publications

1. **Manish Pandey**, Shuichi Nagamatsu, Wataru Takashima, Shyam S. Pandey, Shuzi Hayase *Interplay of Orientation and Blending: Synergistic Enhancement of Field Effect Mobility in Thiophene-based Conjugated Polymers* **Journal of Physical Chemistry C, doi-10.1021/acs.jpcc.7b03416**

2. **Manish Pandey**, Shyam S. Pandey, Shuichi Nagamatsu, Shuzi Hayase and Wataru Takashima *Controlling Factors for Orientation of Conjugated Polymer Films in Dynamic Floating-film Transfer Method* **Journal of Nanoscience and Nanotechnology, (2017) *17*, 1915-1922**

3. **Manish Pandey**, Shuichi Nagamatsu, Shyam S. Pandey, Shuzi Hayase and Wataru Takashima *Solvent driven performance in thin floating-films of PBTTT for organic field effect transistor: Role of macroscopic orientation* **Organic Electronics, (2017) *43*, 240-246**

4. **Manish Pandey**, Shifumi Sadakata, Shuichi Nagamatsu, Shyam S. Pandey, Shuzi Hayase and Wataru Takashima *Layer-by- Layer Coating of Oriented Conjugated Polymer Films towards Anisotropic Architecture* , **Synthetic Metals (2017) *227*, 29-36**

5. Praveen Kumar Sahu, **Manish Pandey**, Chandan Kumar, Shyam S. Pandey, V. N. Mishra, Wataru Takashima and Rajiv Prakash *Air-stable vapor phase sensing of ammonia in sub-threshold regime of Poly(2,5-bis(3-tetradecylthiophen-2yl)thieno(3,2- b)thiophene) based polymer thin-film transistor* , **Sensors and Actuators B: Chemical (2017) *246*, 243-251**

6. **Manish Pandey**, Shuichi Nagamatsu, Shyam S. Pandey, Shuzi Hayase and Wataru Takashima *Enhancement of carrier mobility along with anisotropic transport in non-regiocontrolled poly (3-hexylthiophene) films processed by floating film transfer method* **Organic Electronics (2016) *38*, 115-120**

7. **Manish Pandey**, Shyam S. Pandey, Shuichi Nagamatsu, Shuzi Hayase and Wataru Takashima *Influence of Backbone Structure on Orientation of Conjugated Polymers in the Dynamic Casting of Thin Floating-Films* **Thin Solid Films (2016) *619*, 125-130**

8. **M. Pandey**, S. Nagamatsu, S. S. Pandey, S. Hayase, W. Takashima *Orientation Characteristics of Non-regiocontrolled Poly(3-hexylthiophene) Film by FTM on Various Liquid Substrate* **Journal of Physics: Conference Series (2016)** ***704*****, 012005**

9. A. S. M. Tripathi, **M. Pandey**, S. Nagamatsu, S. S. Pandey, S. Hayase, W. Takashima *Casting Control of Floating-films into Ribbon-shape Structure by modified Dynamic* **Journal of Physics: Conference Series** ***(Accepted Manuscript)***

9. **Manish Pandey**, Ashwathanarayana Gowda, Shuichi Nagamatsu, Sandeep Kumar, Wataru Takashima, Shuzi Hayase and Shyam S. Pandey *Rapid formation of Macroscopic Self-Assembly of Liquid Crystalline, High Mobility, Semi-conducting Thienothiophene* **Submitted in Advanced Materials Interfaces**

Presentations

International Conferences (* Presenting Author)

1. **Manish Pandey*,** Shuichi Nagamatsu, Reeturaj Pandey, Shyam S. Pandey, Shuzi Hayase and Wataru Takashima *Remarkable enhancement in the carrier transport of thiophene based conjugated polymers: Synergistic influence of orientation and blending* 12th International Conference on Nano-Molecular Electronics 14-16 December, 2016

2. Praveen Kumar Sahu, **Manish Pandey***, Chandan Kumar, Shyam Pandey, Wataru Takashima, V. N. Mishra and Rajiv Prakash *Development of highly stable non-invasive ammonia sensor for the detection of sub-ppm level concentration of ammonia* 12th International Conference on Nano-Molecular Electronics 14-16 December, 2016

3. Atul S. M. Tripathi*, **Manish Pandey**, Shuichi Nagamatsu, Shyam Pandey, Shuzi Hayase and Wataru Takashima *Orientation Characteristics in Ribbon Shaped Floating Thin-Films of Conjugated Polymers Prepared by Dynamic FTM* 12th International Conference on Nano-Molecular Electronics 14-16 December, 2016 (Poster : P1-35) **(Selected for ICNME 2016 Best Poster Award)**

4. A. S. M. Tripathi*, **M. Pandey**, S. Sadakata, S. Nagamatsu, S. S. Pandey, S. Hayase and W. Takashima *Orientation Parameters of NR-P3HT macromolecules in a Ribbon-shape Floating-film by Dynamic FTM* 4th International Symposium on Applied Engineering and Sciences (SAES 2016), KIT Japan, December 17-18. (M-19) Dec 18.

5. **M. Pandey***, A. S. M. Tripathi, S. Nagamatsu, S. Hayase, S. S. Pandey and W. Takashima *Solvent Driven Performance in Thin Floating Films of Conjugated polymers for Organic Field Effect Transistor: Role of Macroscopic Orientation* 4th International Symposium on Applied Engineering and Sciences (SAES 2016), KIT Japan, December 17-18, 2016. (M-18) Dec 18.

6. Wataru Takashima*, **Manish Pandey**, Shuichi Nagamatsu, Shyam S. Pandey, Shuzi Hayase *Casting of Floating-film of Organic Semiconductors on Liquid Substrate for Anisotropic Electronics* KJF International Conference on Organic Materials for Electronics and Photonics, Fukuoka, 4-7 Sept, 2016. (Poster PR-233) Sept 5, 2016.

7. **Manish Pandey***, Shuichi Nagamatsu, Shyam S. Pandey and Wataru Takashima *Highly oriented conjugated polymers by FTM method towards anisotropic photonic and electronic devices* International Conference on the Science and Technology of Synthetic Metals (ICSM-2016) Guangzhou Baiyun International Convention Center, June 26 to July 1, 2016. (Poster W-8-31) June 29, 2016.

8. **Manish Pandey**, Shyam S. Pandey*, Shuichi Nagamatsu, Shuzi Hayase and Wataru Takashima *Enhanced Field Effect Mobility with Blends of Organic Semiconductors* 9th International Symposium on Organic Molecular Electronics (ISOME-2016), 18-20 May, 2016 Niigata University, Niigata, Japan, 19th May 2016.

9. **Manish Pandey**, Shuichi Nagamatsu, Shyam S. Pandey, Shuzi Hayase and Wataru Takashima* *Dynamic Casting of Floating-film and Transferring of Oriented π-Conjugated Polymers towards Anisotropic Electronics* India-Japan Expert Group Meeting on Biomolecular Electronics & Organic Nanotechnology for Environment Preservation (IJEGMBE-2015), Kyushu Institute of Technology Japan, December 22-25, 2015. Dec 24, 2015

10. **Manish Pandey***, Shuichi Nagamatsu, Shyam S. Pandey, Shuzi Hayase and Wataru Takashinma *Orientation of Conjugated Polymers Through Floating Film Transfer Method* ICMAT 2015 and IUMRS-ICA 2015, Suntec, Singapore, June 28-July 3, 2015, June 28, 2015.

Domestic Conferences (* Presenting Author)

1. **Manish Pandey***, Atul S. M. Tripathi, Shyam S. Pandey, Shuichi Nagamatsu, Shuzi Hayase, Wataru Takashima *Static vs. Dynamic FTM: Implication of the Solvent Evaporation on Casting*

Thin Floating-Films of Polymer Semiconductor 64th Spring meeting of Japan Society Applied Physics (JSAP)

2. Shifumi Sadakata*, Atul S. M. Tripathi, **Manish Pandey**, Shyam S. Pandey, Shuichi Nagamatsu, Shuzi Hayase and Wataru Takashima *Local mapping of orientation distribution in floating-film* 64th Spring meeting of Japan Society Applied Physics (JSAP)

3.Atul S. M. Tripathi*, **Manish Pandey**, Shifumi Sadakata, Shyam S. Pandey, Shuichi Nagamatsu, Shuzi Hayase and Wataru Takashima *Ribbon-shaped floating-film of polythiophene-based conjugated polymers for orientation analysis* 64th Spring meeting of Japan Society Applied Physics (JSAP)

3. W. Takashima*, **M. Pandey**, S. Nagamatsu, S. S. Pandey and S. Hayase *Orientation Characteristics of Conjugated Polymers on Liquid Substrate* 26th Annual Meeting Material Research Society of Japan (MRS-J), Yokohama, Japan, December 19-22, 2016. [B1-O19-007] Dec 19, 2016.

4. **Manish Pandey***, Shuichi Nagamatsu, Shyam S. Pandey, Shuzi Hayase and Wataru Takashima *Ambient Fabrication of Oriented PBTTT-based FET by FTM* 77th Autumn meeting of Japan Society Applied Physics (JSAP), Niigata University , Niigata Japan, Sept 13-16, 2016. [16a-B5-2] Sept 16, 2016

5. **Manish Pandey***, Shuichi Nagamatsu, Shyam S. Pandey, Shuzi Hayase and Wataru Takashima *Multi-layer coating of oriented conjugated polymer films via FTM method* 63rd Spring meeting of Japan Society Applied Physics (JSAP), Ookayama Campus, Tokyo Institute of Technology, March 19-22, 2016. [19p-W242-5] March 19, 2016.

6. Wataru Takashima*, **Manish Pandey** "*Classical Method to Ananlyze Electrochemical Creep in Polypyrrole Film*" 25th Annual Meeting Material Research Society of Japan (MRS-J), Yokohama, December 8-10, 2015. Dec 8, 2015.

7. Wataru Takashima*, **Manish Pandey**, Shuichi Nagamatsu, Shyam S. Pandey, Shuzi Hayase *Casting Procedure of Conducting Polymers for Delighting Potential Performance* 25th Annual Meeting Material Research Society of Japan (MRS-J), Yokohama, December 8-10, 2015. Dec 8, 2015

8. **Manish Pandey***, Shuichi Nagamatsu, Shyam S. Pandey, Shuzi Hayase and Wataru Takashima *Orientation factors in floating-film transfer method* 76th Autumn meeting of Japan Society Applied Physics (JSAP), Nagoya Congress Center , Nagoya Japan, September 13-16, 2015. [14p-1E-16] Sept 14 2015.

9. **Manish Pandey***, Shuichi Nagamatsu, Shyam S. Pandey, Shuzi Hayase and Wataru Takashima *Orientation of conjugated polymers by FTM method* 62nd Spring meeting of Japan Society Applied Physics (JSAP), Shonan Campus, Tokai University, March 11-14, 2015. [11p-D2-14] 11 Mar 2015.

Acknowledgement

Above all, I am grateful to **Prof. Shyam S. Pandey** who has been more than supervisor for me throughout this 3 years. His contribution was not limited to exploring, planning and solving my research problems but way beyond my studies in learning different aspect of life apart from being a good researcher. Frankly speaking, Japan is country, where surviving without basic Japanese language is very difficult but his continuous support in translating it made my life easy here to survive and focus on my research work. His deep knowledge related to chemistry of conducting polymer, thin films and fabrication of organic electronic devices, which he gained over the past 30 years enabled me at its best. All I can say is he is the ideal person as a teacher to whom I would try to follow in future.

I am grateful to **(Late) Prof. Wataru Takashima** whose contribution in these last two and half years is so much that it is not possible for me to write in a paragraph, I wish his soul to rest in peace. I am very thankful to **Prof. Shuzi Hayase** for providing all required research facilities needed to carry out this research. I am thankful to **Prof. Shuichi Nagamatsu** for his valuable discussions and comments on my work. I am also thankful to other **Prof. Sandeep Kumar** of RRI Bangalore for his consistent help in providing experimental facilities.

I am also very grateful to **Prof. Ayash Kanto Mukherjee** from IIT Patna who recommended me here for my doctoral studies and given continuous suggestions whenever I needed in these 3 years.

I am very grateful to my father **Dr. R. S. Pandey** and my mother **B. Devi** for their belief, patience, support and understanding throughout these 3 years when I was thousands of miles away from them. Also I appreciate my elder brother **Ashutosh Pandey** and sister **Dr. Manju Shukla** who were very supportive in every aspect of encouraging me for higher studies. I am also thankful to dearest long term colleagues **Shalini**, **Abhinav** and **Anant** who always boosted my morale up and their loving conversation made me confident and relaxed while staying away from them.

I am very thankful to my seniors **Dr. Ajay Baranwal**, **Dr. Kapil Gaurav** for providing all sorts of help when I joined my Ph.D. program and other colleagues who have been a very important part of my journey at KIT especially **Vishal Gaurav**. I am grateful to KIT for providing me all kind of facilities including various scholarships throughout these 3 years and different financial support for attending domestic and overseas conferences. I am very thankful to staff of international division for their help.

I would like to thank my beautiful wife **Niharika** whose sacrifice for my doctoral studies is endless. She motivated me, inspired me and always stood with me in every up and down throughout these 3 years. I wish to have a long holiday with her and my other family members after completing this stressful journey of 3 years.